Accounts

Design of High-Performance Heterogeneous Metal Catalysts for Green and Sustainable Chemistry

Kiyotomi Kaneda,[*] **Kohki Ebitani, Tomoo Mizugaki, and Kohsuke Mori**

Department of Materials Engineering Science, Graduate School of Engineering Science,
Osaka University, 1-3 Machikaneyama, Toyonaka, Osaka 560-8531

Received September 20, 2005; E-mail: kaneda@cheng.es.osaka-u.ac.jp

This account reviews a novel approach to designing high-performance heterogeneous metal catalysts using hydroxyapatites, montmorillonites, and hydrotalcites as macroligands of active metal species for aerobic alcohol oxidations, carbon–carbon bond formations, and one-pot syntheses. The catalytic systems using the above heterogeneous catalysts offer significant benefits in achieving environmentally friendly organic syntheses aiming towards Green and Sustainable Chemistry. Furthermore, the present preparation method for the immobilization of metal species is strikingly simple and allows a strong protocol for creating various nanostructured and functionalized heterogeneous catalysts.

Green and Sustainable Chemistry (GSC) is a revolutionary philosophy that aims to bring about a sustainable society by improvement of the safety and environmental aspects of chemical processes and reduction of the risks of chemical products to people and the environment.[1] The emphasis is on eliminating waste at the source—primary pollution prevention—rather than finding incremental end-of-pipe solutions. This concept aims to solve the societal problems of the last century associated with the mass production and consumption of materials, and plays a prime role in providing a venous function in society, encouraging reuse and circulation of resources.

One of the powerful solutions in the move toward GSC is the replacement of traditional synthetic methods using harmful stoichiometric reagents that produce vast amounts of waste with cleaner and simple catalytic alternatives with high atom efficiency[1a] and low E-factors.[1b] Catalytic chemistry, therefore, is of ever-increasing importance because catalysis is a key element in material transformations at atomic and molecular levels, which are an essential realm of chemistry and chemical processes.

Our approach to GSC is to develop a highly functionalized heterogeneous metal catalyst based on the unique characteristics of natural layered inorganic materials such as hydroxyapatite, montmorillonite, and hydrotalcite, by using them as macroligands for metal species.[2] We consider the above inorganic materials to be advanced nano-scaled catalyst supports allowing for the control of the location of catalytically active metal species, which can be found, for example, on the surface, among the layers, or in the interlayer space. Furthermore, these materials are capable of creating catalytically active metal species responsible for targeted organic transformations involving monomers, chain-like species or giant clusters. The creation of well-defined active metal sites on a solid surface, as characterized by X-ray absorption spectroscopy, not only opens up an avenue to materials that boost catalytic performance, but also aids in the understanding of the molecular basis of heterogeneous catalysis. Another advantage of these catalysts is the possibility of a one-pot synthesis based on a cooperative action by several immobilized active species on the solid surface as multifunctional catalysts. The target reactions described here include selective oxidations using molecular oxygen and hydrogen peroxide as a clean oxidant, highly efficient carbon–carbon bond formations, one-pot syntheses involving oxidation reactions coupled with carbon–carbon bond formations, and the chemical fixation of carbon dioxide.

1. Hydroxyapatite

Apatites and related compounds, most notably hydroxyapatite (HAP), $Ca_5(OH)(PO_4)_3$, are of considerable interest due to their potential usefulness as biomaterials, adsorbents, and ion-exchangers.[3] However, few outstanding applications as catalysts or catalyst supports have emerged so far. The hexagonal apatite structure comprises of Ca^{2+} sites surrounded by PO_4^{3-} tetrahedra; OH^- ions occupy columns parallel to the hexagonal axis, as illustrated in Fig. 1.[3]

The crystal structure shows two nonequivalent Ca^{2+} sites: one set of Ca^{2+} ions is aligned in columns (site I: Ca_I), while the other set forms equilateral triangles centered on the screw axes (site II: Ca_{II}). Recently, we have disclosed a new strategy for the design of high-performance heterogeneous catalysts utilizing hydroxyapatite as a macroligand for catalytically active centers (Chart 1).[4]

The choice of hydroxyapatites as catalyst supports is motivated by the following advantages: (i) well-defined monomeric
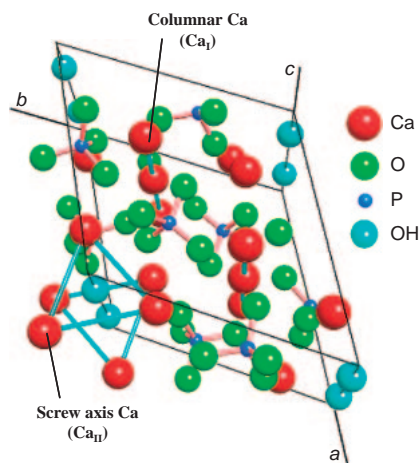
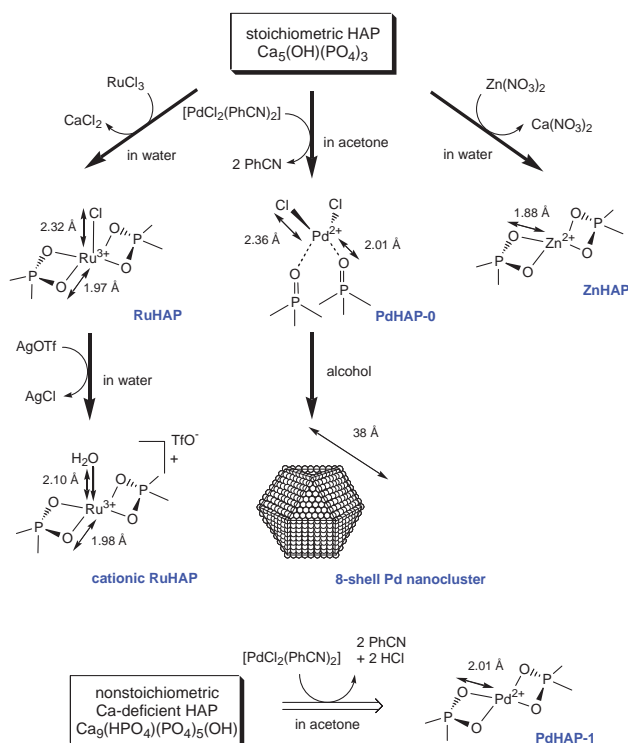Fig. 1.　Structure of hydroxyapatite.

Chart 1.　Strategy for design of hydroxyapatite catalysts.

active species can be immobilized on their surface based on multiple functionality, e.g., cation exchange ability, adsorption capacity, and nonstoichiometry, (ii) their hydrophilic character allows smooth reactions under aqueous conditions, and (iii) due to their robust structure, no metal leaching is observed, the catalysts are recyclable without any loss of activity. In this section, we describe the synthesis and characterization of new classes of hydroxyapatite-bound transition-metal catalysts and their prominent catalytic performances in various types of organic transformations.

1.1　Aerobic Oxidations.　1.1.1　Oxidation of Alcohols Catalyzed by RuHAP: The selective oxidation of alcohols is widely recognized as one of the most fundamental transformations in both laboratory and industrial synthetic chemistry because the corresponding carbonyl compounds serve as im-
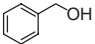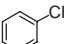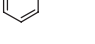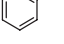
portant and versatile intermediates for the synthesis of fine chemicals.[5–7] Many oxidizing reagents such as hypochlorite, chromium(VI) oxide, permanganate, ruthenium(VIII) oxide, and dichromate have been employed to accomplish this transformation, but these stoichiometric reagents often result in the production of a vast amount of environmental wastes.[8–10] Economical and environmental concerns have resulted in a considerable demand for highly efficient heterogeneous catalytic protocols in combination with a clean, safe, and inexpensive oxidant of molecular oxygen.[11,12]
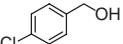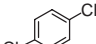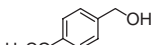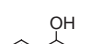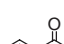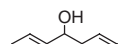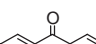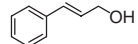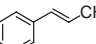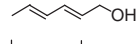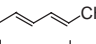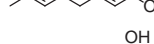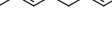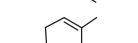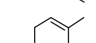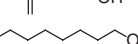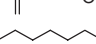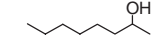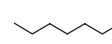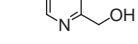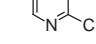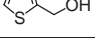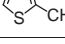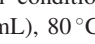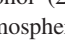
A stoichiometric hydroxyapatite (HAP), $Ca_5(OH)(PO_4)_3$, was synthesized from $Ca(NO_3)_2 \cdot 4H_2O$ and $(NH_4)_2HPO_4$ by the precipitation method described in the literature.[13] The HAP was stirred in an aqueous solution of $RuCl_3 \cdot nH_2O$ at room temperature for 24 h. The obtained slurry was filtered, washed with deionized water, and dried overnight at 110 °C, yielding RuHAP as a dark brown powder.[4a] The X-ray diffraction (XRD) peak positions of the RuHAP were identical to those of the parent HAP. From the elemental analysis, the $(Ru + Ca)/P$ ratio of the RuHAP was estimated to be 1.67, which shows an equimolar substitution of Ru^{3+} for Ca^{2+}. Due to its smaller ionic radius compared to Ca^{2+} ($r = 1.14$ Å), it is thought that the Ru^{3+} cations (0.82 Å) are accommodated into the Ca_I site surrounded by the $PO_4{}^{3-}$ tetrahedra. The presence of chlorine was confirmed by X-ray photoelectron spectroscopy (XPS) and energy-dispersive X-ray (EDX) spectroscopy; the atomic ratio of Ru to Cl was 1:1. The Ru K-edge X-ray absorption near-edge structure (XANES) spectrum of the RuHAP resembles that of $RuCl_3$. In the Fourier transform (FT) of k^3-weighted extended X-ray absorption fine structure (EXAFS) data of the RuHAP, the lack of peaks at around 3.5 Å shows that the RuHAP contains no Ru–Ru bond. The inverse FT of the main peaks was well fitted by use of the Ru–O ($R = 1.97$ Å, $CN = 4.1$) and Ru–Cl ($R = 2.32$ Å, $CN = 1.2$) shells. This proves that the Ru species on the surface of the RuHAP exists as a monomeric phosphatoruthenium complex surrounded by oxygen and chlorine atoms. A proposed surface structure of the RuHAP is represented in Chart 1. The present simple preparation method using the cation-exchange ability of HAP allows a strong protocol to create a monomeric metal species on a solid surface as a hybrid heterogeneous catalyst.

Oxidation of various alcohols using the RuHAP catalyst at 80 °C under an atmospheric O_2 pressure proceeded efficiently to give the corresponding carbonyl compounds, as summarized in Table 1.

Benzylic and allylic alcohols showed particularly high reactivity for this oxidation (Entries 1–11). It is important to note that a primary aliphatic alcohol, 1-octanol, was smoothly converted into 1-octanal without formation of the corresponding carboxylic acid or ester (Entry 12). Moreover, the catalyst was applicable to the oxidation of heterocyclic alcohols containing nitrogen and sulfur atoms. The corresponding aldehydes of 2-pyridinemethanol and 2-thiophenemethanol were achieved in high yields (Entries 14 and 15). Even when air was used in place of pure O_2, the oxidation of 1-phenylethanol proceeded smoothly; a quantitative yield of benzaldehyde was obtained (Entry 2). It was also found that the RuHAP acted as an efficient heterogeneous catalyst for the oxidation of amines and silanes using molecular oxygen, affording the correspond-

K. Kaneda et al.

Bull. Chem. Soc. Jpn. Vol. 79, No. 7 (2006)   983

Table 1. Oxidation of Various Alcohols Catalyzed by RuHAP with Molecular Oxygen[a]

Entry	Substrate	Product	Time /h	Convn. /%	Yield /%
1	[benzyl alcohol]	[benzaldehyde]	3	100	>99
2[b]			3	100	95
3	[4-chlorobenzyl alcohol]	[4-chlorobenzaldehyde]	3	100	>99
4	[4-methoxybenzyl alcohol]	[4-methoxybenzaldehyde]	3	100	92
5	[1-phenylethanol]	[acetophenone]	2	100	98
6	[diphenylmethanol]	[benzophenone]	2	100	>99
7	[cinnamyl alcohol]	[cinnamaldehyde]	1	100	99
8	[2,4-hexadien-1-ol]	[2,4-hexadienal]	4	99	99
9	[unsaturated alcohol]	[unsaturated aldehyde]	3	90	85
10	[unsaturated alcohol]	[unsaturated ketone]	5	93	91
11	[terpene alcohol]	[terpene ketone]	6	83	80
12[c]	[primary alcohol]	[aldehyde]	16	95	94
13	[secondary alcohol]	[ketone]	6	96	96
14	[2-pyridinemethanol]	[pyridine-2-carbaldehyde]	10	100	>99
15	[2-thiophenemethanol]	[thiophene-2-carbaldehyde]	2	100	94

a) Reaction conditions: Alcohol (2 mmol), RuHAP (0.2 g), toluene (5 mL), 80 °C, O_2 atmosphere. b) Under 1 atm of air instead of pure O_2. c) The reaction temperature was 60 °C.

ing nitriles and silanols in high yields (Eqs. 1 and 2).[4b,c]

$$\underset{R_1}{\overset{H}{\underset{H}{\diagdown}}}NH_2 + O_2 \xrightarrow[\text{toluene, 110°C}]{\text{RuHAP}} R_1-C\equiv N + 2H_2O \quad (1)$$

R_1=alkyl, aryl

$$\underset{R_3}{\overset{R_1}{R_2-Si-H}} \xrightarrow[\substack{O_2, H_2O, \\ \text{ethylacetate, 80°C}}]{\text{RuHAP}} \underset{R_3}{\overset{R_1}{R_2-Si-OH}} \quad (2)$$
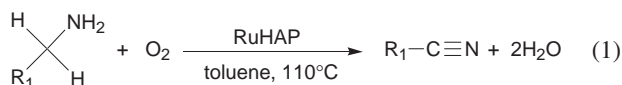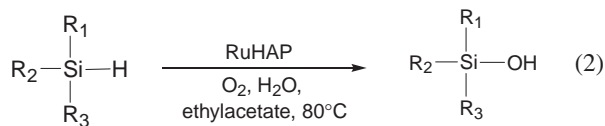
R_1, R_2, R_3=alkyl, alkenyl, alkynyl, aryl

Furthermore, the RuHAP catalyst could be reused without any loss of its high catalytic activity and selectivity; the yield of benzaldehyde in the oxidation of benzyl alcohol was kept over 93% during three recycling experiments. The Ru content of the spent RuHAP catalyst did not change compared to the fresh catalyst, and no Ru leaching was observed in the filtrate during the above recycling using the ICP method.

In the present RuHAP catalytic system, competitive oxida-
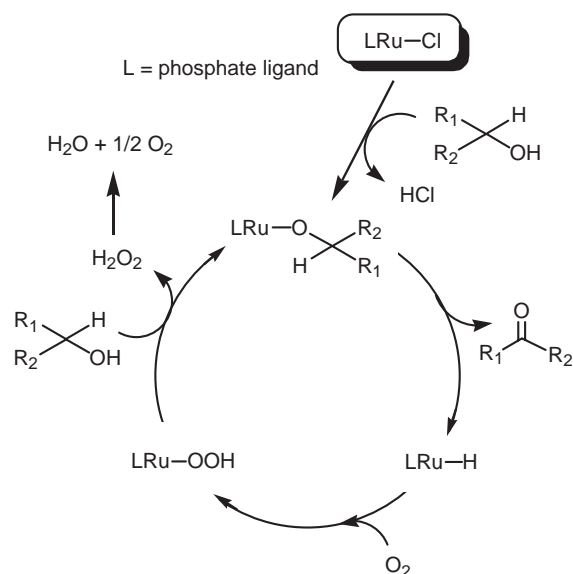
Scheme 1. A proposed mechanism for the oxidation of alcohols using RuHAP catalyst.

tion in an equimolar mixture of p-substituted benzyl alcohols gave a Hammett ρ value of -0.429, which is much smaller than the -1.9 given with oxoruthenium compounds, e.g., cis-[$(N_4)Ru^{VI}O_2$]$^{2+}$,[14] but is close to the -0.431 afforded with a stoichiometric reagent of a monomeric [$RuCl_2(PPh_3)_3$] complex. These results suggest that the present RuHAP catalyst does not contain oxoruthenium species as the active oxidant. When an equimolar mixture of 1-octanol and 4-octanol was used as the substrate, 95% of 1-octanal was selectively obtained together with 5% of 4-octanone. In the intramolecular competitive oxidation of 1,7-octanediol, the RuHAP catalyst gave 7-hydroxyoctanal chemoselectively in 81% yield. The above high chemoselectivity for primary hydroxy functions is not similar to that of bulk Ru catalysts. It is, however, similar to that of a monomeric [$RuCl_2(PPh_3)_3$] complex,[15] suggesting that the present RuHAP-catalyzed alcohol oxidation involves an alcolatoruthenium intermediate, which is dominated by the formation of a monomeric Ru species on the RuHAP surface.

In consideration of the reaction mechanism for monomeric Ru complexes, we propose a possible catalytic cycle using the RuHAP, as illustrated in Scheme 1. The oxidation is initiated by a ligand-exchange between an alcohol and a Cl species from the RuHAP to give a alcolatoruthenium species, which undergoes β-hydride elimination to produce the corresponding carbonyl compound and a hydrideruthenium species. Reaction of the hydride species with O_2 affords a hydrogenperoruthenium species, followed by ligand-exchange to regenerate the alcolatoruthenium species concomitant with the formation of O_2 and H_2O. In the case of [$RuCl_2(PPh_3)_3$], the catalytic cycle was not completed without hydroquinone[15a] or 2,2′,6,6′-tetramethylpiperidine N-oxyl (TEMPO).[15c,e] It is notable that our RuHAP catalyst does not require additives for catalytic aerobic oxidation. Furthermore, the above mechanism can be well evidenced by the following experiments using benzyl alcohol: (i) Addition of a radical trap, 2,6-di-$tert$-butyl-p-cresol, to the reaction medium hardly influenced the oxidation. (ii) One mole

of H_2O was produced for every mole of benzaldehyde formed. (iii) In monitoring the O_2 uptake, the ratio of O_2 consumed to benzaldehyde was ca. 1:2. (iv) Under a N_2 atmosphere, benzaldehyde was obtained only in a stoichiometric amount relative to the Ru element on the RuHAP catalyst. The β-elimination is the rate-determining step of the overall oxidation process because k_H/k_D values of 7.0 and 4.7 were observed in the competitive oxidation of benzyl alcohol with benzyl-d_7 alcohol ($C_6D_5CD_2OH$) and in the intramolecular oxidation of *p*-methyl-α-deuterobenzyl alcohol, respectively.

1.1.2 Alcohol Oxidations in the Presence of PdHAP-0 Catalyst: Since the first successful example of palladium-catalyzed aerobic oxidation of alcohols in 1977 by Blackburn and Schwartz,[16] subsequent efforts have extended the substrate scope and efficiency of palladium catalysts. Although some progress has been achieved by homogeneous Pd catalysts,[17] only a few heterogeneous Pd ones have become available to date, e.g. Pd on activated carbon,[18] Pd on pumice,[19] Pd-hydrotalcite,[20] Pd clusters on TiO_2,[21c,e] and polymer-supported Pd.[22] Unfortunately, these heterogeneous Pd systems suffer from low catalytic activities and a limited substrate scope.

Treatment of the stoichiometric HAP with $[PdCl_2(PhCN)_2]$ in acetone solution gives a new type of palladium-grafted HAP (PdHAP-0) as a yellow powder.[4h] XPS and EDX showed that the atomic ratio of Pd to Cl was 1:2. ICP analysis revealed that no Ca^{2+} was present in the filtrate after palladium loading. This shows that isomorphic substitution of Pd^{2+} for Ca^{2+} did not occur in organic media, which is in sharp contrast to the RuHAP catalyst prepared by the cation-exchange method in water. The Pd K-edge XANES spectrum for PdHAP-0 confirmed that all Pd species were in the divalent state. The absence of peaks at around 2.5 Å in the FT of k^3-weighted EXAFS data is evidence for a monomeric Pd species (Fig. 2A).
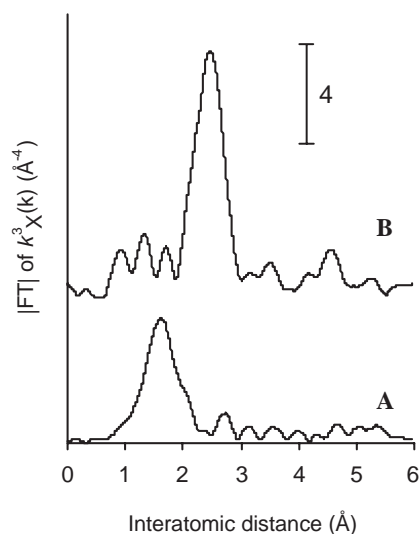
The inverse FT of the peaks at around 1–2 Å for the PdHAP-0 was well fitted using Pd–Cl and Pd–O shells (Table 2A). It was conclusively established that a monomeric $PdCl_2$ species was grafted onto the HAP surface by chemisorption, as illustrated in Chart 1.

The time course for the oxidation of 1-phenylethanol was monitored periodically, as shown in Fig. 3. The PdHAP-0 had an induction period of about 10 min, in which a concomitant color change of the catalyst from yellow to light gray was observed and no noticeable O_2 absorption was detected. During the induction period, the monomeric Pd^{2+} species were converted into Pd nanoparticles, as described below. After the induction period, consumption of molecular oxygen began, and finally the molar ratio of O_2 uptake to acetophenone yield was ca. 1:2. Taken together these data suggest that the reaction medium transforms the putative catalyst into the real one, due to significant chemical changes in the surface Pd species.

The Pd K-edge XANES spectrum of the recovered PdHAP-0 was similar to that of the Pd foil (Fig. 2B). The FT of k^3-weighted EXAFS exhibited a single peak at approximately

Table 2. Curve-Fitting Analysis for PdHAP-0 Catalysts[a]

Sample	Shell	C.N.[b]	R/Å[c]	$\Delta\sigma$/Å^2 [d]
PdHAP-0 (A)	Pd–Cl	2.0	2.36	0.0087
	Pd–O(1)	2.1	2.01	0.0006
	Pd–O(2)	3.0	2.37	0.0199
Recovered PdHAP-0 (B)	Pd–Pd	10.0	2.76	0.0018

a) Inverse Fourier transformations were performed for the regions of 0.9–2.2 Å in Fig. 2A and 1.95–3.0 Å in Fig. 2B. b) Coordination number. c) Interatomic distance. d) Difference between Debye–Waller factor of PdHAP and that of the reference sample.

Fig. 2. Fourier-transforms of k^3-weighted Pd K-edge EXAFS experimental data for (A) PdHAP-0, (B) recovered PdHAP-0 for the oxidation of 1-phenylethanol. Phase shift was not corrected. Reactions were conducted with 1-phenylethanol (1 mmol), PdHAP-0 (0.1 g, Pd: 2 μmol), and trifluorotoluene (5 mL) at 90 °C for 1 h under an O_2 atmosphere.

Fig. 3. Time profile for the oxidation of 1-phenylethanol catalyzed by PdHAP-0. Reaction conditions: PdHAP (0.1 g, Pd: 2 μmol), 1-phenylethanol (1 mmol), trifluorotoluene (5 mL), 90 °C, O_2 atmosphere.

K. Kaneda et al.

Bull. Chem. Soc. Jpn. Vol. 79, No. 7 (2006)   985

Fig. 4. (A) Size distribution diagram and (B) HR-TEM image of an 8-shell Pd nanocluster, for the recovered PdHAP-0 catalyst after oxidation of 1-phenylethanol.

2.5 Å due to the contiguous Pd–Pd bond in the metallic form with R and CN values of 2.76 Å and 10, respectively, as listed in Table 2B. These results are in good agreement with those of the TEM analysis of the Pd nanoclusters with a mean diameter (d) of ca. 38 Å and a narrow size distribution (standard deviation: $\sigma = 5.7$ Å) that formed on the PdHAP-0 (Chart 1 and Fig. 4A). From high-resolution TEM analysis, the regular arrangement of Pd atoms on the Pd nanocluster surface can be clearly observed with 17 Pd atoms along the {111} planes (Fig. 4B). Hence, the present nanoclusters have an fcc cuboctahedral shape with an eight-shell structure composed of ca. 2060 Pd atoms as the magic number.[21] These results suggest that the catalytically active species is not the original monomeric Pd^{2+} species, but the Pd nanoparticles generated in situ on the hydroxyapatite surface during the oxidation of alcohol.

The PdHAP-0 proved to be an effective heterogeneous catalyst for the aerobic oxidation of a wide variety of alcohols such as benzylic, allylic, aliphatic, and heterocyclic alcohols, giving the corresponding ketones and aldehydes in excellent yields. In order to highlight the applicability of the present protocol, a 250 mmol-scale reaction of 1-phenylethanol was undertaken using 4×10^{-4} mol % of the Pd catalyst without organic solvents: The oxidation proceeded smoothly and the turnover number (TON) of acetophenone based on Pd approached 236000 with an excellent TOF of approximately 9800 h^{-1} (Eq. 3).
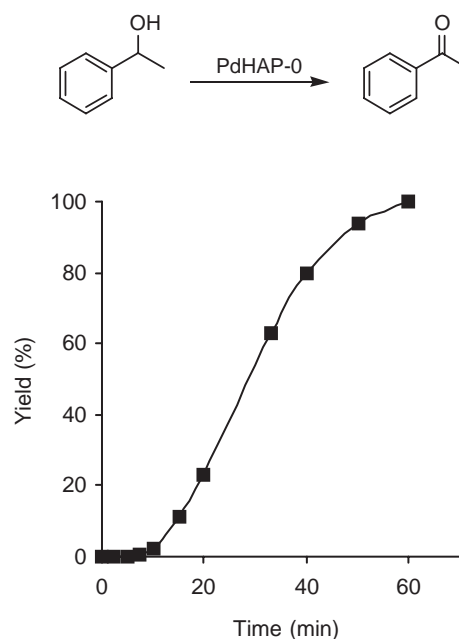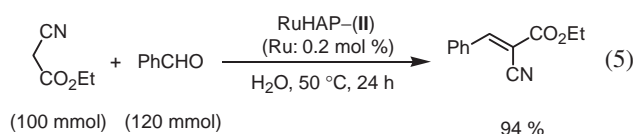
$$\text{Ph}\overset{\text{OH}}{\underset{}{|}} + 1/2\ O_2 \xrightarrow[\substack{160\ ^\circ C,\ 24\ h}]{\substack{\text{PdHAP-0} \\ (\text{Pd: }4 \times 10^{-4}\ \text{mol\%})}} \text{Ph}\overset{\text{O}}{\underset{}{||}} + H_2O \quad (3)$$

(250 mmol)

TON = 236000
TOF = 9800 h^{-1}

These TON and TOF values achieved by PdHAP-0 are significantly higher than those reported for other active catalyst systems, such as {K$_2$[OsO$_2$(OH)$_4$]} (TON and TOF, 16600 and 700 h^{-1}),[23] Ru/Al$_2$O$_3$ (950 and 300 h^{-1}),[24] [RuCl$_2$(PPh$_3$)$_3$]/ TEMPO (466 and 104 h^{-1}),[15e] Ru/quinone/[Co–(salene)] (194 and 97 h^{-1}),[25] [Pd(IiPr)(OAc)$_2$(H$_2$O)]/HOAc/MS3 Å (1000 and 50 h^{-1}),[17g] Pd(OAc)$_2$/PhenS*/NaOAc (400 and 10 h^{-1}).[17c] The oxidation also could be performed even under biphasic water–alcohol conditions owing to the high hydrophilic character of the hydroxyapatite. For example, 1-phenylethanol in water using 0.04 mol % of the PdHAP-0 catalyst afforded acetophenone in a 94% yield for 24 h; the corresponding TON and TOF were 2350 and 98 h^{-1}, respectively. Most

reported catalyst systems require additional bases, electron/proton-transfer mediators, and high O$_2$ pressure. Our PdHAP-0 catalyst does not need any additives or co-catalysts to facilitate its efficient catalytic cycle under an atmospheric O$_2$ pressure. The present Pd catalytic system therefore provides an opportunity for simple and practical organic synthesis, meeting the increasing demands for environmentally friendly chemical processes.

1.2 Carbon–Carbon Bond-Forming Reactions Using Cationic RuHAP Catalysts.   1.2.1 Aldol and Diels–Alder Reactions Using Cationic RuHAP Catalysts: Lewis-acid catalysts have attracted considerable interest in organic synthesis because of their unique properties across a diverse array of carbon–carbon bond-forming reactions.[26] The most conventional Lewis acids are the halides of B(III), Al(III), Ti(IV), and Sn(IV).[27] However, these acids generally require stoichiometric amounts in order to achieve maximum acceleration and must be employed under strictly anhydrous conditions. In a quest for improving the reaction, the development of new types of heterogeneous Lewis-acid catalysts is particularly important.

We have synthesized a new type of hydroxyapatite-bound cationic Ru complex with potentially vacant coordination sites by simple modulation of the neutral RuHAP.[4g] Treatment of the RuHAP, at room temperature under an Ar atmosphere, with an aqueous solution of AgX (1.1 equiv of Ru), gives the cationic RuHAP-(**I**) and -(**II**) (**I**: X = SbF$_6$$^-$, **II**: TfO$^-$, respectively). The absence of chlorine was confirmed by XPS analysis of the cationic RuHAPs. The Ru K-edge XANES spectra were quite similar to that of the parent RuHAP, showing that the Ru species exists in the +3 oxidation state. The absence of a 3.5 Å peak in the FT of the k^3-weighted Ru K-edge EXAFS showed that the Ru species remained in the monomeric form. The inverse FTs of the cationic RuHAPs were well fitted by replacing the Ru–Cl bond in the RuHAP with a Ru–O bond (R = 2.1 Å, CN = 1.0), which was assigned to a weakly coordinated aqua ligand. Consequently, a well-defined cationic phosphatoruthenium complex may be created on the hydroxyapatite surface, as illustrated in Chart 1.

The use of the cationic RuHAP-(**I**) as a heterogeneous Lewis-acid catalyst successfully accelerated several Diels–Alder reactions in nitromethane at room temperature. The reaction between cyclopentadiene and methyl vinyl ketone proceeded smoothly to afford 5-acetyl-2-norbornene in 92% yield with a favorable *endo*:*exo* selectivity (Eq. 4).

$$\xrightarrow[\text{CH}_3\text{NO}_2,\ \text{r.t.,}\ 4\ h]{\text{RuHAP-(\textbf{I})}} \quad (4)$$

92 %
(endo/exo=90/10)

In marked contrast to the homogeneous [Ru^{III}(salen)(NO)-H$_2$O]$^+$SbF$_6$$^-$ complex, the RuHAP-(**I**) was applicable to a less reactive dienophile of methyl acrylate.[28] It is generally known that product inhibition is a crucial drawback in traditional Al-, Ti-, or B-based Lewis-acid catalysis. When the above reaction of cyclopentadiene with methyl vinyl ketone went to completion, two substrates were added and the new mixture was
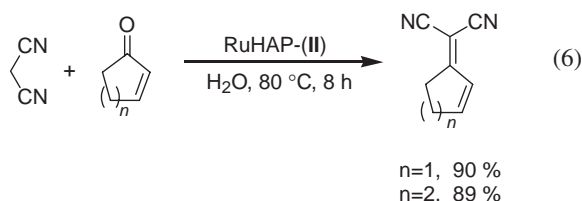
allowed to react further. The subsequent three reactions afforded the corresponding cycloadduct in yields of over 92% at essentially the same rates, showing that the present catalyst could maintain its inherent activity during successive reactions.

The development of water-tolerant Lewis-acid catalysts is particularly attractive from the viewpoint of practical and environmental concerns.[29] The cationic RuHAP-(**II**) has proved to be a useful catalyst for the aldol reaction of nitriles with carbonyl compounds in water, affording the corresponding α,β-unsaturated nitriles in excellent yields. For example, a 100 mmol-scale reaction of ethyl cyanoacetate with benzaldehyde using 0.2 mol % of the Ru catalyst provided a 94% yield of (*E*)-ethyl 2-cyano-3-phenyl-2-propenoate within 24 h (Eq. 5).

$$
\begin{array}{c}
\text{CN} \\
| \\
\text{CO}_2\text{Et}
\end{array}
+ \text{PhCHO}
\xrightarrow[\text{H}_2\text{O, 50 °C, 24 h}]{\begin{array}{c}\text{RuHAP–(\textbf{II})}\\(\text{Ru: 0.2 mol \%})\end{array}}
\text{Ph}\diagup\diagdown\begin{array}{c}\text{CO}_2\text{Et}\\\text{CN}\end{array}
\qquad (5)
$$

(100 mmol)   (120 mmol)   94 %

The present catalyst exhibited a specific activity only toward nitriles as aldol donors. Other active methylene compounds such as 2,4-pentanedione, dimethyl malonate, and nitroethane, whose pK_a values are similar to that of ethyl cyanoacetate, did not yield aldol products under the above conditions. It is notable that treatment of α,β-unsaturated carbonyl compounds with malononitrile gave the products via 1,2-addition in high yields (Eq. 6); attack of an enolate species on the carbonyl function occurred exclusively without the 1,4-addition.

$$
\begin{array}{c}\text{CN}\\\text{CN}\end{array}
+ \underset{(\ )_n}{\overset{\text{O}}{\bigcirc}}
\xrightarrow[\text{H}_2\text{O, 80 °C, 8 h}]{\text{RuHAP-(\textbf{II})}}
\underset{(\ )_n}{\overset{\text{NC}\diagdown\diagup\text{CN}}{\bigcirc}}
\qquad (6)
$$

n=1, 90 %
n=2, 89 %

This phenomenon was quite distinct from that of the [Ru^{II}-(H)$_2$(PPh$_3$)$_4$]-catalyzed reaction, whose products were predominantly a result of the 1,4-addition.[30] In terms of the HSAB principle, a trivalent Ru enolate species generated from the RuHAP may behave as a harder nucleophile than that from the divalent Ru one, which allows a favorable interaction with the carbonyl groups to enhance the 1,2-addition.

For the aldol reaction of methyl isocyanoacetate with benzaldehyde, the cationic RuHAP-(**II**) gave the corresponding oxazoline in 90% yield without any additives (Eq. 7), whereas the [Ru(salen)(NO)H$_2$O]$^+$SbF$_6^-$ complex required a Hunig's base (*i*-Pr$_2$NEt) to complete the catalytic cycle.

$$
\begin{array}{c}\text{NC}\\\text{CO}_2\text{Me}\end{array}
+ \text{PhCHO}
\xrightarrow[\text{CH}_2\text{Cl}_2, \text{r.t, 20 h}]{\text{RuHAP-(\textbf{II})}}
\underset{\text{O}\diagdown\text{N}}{\overset{\text{Ph}\diagdown\diagup\text{CO}_2\text{Me}}{\bigcirc}}
\qquad (7)
$$

90 %
(*trans:cis*=9:1)
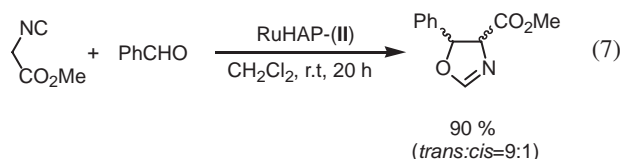
Upon treatment with ethyl cyanoacetate, the IR spectrum of the cationic RuHAP-(**II**) showed a shift of the ν(CN) band toward 2093 cm^{-1} in comparison with the free cyano group at 2260 cm^{-1}, along with a new peak at 870 cm^{-1} assigned to the P–OH group of a HPO$_4^{2-}$ ion on the hydroxyapatite surface.[3] The FT-EXAFS analysis of the above treated sample
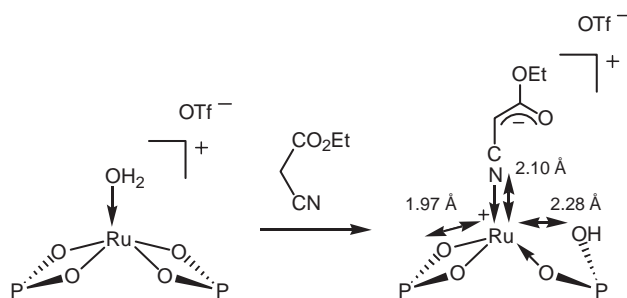

Fig. 5.   Generation of the enolatoruthenium intermediate.

showed a decrease in the coordination number of the nearest neighboring Ru–O bond from 4 to 3, and the appearance of an additional second Ru–O bond attributable to a weak interaction between Ru and P–OH. These results are in agreement with the formation of an enolatoruthenium species surrounded by three oxygen atoms, as shown in Fig. 5. It is thus reasonable to suggest that the cationic RuHAP-(**II**)-catalyzed aldol-type reaction using nitriles involves the enolatoruthenium intermediate, which is generated through cooperative catalysis between the cationic Ru species and the basic phosphate ligand; the former activates the nitrile as a Lewis acid, while the latter phosphate abstracts an acidic α-proton of the nitrile to generate the enolate species. The Diels–Alder reaction can be induced by the Lewis-acid site that originates from the cationic Ru species.

1.2.2   Mizoroki–Heck and Suzuki–Miyaura Reactions Catalyzed by PdHAP-1:   Palladium-mediated cross-coupling reactions between aryl halides and nucleophiles, such as the Mizoroki–Heck and Suzuki–Miyaura coupling reactions, have received considerable attention due to their enormous synthetic potentials to form new carbon–carbon bonds.[31] New classes of Pd^{II} complexes having Pd–carbon σ bonds, e.g., palladacycle complexes,[32] PCP pincer-type complexes,[33] and *N*-heterocyclic carbenes (NHCs),[34] have led to significant breakthroughs in this area. From practical and economical considerations, however, the demand for phosphine-free heterogeneous systems is still extremely high in order to circumvent drawbacks imposed by homogeneous complexes.

The chemical composition of HAP can be modified from the stoichiometric form, Ca$_{10}$(PO$_4$)$_6$(OH)$_2$ (Ca/P = 1.67), to the nonstoichiometric Ca-deficient form, Ca$_{10-Z}$(HPO$_4$)$_Z$-(PO$_4$)$_{6-Z}$(OH)$_{2-Z}$ (0 < Z ≤ 1, 1.5 ≤ Ca/P < 1.67). The crystallographic structures of Ca-deficient HAPs are identical to that of the stoichiometric one. The charge deficiency, due to the lack of Ca^{2+} in the lattice, is compensated by the introduction of H$^+$ into the PO$_4^{3-}$ ion and removal of OH$^-$ in the parent unit cell. Treatment of the nonstoichiometric Ca-deficient HAP Ca$_9$(HPO$_4$)(PO$_4$)$_5$(OH) (HAP-1; Z = 1, Ca/P = 1.50) with an acetone solution of [PdCl$_2$(PhCN)$_2$] yielded the PdHAP-1 as a white powder. Analysis by means of XRD, XPS, EDAX, IR, and Pd K-edge XAFS proved that a monomeric phosphatopalladium(II) complex surrounded by four oxygen atoms in square planar coordination, which is formed at the Ca-deficient site of the HAP-1 with the loss of 2 equivalents of PhCN and HCl, as shown in Chart 1. The proposed surface structure of the PdHAP-1 is in sharp contrast to that of the PdHAP-0 prepared by the same method using stoichiometric HAP.

We found that the PdHAP-1 was an outstanding catalyst for the Mizoroki–Heck reaction. In the case of bromobenzene with styrene using 2×10^{-3} mol % Pd, the reaction was completed within 24 h, in which the TON based on Pd approached up to 47000 (Eq. 8). Electronic variation of the *p*-substituted aryl bromides did not significantly affect the reaction rates. It has also been found that the PdHAP-1 acts as an outstanding catalyst for the Suzuki–Miyaura coupling reaction: The TON reached 45500 after 6 h for the reaction of deactivated 4-bromoanisole with phenylboronic acid (Eq. 9). Notably, the recovered PdHAP-1 had an original monomeric Pd^{2+} structure and was recyclable with retention of its catalytic activity.

$$\text{(8)}$$

R	TON
H	47000
OMe	45000
C(O)CH$_3$	48000

$$\text{(9)}$$

R	TON
H	45500
OMe	47000
C(O)CH$_3$	49000
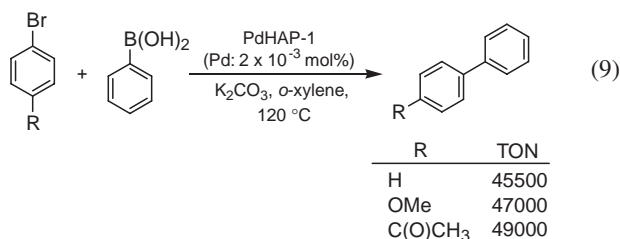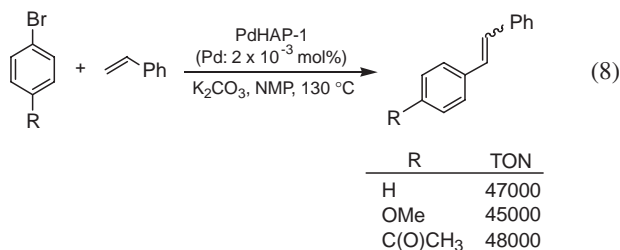
In the present PdHAP-1 catalytic system, the competitive Mizoroki–Heck reactions in an equimolar mixture of *p*-substituted iodobenzenes using styrene gave a Hammett ρ value of 1.1, which differs from the value of 2.0 obtained with [Pd(PPh$_3$)$_4$].[35] In a competitive reaction between styrene and *n*-butylacrylate with iodobenzene, the PdHAP-1 gave a relatively high product ratio of 9.6 between *n*-butylcinnamate and stilbene. This value significantly exceeds the 4.1 value observed for [Pd(PPh$_3$)$_4$]. The above phenomena associated with extremely high activity toward deactivated aryl bromides suggests that the rate-determining step in the Mizoroki–Heck reaction catalyzed by the PdHAP-1 is not oxidative addition, but rather insertion of the olefin into the arylpalladium intermediate. This finding is also supported by kinetic studies of the reaction between bromobenzene and styrene, in which the reaction rate is zero order for bromobenzene and first order for styrene. These performances of PdHAP-1 are attributed to the extremely robust monomeric Pd^{2+} structure surrounded by phosphate ligands on the hydroxyapatite surface, which effectively serves as a powerful alternative to organic ligands.

The utilization of readily available and inexpensive aryl chlorides in palladium-catalyzed cross-coupling reactions is a challenging task for industrial applications.[36] It was also shown that the PdHAP-1 was able to catalyze the Suzuki–Miyaura coupling of activated aryl chlorides in the presence of TBAB (Bu$_4$N$^+$Br$^-$: 10 mol %) and a small amount of water (volumetric ratio: DMF/H$_2$O = 50/1) (Eq. 10). In all cases, the selectivity was almost 100%, with no formation of the homo-coupled product. A TEM image of the isolated PdHAP-1 catalyst

after the Suzuki–Miyaura coupling reaction of *p*-chloroacetophenone with phenylboronic acid showed the presence of Pd^0 nanoparticles with a mean diameter of ca. 50 Å. It can be concluded that the catalytically active species was a Pd nanocluster generated in situ on the surface of the hydroxyapatite under such conditions.

$$\text{(10)}$$

R	Yield (%)
C(O)CH$_3$	92
NO$_2$	>99
CN	>99
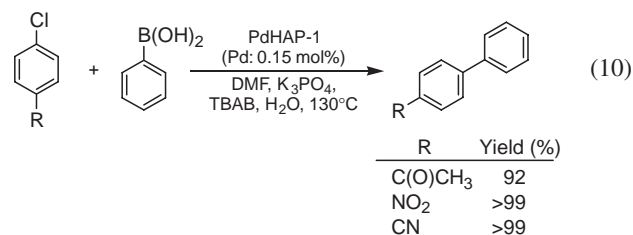
1.3 Waste Elimination and Utilization of Waste. The ultimate principal of Green Chemistry is the elimination of waste at the source, i.e., primary pollution prevention. Needless to say, harmful waste removal (end-of-pipe solutions) and the utilization of waste as a raw material for conversion into industrially beneficial organic compounds are also necessary and make invaluable contributions to preserving our quality of life.

1.3.1 Dehalogenation of Haloarenes Catalyzed by PdHAP-0 in the Presence of Molecular Hydrogen: The dehalogenation of organic halides is a significant process in the removal of halogenated organic pollutants such as chlorophenols and polychlorinated biphenyls (PCBs).[37] Compared with oxidative methods,[38] reductive dehalogenation processes are advantageous in that no toxic by-products are formed. Various hydrogen donors such as metal alkoxide,[39] hydrosilanes,[40] Grignard reagents,[41] hydrazine hydrochloride,[42] and sodium formate[43] are generally available for this transformation. These reagents, however, are often harmful and toxic, and considerable amounts are required.

The PdHAP-0 catalyst smoothly reduced various haloarenes to the corresponding arenes using molecular hydrogen in methanol solvent, as summarized in Table 3.[4i] This catalytic activity was significantly higher than those of commercially available heterogeneous Pd catalysts. The use of typical homogeneous Pd complexes resulted in low yields, accompanied with the formation of Pd black. An intramolecular competitive dehalogenation of 4-bromochlorobenzene chemoselectively gave a 95% yield of chlorobenzene together with a 5% yield of benzene under the present conditions (Entry 2). The PdHAP-0 was also applicable to chlorinated substrates containing nitrogen atoms (Entries 10 and 11).

Notably, the quantitative conversion of chlorobenzene to benzene with excellent TON (10000) and TOF (1000 h^{-1}) could be achieved using low concentrations of the PdHAP-0 catalyst (1×10^{-2} mol %). These values are significantly higher than those previously reported for other catalytic systems, such as Ru(II) phosphine complex (TON = 40, TOF = 40 h^{-1}),[44] [{Rh(C$_5$Me$_5$)Cl$_2$}$_2$] catalyst (TON = 33, TOF = 16.5 h^{-1}),[45] poly(*N*-vinyl-2-pyrrolidone) anchored Pd catalyst (TON = 1000, TOF = 500 h^{-1}),[46] and Pd/carbon (TON = 130, TOF = 260 h^{-1}).[47] TEM analysis for the isolated PdHAP-0 during the dechlorination in methanol solvent confirmed the formation of Pd nanoclusters with a mean diameter of 3 nm. These are clear evidence that the monomeric PdCl$_2$ species grafted by chemisorption on the surface of the HAP
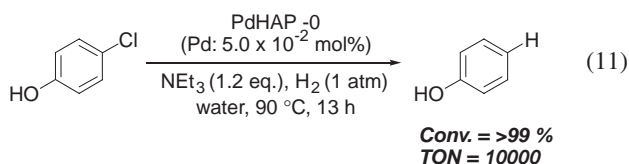
Table 3. Hydrodehalogenation of Various Organic Halides Using PdHAP-0 Catalyst[a]

Entry	Substrate	Time/h	Yield/%[b]
	R—⟨benzene⟩—Cl		
1	R = H	3	>99
2	Br	2	95[c]
3	CH$_3$	3	98
4[d]	C(O)CH$_3$	1	>99[e]
5	CN	2	80
6	NH$_2$	1	96
7	OH	3	>99
8	⟨benzyl⟩—Br	1	99
9	⟨benzyl⟩—CH$_2$Cl	2	>99
10	⟨pyridyl⟩—Cl	2	>99
11[f]	⟨6-chloroindole⟩	3	>99

a) Reaction conditions: Substrate (1 mmol), PdHAP-0 (0.2 mol % of Pd), MeOH (5 mL), 60 °C, H$_2$ atmosphere. b) Determined by GC and GC-MS using an internal standard technique. Values in parenthese are isolated yields. c) Chlorobenzene yield. d) KO^{t}Bu (1.2 mmol). e) Acetophenone yield. f) 0.6 mol % of Pd.

was readily transformed into Pd nanoclusters and effectively promoted the dehydrogenation.

Halogenated compounds are often detected in contaminated wastewater; therefore, achieving efficient dehalogenation in aqueous media is particularly important for practical applications. It is noteworthy that our PdHAP-0 has proved to be an efficient heterogeneous catalyst in water under an H$_2$ atmosphere. For example, the reduction of 4-chlorophenol, a precursor to dioxins, was achieved at a low concentration of the PdHAP-0: The corresponding TON and TOF were 10000 and 769 h^{-1}, respectively (Eq. 11). In contrast, previously reported catalyst systems in aqueous media required high hydrogen pressures and high catalyst concentrations in order to accomplish efficient dehalogenations.[48] The superior performances of the PdHAP-0 catalyst is thought to be due to the highly hydrophilic character of the hydroxyapatite, which helps to overcome problems related to diffusion limitations.

$$\text{HO—⟨C}_6\text{H}_4\text{⟩—Cl} \xrightarrow[\substack{\text{NEt}_3\text{ (1.2 eq.), H}_2\text{ (1 atm)} \\ \text{water, 90 °C, 13 h}}]{\substack{\text{PdHAP-0} \\ \text{(Pd: } 5.0 \times 10^{-2}\text{ mol\%)}}} \text{HO—⟨C}_6\text{H}_4\text{⟩—H} \quad (11)$$

Conv. = >99 %
TON = 10000

1.3.2 Chemical Fixation of Carbon Dioxide into Epoxide by ZnHAP Catalyst: In order to avoid the greenhouse effects, much effort has been devoted to reduce the amount of carbon dioxide (CO$_2$) exhausted from industry. The chemical fixation of CO$_2$ into synthetically beneficial compounds is of great interests because CO$_2$ can be considered as an inexpensive, nontoxic, and abundant C$_1$ feed stock.[49] One of the most powerful approaches is the coupling of CO$_2$ and epoxides

Table 4. Coupling of CO$_2$ and Epoxides Catalyzed by ZnHAP[a]

Entry	Epoxide	Zn/mol %	Yield/%[b]	TON[b]
1	Cl⟨epoxide⟩	0.003	90	30000
2[c]			86	28600
3[d]	Ph–O⟨epoxide⟩	0.003	95	31600
4[c],[d]			90	30000
5	HO⟨epoxide⟩	0.006	96	16000
6[c]			84	14000
7[e]	⟨—O⟨epoxide⟩	0.006	95	15800
8[f],[g]	Ph⟨epoxide⟩	0.012	89	7400
9[f]	⟨(CH$_2$)$_3$⟩⟨epoxide⟩	0.012	86	7100
10[f]	⟨(CH$_2$)$_5$⟩⟨epoxide⟩	0.012	81	6700

a) Reaction conditions: epoxide (100 mmol), DMAP (0.02 mmol), ZnHAP (0.01 g, Zn: 0.003 mmol), CO$_2$ (10 atm), 100 °C, 24 h. b) Determined by GC using an internal standard technique. c) CO$_2$ (1 atm). d) DMF (5 mL) was used as solvent because of the solid nature of substrate. e) Epoxide (50 mmol). f) Epoxide (25 mmol). g) 130 °C.
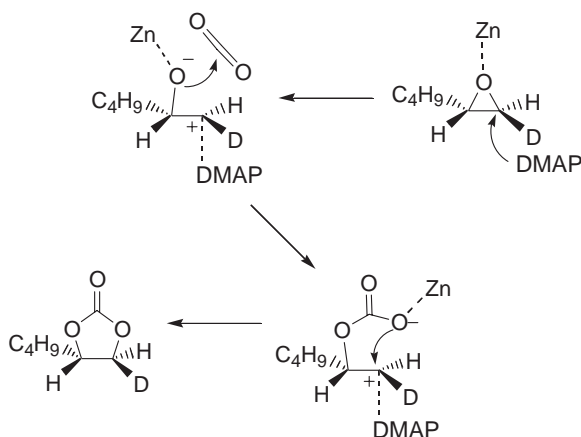
to provide five-membered cyclic carbonates with 100% atom efficiency, which are prominently utilized for the production of engineering plastics as well as for the synthesis of pharmaceuticals and fine chemicals.[50]

Using a cation-exchange approach, zinc-exchanged HAP (ZnHAP, Zn content: 0.3 mmol g^{-1}) was synthesized by treatment of stoichiometric HAP with an aqueous solution of Zn(NO$_3$)$_2$·6H$_2$O.[4k] The XPS spectra of the ZnHAP and ZnO showed identical binding energy values of 1021.5 and 1021.4 eV for Zn 2p$_{3/2}$, respectively. The edge position of the Zn K-edge XANES spectra of the ZnHAP was also comparable with that of ZnO. It is clear that the Zn species of the ZnHAP exist in a tetrahedral geometry with a +2 oxidation state. The lack of peaks assignable to the Zn–O–Zn bond in the Fourier transform of k^3-weighted Zn K-edge EXAFS, which was detected for ZnO at around 2.8 Å, showed that the Zn species is monomeric. The curve-fitting analysis for the inverse FT of the main peaks revealed the existence of a Zn–O bond having an interatomic distance and coordination number of 1.88 Å and 4.0, respectively. The above results demonstrate the creation of a monomeric phosphatozinc(II) complex surrounded by four oxygen atoms in tetrahedral coordination on the surface of the HAP, as illustrated in Chart 1.

As can be seen from Table 4, a variety of terminal epoxides possessing aromatic, aliphatic, and both electron-donating and -withdrawing substituents were successfully converted into the corresponding cyclic carbonates in excellent yields. For example, a 100 mmol-scale reaction of epichlorohydrin provided a 90% yield of 4-(chloromethyl)-1,3-dioxolan-2-one within 24 h in the presence of Lewis base co-catalysts of 4-(dimethylamino)pyridine (DMAP) (Entry 1). Both ZnHAP and Lewis base were indispensable components for attaining high carbonate yields.

It is noteworthy that the coupling reaction could be performed even under a CO$_2$ atmosphere, giving a remarkably

Scheme 2. Proposed reaction mechanism.

Fig. 6. Crystal structure of montmorillonites, $Na_{0.66}(OH)_4$-$Si_8(Al_{3.34}Mg_{0.66}Fe_{0.19})O_{20}$.

high TON of up to 28600 with a TOF of approximately $1100\,h^{-1}$ (Entry 2). These values for epichlorohydrin are considerably higher than those of analogous binary catalyst systems comprising a metal complex and a Lewis base under high CO_2 pressures, such as $[Cr^{III}(salen)]$ (50 psig, TON and TOF, 98 and $65\,h^{-1}$),[51] $[Zn^{II}(binaphthyldiaminosalen)]$ (500 psig, 100 and $6\,h^{-1}$),[52] and $[Co^{III}(porph)]$ (300 psig, 250 and $250\,h^{-1}$).[53] Furthermore, the ZnHAP-catalyzed coupling reactions proceeded exclusively with retention of the configuration of epoxides; the reactions of enantiomerically pure (R)- and (S)-benzyl glycidyl ethers with CO_2 yielded (R)- and (S)-4-(benzyloxymethyl)-1,3-dioxolan-2-one in 82 and 84% chemical yields with over 99% ee, respectively.

We propose a possible catalytic cycle of the ZnHAP in consideration of the reaction mechanism for the $[Zn^{II}(binaphthyldiaminosalen)]$ complex system.[53] The coupling reaction proceeds through effective cooperation between the ZnHAP and the Lewis base; the former activates the epoxide as a Lewis acid, while the latter attacks the less sterically hindered carbon atom to open the epoxide ring. The generated oxo anion species then reacts with CO_2 to give the corresponding cyclic carbonate, as shown in Scheme 2. Evidenced for this mechanism could be found in the reaction of trans-1-deuterio-1,2-hexene oxide with CO_2, in which the corresponding trans-1-deuterio-1,2-hexene carbonate was formed with 82% selectivity.

2. Montmorillonite

Montmorillonites are layered clay minerals, composed of alumina octahedral sheets sandwiched by two silica tetrahedral layers as shown in Fig. 6.[54] Some of the aluminum atoms in the center of the octahedral sheets are replaced by magnesium atoms, resulting in cation deficiency over the whole clay. To compensate for the cationic deficiency, some ion-exchangeable cations are present in the interlamellar spaces between two-dimensional sheets of montmorillonite. They can be used as inorganic supports for reagents, and efficient and versatile catalyst for various organic reactions. In montmorillonite clay, both Brønsted and Lewis-acidic catalytic sites are available, hence its natural occurrence as well as its ion-exchange properties allow it to act as a catalyst. Various types of metal cations can be introduced readily into the expansible interlayer spaces, thus making it possible to alter the acidic nature of the
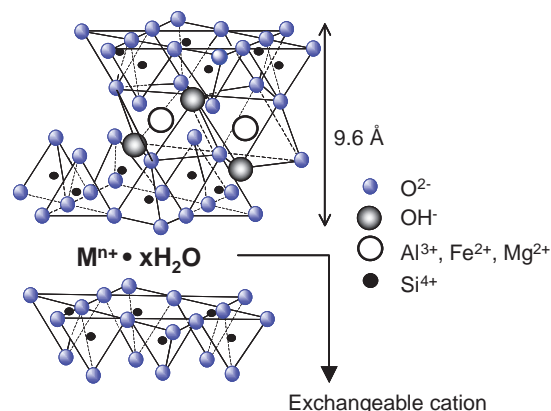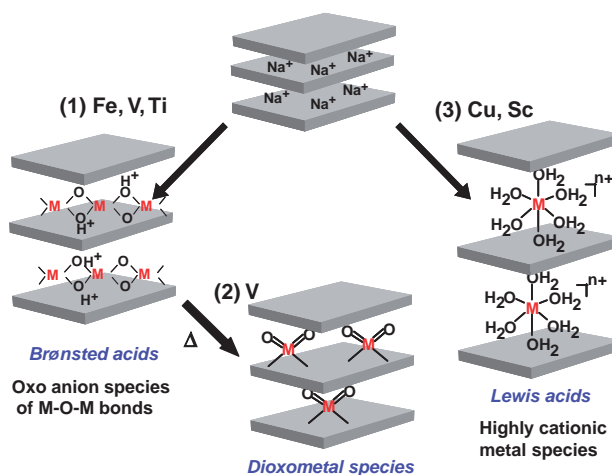
Chart 2. Heterogenization of metal complexes using montmorillonites.

material by simple ion-exchange procedure.[55,56] In the course of our studies on metal-cation-exchanged montmorillonite catalysts (M^{n+}-monts), we have defined three types of metal ion species with unique structures within the interlayers of the mont: a chain-like metal species for Fe and Ti (Chart 2(1)), a monomeric dioxo complex of V (Chart 2(2)), and a monomeric aqua complex for Cu and Sc (Chart 2(3)). These M^{n+}-monts exhibited excellent catalytic performance in various heterogeneous organic transformations,[57] which resulted in the advantage of eliminating waste production and simplifying the workup procedure. Furthermore, the mont catalysts are reusable without appreciable loss of their activities or selectivities. The application of catalytic systems based on monts as macroanions goes beyond mere immobilization and will lead to the development of high-performance heterogeneous Brønsted and Lewis-acid catalysts for "green" organic syntheses.

2.1 Preparation and Characterization of Montmorillonite-Enwrapped Metal Cations. Our approach in the design of M^{n+}-mont catalysts is exemplified in Chart 2. The strategy involves precise control of structures of the metal cation based on the layered-structure of montmorillonites. Chain-like metal species along the silicate sheets generate strong Brønsted-acid sites located on the oxo anion species of M–
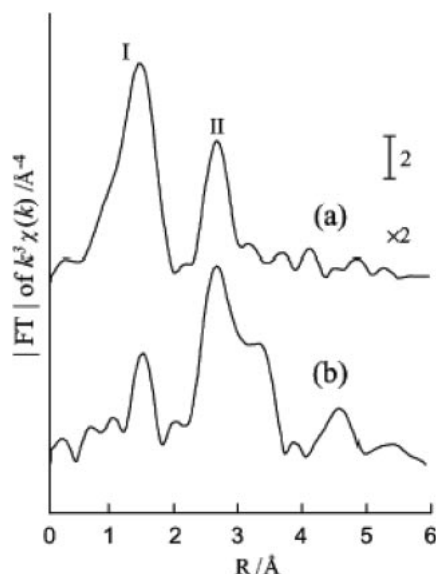
Fig. 7. Fourier transforms for k^3-weighted Fe K-edge EXAFS of (a) Fe^{3+}-mont and (b) Fe_2O_3. Phase shift was not corrected.

Table 5. Cueve-Fitting Analysis of the Fe^{3+}-Mont Catalyst

Shell	C.N.[a]	$R/Å$[b]	$\Delta\sigma/Å^2$ [c]
Fe–O(1)	2.0	1.90	−0.0029
Fe–O(2)	2.0	2.03	−0.0027
Fe–Fe	1.8	3.05	−0.0005

a) Coordination number. b) Interatomic distance. c) $\Delta\sigma$ is the difference between Debye–Waller factor of Fe^{3+}-mont and that of the reference material.
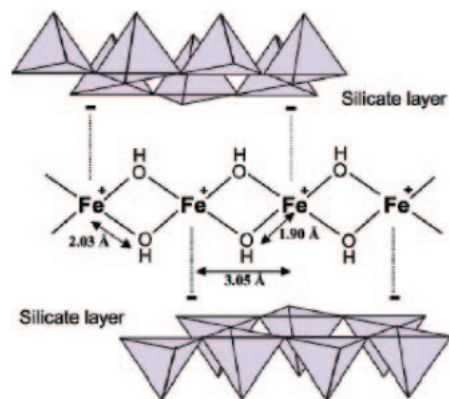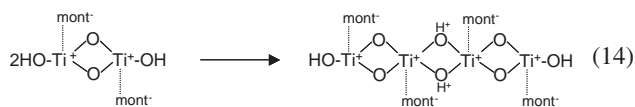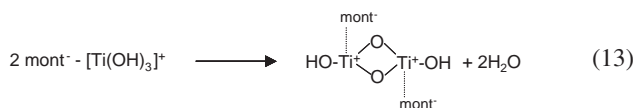

Fig. 8. Proposed schematic structure of Fe^{3+} species within the interlayer space of montmorillonite. Two Fe ions are linked by two hydroxy anions to form an $Fe_2(\mu\text{-OH})_2$ core structure. The cationic Fe species are bound with anionic silicate layers.

O–M bonds. The monomeric dioxometal structure is constructed by calcination of metal-cation-exchanged monts. In contrast, the Lewis-acidic monomeric aqua complex was created in the case of metal cations with high pK_h (K_h = hydrolysis constant) values.[58]

2.1.1 Fe^{3+}-Mont and Ti^{4+}-Mont: 2.1.1.1 Fe^{3+}-Mont; Fe^{3+}-exchanged montmorillonite (Fe^{3+}-mont) was prepared by the conventional ion-exchange of a parent Na^+-montmorillonite, $Na_{0.66}(OH)_4Si_{7.7}(Al_{3.34}Mg_{0.66}Fe_{0.19})O_{20}$, with aqueous solution of $Fe(NO_3)_3 \cdot 9H_2O$. The exchange degree of the Na cation in the Fe^{3+}-mont was 97.7%. Retention of the crystallinity was confirmed by its XRD pattern: Interlayer space was 2.2 Å which is smaller than that of the parent Na^+-mont (2.9 Å). XPS and Fe K-edge XANES spectra confirmed a trivalent Fe species in the Fe-mont. As depicted in Fig. 7, the Fourier-transform of Fe K-edge EXAFS for the Fe^{3+}-mont is not similar to those for the bulk α-Fe_2O_3, γ-Fe_2O_3, Fe_3O_4, and $Fe_2(SO_4)_3$, but is similar to that of α-iron(III) hydroxide oxide (α-FeOOH) with very small particle sizes. Curve-fitting analysis of peak I of the Fe^{3+}-mont showed that the cationic iron species were coordinated with two long Fe–O distances (2.03 Å) and two short Fe–O distances (1.90 Å), as summarized in Table 5. Each distance is slightly shorter than the values of 2.02 and 1.97 Å found in α-FeOOH, respectively, whereas it is longer than the value of 1.86 Å found in the FeAlPO-5 molecular sieve, $FePO_4$, and Fe^{3+}-containing ZSM-5, in which the Fe^{3+} ions are monomerically situated in a tetrahedral coordination.[59] Peak II at 2.7 Å is assignable to an Fe–Fe moiety in the Fe^{3+}-mont; the interatomic distance between the two irons and the coordination number are 3.05 Å and 2, respectively. The 3.05 Å Fe–Fe distance is associated with an Fe–Fe bond found in α-FeOOH, where each Fe cation is bound by hydroxy groups at the corner.

Therefore, in the present Fe species, it is most likely that two Fe ions are bound by oxygen anions to form an $Fe_2(\mu$-$OH)_2$ core structure. Based on the above results, a coordination structure around iron species in the Fe^{3+}-mont is proposed as in Fig. 8, in which two Fe cations are linked by hydroxide anions along the interlayer space as a chain-like shape. To our knowledge, this is the first example of the synthesis of Fe cation linkages containing an Fe–O–Fe unit in inorganic material by a simple ion-exchange method. Such a linkage structure might be generated by a successive reaction of two neighboring iron(III) hydroxides.

2.1.1.2 Ti^{4+}-Mont; Ti^{4+}-mont was obtained by treatment of aqueous solution of $TiCl_4$ and Na^+-mont.[57a] The Ti K-edge XANES of the Ti^{4+}-mont resembles the spectrum of the anatase TiO_2 and is different from that of an isolated Ti^{4+} species with a tetrahedral symmetry located in the framework of molecular sieves.[60] The coordination number (CN) and distance (R) for the Ti–O shell of the Ti^{4+} species in the montmorillonite are 4 and 1.94 Å, respectively, while both values for the Ti–Ti shell are 1.5 and 3.04 Å, respectively. These values are different from those of the bulk anatase TiO_2 ($CN_{Ti-O} = 6$, $R_{Ti-O} = 1.96$ Å, $CN_{Ti-Ti} = 4$, and $R_{Ti-Ti} = 3.06$ Å).[61] Small coordination numbers in Ti–O and Ti–Ti shells as well as the interlayer space of the Ti^{4+}-mont of 2.7 Å support the conclusion that a two-dimensional titanium oxide structure might be formed along a layer of the montmorillonite. Sodium cations in the interlayer space are replaced by $Ti(OH)_4$ species formed by the reaction of $TiCl_4$ with H_2O (Eq. 12). The successive dehydration of two neighboring $Ti(OH)_4$ species would occur to generate the two-dimensional titanium oxide species along the negatively charged layers (Eqs. 13 and 14).

$$Ti(OH)_4 + \text{mont-}Na^+ \longrightarrow \text{mont}^-\text{-}[Ti(OH)_3]^+ + NaOH \quad (12)$$

K. Kaneda et al.

Bull. Chem. Soc. Jpn. Vol. 79, No. 7 (2006)   991

$$2 \text{ mont}^- - [\text{Ti(OH)}_3]^+ \longrightarrow \text{HO-Ti}^+ \underset{\text{mont}^-}{\overset{\text{mont}^-}{\diamondsuit}} \text{Ti}^+\text{-OH} + 2\text{H}_2\text{O} \qquad (13)$$

$$2\text{HO-Ti}^+ \underset{\text{mont}^-}{\overset{\text{mont}^-}{\diamondsuit}} \text{Ti}^+\text{-OH} \longrightarrow \text{HO-Ti}^+ \underset{\text{mont}^-}{\overset{\text{mont}^-}{\diamondsuit}} \text{Ti}^+ \underset{\text{H}^+}{\overset{\text{H}^+}{\diamondsuit}} \text{Ti}^+ \underset{\text{mont}^-}{\overset{\text{mont}^-}{\diamondsuit}} \text{Ti}^+\text{-OH} \qquad (14)$$

2.1.2 V^{5+}-Mont: V-mont was prepared by ion exchange of Na$^+$-mont with aqueous solution of VCl$_3$ followed by calcination at 800 °C. XRD measurement showed that the lamellar structure of the uncalcined V-mont with an interlayer space of 2.9 Å was transformed into a card-house structure by the above calcination process.

The height of the pre-edge peak in the V K-edge XANES spectrum of the calcined V-mont was similar to that of Na$_3$VO$_4$, but differed from that of VOSO$_4$.[62] This result showed that the vanadium species existed in a tetrahedral-like geometry. Furthermore, the energy position of the pre-edge peak and the absorption edge for V-mont were higher than those of VOSO$_4$, suggesting that the oxidation state of the V-mont is 5+. In the Fourier transform (FT) of k^3-weighted V K-edge EXAFS, no peaks due to a V–O–V bond, detectable in the spectrum of V$_2$O$_5$ at around 2.7 Å, was observed for V-mont (Fig. 9). The inverse FT of the peak around 1–2 Å was well fitted using two short (1.59 Å) and two long (1.70 Å) V–O bonds. The short V–O distance is associated with a V=O bond, as found in V$_2$O$_5$.[63] The above results suggest that a highly dispersed monomeric dioxovanadium(V) species surrounded by four oxygen atoms can be created on the mont.

2.1.3 Cu^{2+}-Mont and Sc^{3+}-Mont: Mont-enwrapped metal cation species containing Cu and Sc were prepared by treating Na$^+$-mont with an aqueous solution of the appropriate metal nitrates or triflates.

2.1.3.1 Cu^{2+}-Mont; The Cu^{2+}-mont was prepared by treatment of Na$^+$-mont with aqueous solution of Cu(NO$_3$)$_2$·3H$_2$O. On the basis of the XRD analysis, the layered structure was identified and the basal spacing for Cu^{2+}-mont was estimated to be 2.9, which is comparable to that of the parent Na$^+$-mont. Elemental analysis confirmed that two Na$^+$ ions

are replaced by one Cu^{2+} ion during ion-exchange (Cu, 3.21; Na, 0.09%). UV–vis and Cu K-edge XANES spectra of Cu-mont exhibited that Cu species is divalent and has distorted octahedral coordination environment.[64] The peak at 1.5 Å in the FT of k^3-weighted Cu K-edge EXAFS was assignable to a Cu–O moiety.[65]

The results of the curve-fitting analysis are summarized in Table 6, showing a slightly distorted CuO$_6$ octahedron with four short (1.90 Å) and two long (2.03 Å) Cu–O shells. The Cu–O distance of 2.03 Å was shorter than an axial Cu–O bond of 2.43 Å observed in a [Cu(H$_2$O)$_6$]$^{2+}$ complex in perchlorate solution,[66] due to the restricted interlayer space of the mont. The peaks above 2 Å in the FT EXAFS due to the presence of contiguous Cu sites were not detectable for Cu^{2+}-mont. Based on the basal spacing and Cu–O distances of Cu^{2+}-mont, it is reasonable to consider that the monomeric aquacopper complex in the interlayer is inclined at about 45° with respect to the c-axis of the mont. An analogous [Cu(H$_2$O)$_6$]$^{2+}$ species has been reported within the interlayer space of hectrites[55b,67] and the pores of zeolite-X.[68]

2.1.3.2 Sc^{3+}-Mont; Treatment of Na$^+$-mont with aqueous solution of Sc(OTf)$_3$ afforded Sc-mont. Elemental analysis (Sc, 1.78; Na, 0.04%) of Sc-mont showed one Sc ion substituting for three Na$^+$ ions (Eq. 15).

$$\text{Sc(OTf)}_3 + 3\text{Na}^+\text{-(mont)}^{3-}$$
$$\xrightarrow[\text{in water}]{} [\text{Sc(H}_2\text{O)}_6]^{3+}\text{-(mont)}^{3-} + 3\text{NaOTf}. \qquad (15)$$
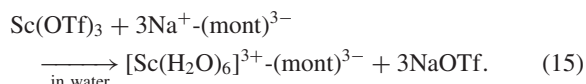
XRD studies verified retention of a layered structure of Sc-mont with a basal spacing of 3.6 Å. XPS revealed formation of a trivalent Sc species. FT of k^3-weighted Sc K-edge EXAFS of the Sc^{3+}-mont sample showed a peak at 1.7 Å assignable to a Sc–O shell, and curve-fitting results disclosed that the inter-
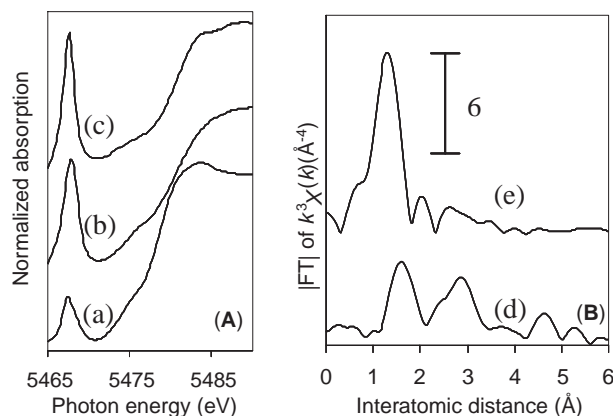

Fig. 9. (A) V K-edge XANES spectra of (a) VOSO$_4$, (b) V-mont, and (c) Na$_3$VO$_4$. (B) Fourier transforms of k^3-weighted V K-edge EXAFS for (d) V$_2$O$_5$, and (e) V-mont.

Table 6. Results of Curve-Fitting Analysis of the Cu–O and Sc–O Shell for the Mont-Enwrapped Cu^{2+}- and Sc^{3+}-Catalysts

| Sample	Shell	C.N.[a]	R/Å[b]	$\Delta\sigma$/Å^2 [c]
Cu^{2+}-mont				
Fresh	Cu–O(1)	4.0	1.90	0.0005
	Cu–O(2)	2.0	2.03	0.0004
Recovered[d]	Cu–O(1)	4.0	1.92	0.0025
	Cu–O(2)	2.0	2.03	0.0028
In substrate[e]	Cu–O(1)	2.1	1.93	0.0006
	Cu–O(2)	1.0	2.39	0.0065
	Cu–O(3)	2.1	1.86	0.0009
	Cu–O(4)	1.0	2.60	0.0063
Sc^{3+}-mont				
Fresh	Sc–O	6.0	2.13	0.0019
Recovered[f]	Sc–O	6.1	2.13	0.0014

a) Coordination number. b) Interatomic distance. c) $\Delta\sigma$ is the difference between Debye–Waller factor of catalysts and that of the reference material. d) The recovered catalyst by filtration after the Michael reaction of ethyl 2-oxocyclopentanecarboxylate with 2-cyclohexen-1-one under solvent-free conditions. e) The catalyst treated with both 2-cyclohexen-1-one and acetylacetone. f) The recovered catalyst after the Michael reaction of 2-oxocyclopentanecarboxylate with 3-buten-2-one in water.

atomic distance and coordination number of the Sc–O bond were 2.13 Å and 6.0, respectively, which was evidence for the formation of a monomeric Sc species (Table 6).

The situations involving Cu^{2+} and Sc^{3+} cations sharply contrast with those of Fe^{3+} and Ti^{4+} in the mont interlayer, in which the Fe and Ti cations form a chain-like structure linked by M–O–M moieties (vide supra).[57a–d] We think that this difference can be explained by the hydrolysis constant (K_h) of the metal cations.[58] Generally, metal cations with small pK_h values (2.3 for Ti^{4+}) are easy to hydrolyze to the corresponding $[M(OH)_n]$ cation species that precede the M–O–M moiety. However, Cu and Sc cations have large pK_h values (7.53 for Cu^{2+} and 4.3 for Sc^{3+}), and thus are stable against hydrolysis to remain monomeric.

The present preparation method, which utilizes the cation-exchange ability of monts and the choice of metal element to be exchanged, is a powerful protocol for the stabilization of monomeric aqua metal species of Cu and Sc within the interlayer of monts to serve as heterogeneous acid catalysts.

2.2 Oxygenation Reactions. 2.2.1 Oxygenation of Cyclic Alkanes Catalyzed by Fe^{3+}-Mont: The potential catalytic abilities of the unique diiron species of Fe^{3+}-mont was explored in the liquid-phase oxygenation of cyclohexane using H_2O_2.[57e] Fe^{3+}-mont showed a high catalytic activity for selective cyclohexane oxygenation to cyclohexyl hydroperoxide in the presence of trifluoromethane sulfonic acid (TFSA); a TON based on Fe ions reached 23200 after 60 h (Eq. 16).

$$\text{(16)}$$

TON 23200
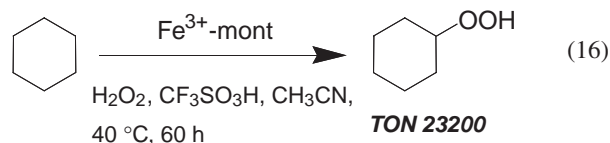
The turnover frequency for Fe^{3+}-mont of 386 h^{-1} is much higher than those of 1.3, 2.4, 4, and 46 h^{-1} for $[\gamma\text{-SiW}_{10}\text{-}\{Fe(OH_2)\}_2O_{38}]^{6-}$,[69] $[Fe_2O(OAc)(tmima)_2]^{3+}$ (tmima = tris-[(1-methylimidazol-2-yl)methyl]amine),[70] NaAuCl$_4$,[71] and $[VO(Hpda)_2(H_2O)]$ (H$_2$pda = pyrazine-2,3-dicarboxylic acid)[72] catalyst systems, respectively. Under the present conditions, Fe_2O_3 did not show any catalytic activity.

One of the prominent characteristics of montmorillonites is enlargement of the interlayer distance in polar solvents.[73] Indeed, the interlayer space of Fe^{3+}-mont was expanded from 2.2 to 10.6 Å when soaked in acetonitrile, as confirmed by its XRD pattern; most Fe species within the interlayer become available for oxygenation. Correspondingly, the Fe^{3+}-mont catalyst system was also able to oxidize the larger cyclic alkane of cyclooctane to cyclooctyl hydroperoxide with a TON of 21000 after 60 h (Eq. 17).

$$\text{(17)}$$

TON 21000
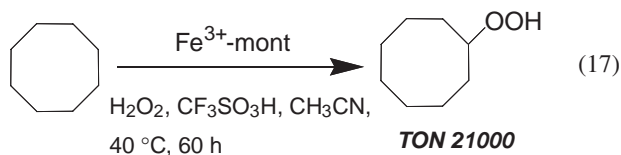
The Fe^{3+}-mont catalyst was easily separated from the reaction mixture, and could be reused four times, keeping its high reaction rate and product selectivity for the oxygenation. Presumably, this alkane oxygenation may occur via a high valent oxoiron species, i.e. $Fe^{5+}=O$. In the presence of TFSA, H_2O_2

Table 7. Epoxidation of Cyclooctene by Various Catalysts Using O_2[a]

$$\text{Scheme: } O_2,\ \text{catalyst};\ \text{trifluorotoluene, 90 °C}$$

Entry	Catalyst	Yield of epoxide/%[b]
1[c]	V-mont[d]	80
2	V-mont[d]	31
3	V-mont[d,e]	trace
4	Fe-mont	trace
5	Mn-mont	trace
6	Mo-mont	trace
7	Ru-mont	trace
8	Na-mont	trace
9	V_2O_5[d]	4
10	V-X zeolite[d]	1
11	V/Al_2O_3[d]	trace
12	$VO(acac)_2$[d]	trace

a) Reaction conditions: cyclooctene (3 mmol), catalyst (0.1 g), trifluorotoluene (5 mL), O_2 atmosphere, 90 °C, 48 h. b) Determined by GC analysis using an internal standard technique. c) Trifluorotoluene (1 mL), 72 h. d) V (0.019 mmol). e) Uncalcined V-mont was used.

oxidizes the Fe^{3+}–O–Fe^{3+} species to give an $Fe^{5+}=O$ intermediate,[74] which reacts with cyclohexane, followed by attack of molecular oxygen leading to the formation of cyclohexyl hydroperoxide and Fe^{3+}–OH.

2.2.2 Oxygenation of Cyclic Alkanes Catalyzed by V^{5+}-Mont: Epoxidation is one of the most fundamental and important reactions in organic synthesis.[75] Various methods have been developed and exploited, and the search for new environmentally friendly methods using molecular oxygen (O_2) as the sole oxidant has attracted much interest. However, there have been few reports concerning the epoxidation of alkenes using 1 atm of O_2 without the use of reducing reagents.[57h,76]

Epoxidations of cyclooctene were carried out using various metal-exchanged monts under 1 atm of O_2 in α,α,α-trifluorotoluene solvent, as shown in Table 7. Among the catalysts examined, the calcined V-mont proved the most efficient for the epoxidation of cyclooctene (Entry 2). Interestingly, the uncalcined V-mont was found to be less effective (Entry 3). Other vanadium catalysts such as V_2O_5, V–X Zeolite, V–alumina, and $VO(acac)_2$ gave poor results (Entries 9–12). Under optimized reaction conditions, the yield of cyclooctene oxide reached up to 80 % with >99% selectivity after 72 h (Entry 1). To the best of our knowledge, this is the first example of selective liquid-phase epoxidation of cyclooctene using a heterogeneous catalyst with an atmospheric pressure of O_2 as the sole oxidant.[57h,75,77]

This V-mont selectively catalyzed the epoxidation of various kinds of cyclic and linear alkenes with 1 atm of O_2, affording the corresponding epoxides as sole products. Upon completion of the epoxidation of cyclooctene, V-mont was separated from the reaction mixture by simple filtration, and could be reused without any appreciable loss of its high catalytic activity and selectivity.

The above V-mont also exhibited high catalytic activity for the oxygenation of adamantane in *tert*-butyl acetate solvent

K. Kaneda et al.

Bull. Chem. Soc. Jpn. Vol. 79, No. 7 (2006)   993

under an O_2 atmosphere, affording 1-adamantanol, 1,3-ada-mantanediol, and 2-adamantanone; the total yield of oxygenated products reached 93% at 96 h (Eq. 18). Oxidation did not proceed in the absence of V-mont under identical reaction conditions. This yield is higher than those reported for other methods of adamantane oxidation with O_2 as the sole oxidant.[78]

$$(18)$$

(**1**)   (**2**)   (**3**)
Total Yield 93 %
Selectivity; (**1**) : (**2**) : (**3**) = 41: 44: 15
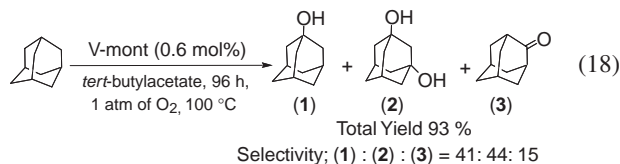
The above two oxidation reactions were inhibited by the addition of radical scavengers such as *p-tert*-butylcatechol and 2,6-di-*tert*-butylphenol. Furthermore, the ratio of oxidation at tertiary vs secondary positions in the oxygenation of adamantane was 8.6:1, which is similar to the ratio observed for radical oxidations.[79] These facts suggest that the above oxidations by V-mont involve a radical oxidation mechanism.[78a,79]

2.3 Carbon–Carbon Bond-Forming Reactions.   2.3.1 Acid-Catalyzed Reactions by Ti⁴⁺-Mont as a Solid Brønsted Acid: The acidic nature of M^{n+}-monts can be utilized in the aromatic alkylation of phenoxyethanol with fluoren-9-one to afford 9,9-bis[4-(2-hydroxyethoxy)phenyl]fluorene (BHEPF), which is a highly stable and valuable raw material for the highly functionalized polymers used in optical products.[80] BHEPF is usually obtained by a multi-step procedure[81] or a one-step synthesis in the presence of concentrated sulfuric acid and 3-mercaptopropionic acid.[82] However, the above two synthetic methods suffer from some serious disadvantages: 1) Large amounts of acids result in the production of hazardous wastes which entails environmental pollution, and 2) the use of corrosive acids corrodes reactor walls.

The reaction of phenoxyethanol with fluoren-9-one in the presence of Ti⁴⁺-mont catalyst gave an 82% yield of BHEPF under solvent-free conditions at 170 °C after 2 h (Eq. 19).

$$(19)$$

yield: 82 %
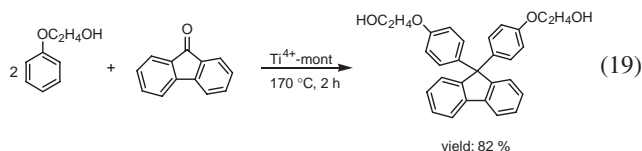
Reactions using various M^{n+}-monts were carried out as summarized in Table 8. M^{n+}-monts containing high-valent metal cations such as Ti⁴⁺, Al³⁺, and Zr⁴⁺ were found to be effective (Entries 1–3). The parent Na⁺-mont had no catalytic activity for the above alkylation reaction (Entry 8). The yields of the BHEPF increased in line with the amount of strongly adsorbed NH_3 observed for the M^{n+}-mont catalysts. The amount of strongly adsorbed NH_3 on Ti⁴⁺-mont was over twice as much as those of the Al³⁺- and Fe³⁺-mont catalysts. M^{n+}-monts showed higher catalytic activities as well as surface acidities than sulfate ion-treated zirconium oxide (SO_4^{2-}-ZrO_2)[83,84] and H⁺-exchanged zeolites such as H⁺-mordenite, H⁺-ZSM-5, and USY (Entries 1–4 vs Entries 9–12). These results imply that the above alkylation reaction may be catalyzed by the strong acid sites of the M^{n+}-mont catalysts. Bulk TiO_2 itself was inactive for this alkylation reaction; we therefore propose that the prominent catalysis of Ti⁴⁺-mont could be

Table 8. Aromatic Alkylation of Phenoxyethanol with Fluoren-9-one Catalyzed by the Mn^{n+}-Monts and Typical Solid Acids[a]

| Entry	Catalyst	Convn. /%	Yield of BHEPF /%[b]	Amount of adsorbed NH_3 /mmol g^{-1} [c]
1	Ti⁴⁺-mont	100	82	1.89
2	Al³⁺-mont	80	62	0.75
3	Zr⁴⁺-mont	58	50	0.81
4	Fe³⁺-mont	58	27	0.95
5	Ni²⁺-mont	32	16	n.m.[d]
6	Cu²⁺-mont	16	12	0.74
7	Zn²⁺-mont	0	0	n.m.
8	Na⁺-mont	0	0	0.17
9	SO_4^{2-}-ZrO_2[e]	27	14	0.44
10	H⁺-mordenite	12	trace	0.24
11	H⁺-ZSM-5	trace	trace	n.m.
12	USY	24	trace	0.36
13	TiO_2[f]	20	trace	n.m.

a) Reaction conditions: fluoren-9-one (1 mmol), catalyst (0.15 g), phenoxyethanol (5 mL), 170 °C, 2 h. b) Yeild was based on fluoren-9-one. c) Acid amount was volumetrically measured. The value corresponds to the number of strongly adsorbed NH_3. d) Not measured. e) From Wako Pure Chemicals. f) JRC-TIO-1 was used.

ascribed to the novel structure of titanium oxide within the layer of the montmorillonite (vide supra).

The catalytic activity of the spent Ti⁴⁺-mont was regenerated by treatment with H_2O. The protonic acid sites are probably located on the oxygen anions of the Ti–O–Ti bonds and efficient interactions through the oxygen anions between Ti⁴⁺ and Si⁴⁺ of SiO_4 tetrahedra in the layer can strengthen the acidity of the protons. The protonic acids[85] associated with Ti⁴⁺ cations might act as active sites for this alkylation. The interlayer space of Ti⁴⁺-mont was expanded from 2.7 to 8.4 Å when soaked in phenoxyethanol. After soaking, phenoxyethanol molecules form π-arene complexes with Ti cations in the interlayer space. The interlayer distance of 8.4 Å is comparable to the molecular sizes of fluoren-9-one of ca. 9.36 Å. Fluoren-9-one can react with the protonic acid sites within the interlayer space.

Scheme 3 shows a possible reaction path for BHEPF. Fluoren-9-one is protonated at an acid site on the Ti⁴⁺ ions within the interlayer space. An electrophilic attack of phenoxyethanol at a benzyl position of fluoren-9-one gives a monoalkylated intermediate, followed by successive reactions with a proton and phenoxyethanol to lead to the formation of BHEPF, together with the regeneration of the protonic acid sites. A prominent catalysis of Ti⁴⁺-mont could be ascribed to the expansion of the interlayer space in phenoxyethanol as well as their strong acidity associated with the metal cation in the interlayer.

2.3.2 Miscellaneous Acid-Catalyzed Reaction: The strong acidity and the expansion of interlayer space of Ti⁴⁺-mont under reaction conditions can be further utilized for other acid-catalyzed reactions, such as acetalization,[57c] deacetalization,[57b] and esterification.[57a] These reactions are usually conducted using homogeneous acids, such as *p*-toluenesulfonic acid (PTSA), $(C_2H_5)O\cdot BF_3$, $FeCl_3$, or trimethylsilyl trifluoromethanesulfonate (Me_3SiOTf). These homogeneous acids
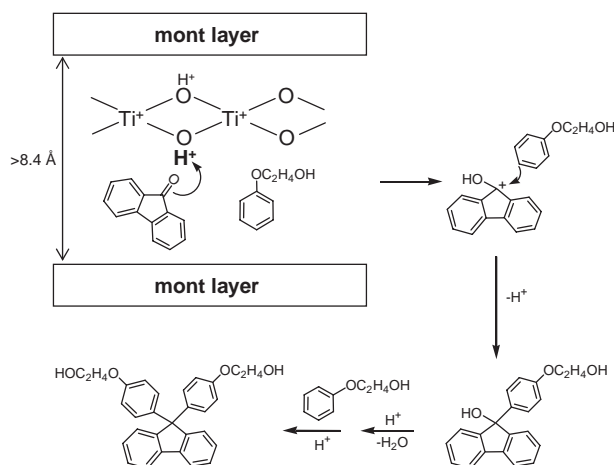
Scheme 3. Possible reaction mechanism of Ti^{4+}-mont-catalyzed alkylation of phenoxyethanol with fluoren-9-one.

often suffer from drawbacks, such as troublesome isolation of products and the production of large volumes of salt wastes during neutralization of the acids.

Acetalization is commonly utilized as a protecting method for carbonyl functions because dimethylacetals and 1,3-dioxolanes are stable under neutral and basic conditions.[86] Ti^{4+}-mont could smoothly transform various kinds of cyclic, aliphatic, and aromatic ketones into cyclic acetals. Remarkably, a bulky ketone of 1,3-diphenyl-2-propanone gave a quantitative yield of the corresponding acetal, whereas some zeolite catalysts do not efficiently promote the acetalization of this ketone because of the steric hindrance of the bulky compound in the acid sites.[87] Chemoselective acetalizations are exemplified. In the presence of Ti^{4+}-mont, the acetalization of 4-oxo-4*H*-1-benzopyran-3-carboxaldehyde occurred exclusively at a formyl group to give 2-(4-oxo-4*H*-1-benzopyran-3-yl)-1,3-dioxolane (Eq. 20), and also ethyl 2-oxocyclopentanecarboxylate afforded an acetal, leaving an ester function intact in a high yield (Eq. 21). An unconjugated keto function of the Wieland–Miescher ketone was selectively protected to 3′,4′,8′,8′a-tetrahydro-8′a-methylspiro[1,3-dioxolane-2,1′(2′*H*)-naphthalen]-6′(7′*H*)-one (Eq. 22). Furthermore, Ti^{4+}-mont could efficiently catalyze deprotection of various acetal compounds in aqueous acetone solution.[57b]

(20)

91% isolated yield

(21)

90% isolated yield

(22)

87% isolated yield
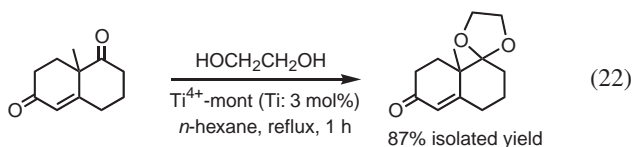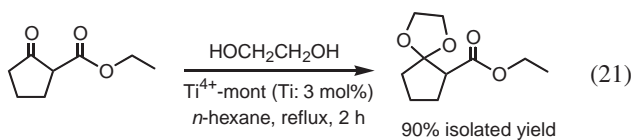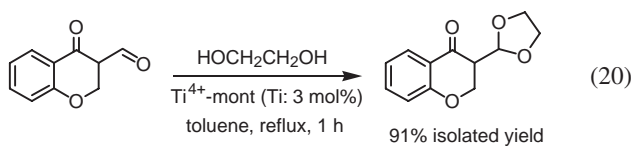
Esters are widely found among naturally occurring compounds and are also greatly important intermediates in organic syntheses. Of the methods available for their preparation, catalytic condensation of a carboxylic acid with an alcohol[88] provides "green" protocol; particularly, use of equimolar amounts of carboxylic acids and alcohols[88b,d] is preferable from the standpoint of atom efficiency.

The Ti^{4+}-mont catalyst provides a new practical method for the esterification of carboxylic acids with alcohols using equimolar amounts of carboxylic acids and alcohols under solventless conditions.[57b] As depicted in Eq. 23, a 100 mmol scale esterification of hexanoic acid with 3-phenyl-1-propanol was successfully carried out in the absence of solvents to afford 3-phenyl-1-propyl hexanoate in a 93% yield. To the best of our knowledge, this is the first example of a highly efficient and recyclable solid catalyst for esterifications using equimolar amounts of carboxylic acids and alcohols.

(23)

93% isolated yield
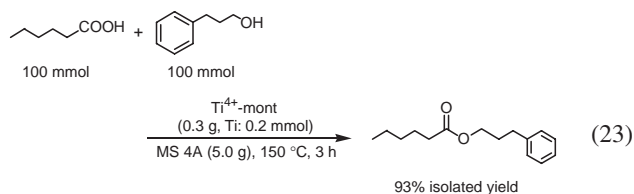
Several primary carboxylic acids were readily esterified to the corresponding methyl esters (Table 9). Suberic acid afforded the dimethyl ester in a 99% yield (Entry 7). Notably, the esterification of homophthalic acid occurred chemoselectively at the non-conjugated carboxylic group to yield methyl 2-carboxyphenylacetate without formation of the diester; similar results were also observed for itaconic acid (Entry 9).

It is noteworthy that hydrolysis of the methyl esters, even in the presence of both Ti^{4+}-mont and large amounts of water, was not observed under reflux conditions using methanol. Presumably, the prominent catalytic activity of Ti^{4+}-mont might arise from the strong acid sites associated with the chain-like

Table 9. Esterification of Carboxylic Acids with MeOH Using the Ti^{4+}-Mont Catalyst[a]

Entry	Carboxylic acid	Product[b]	Time /h	Yield /%[c]
1	$CH_3(CH_2)_4CO_2H$	$CH_3(CH_2)_4CO_2Me$	6	98
2[d]	$CH_3(CH_2)_4CO_2H$	$CH_3(CH_2)_4CO_2Me$	6	98
3[e]	$CH_3(CH_2)_4CO_2H$	$CH_3(CH_2)_4CO_2Me$	6	98
4[f]	$CH_3(CH_2)_4CO_2H$	$CH_3(CH_2)_4CO_2Me$	6	98
5	$CH_3(CH_2)_8CO_2H$	$CH_3(CH_2)_8CO_2Me$	12	90
6	$Ph(CH_2)_2CO_2H$	$Ph(CH_2)_2CO_2Me$	12	90
7	$HO_2C(CH_2)_6CO_2H$	$HO_2C(CH_2)_6CO_2Me$	12	99
8			12	90
9			12	89

a) Reaction conditions: carboxylic acid (1 mmol), Ti^{4+}-mont (0.15 g, Ti: 0.1 mmol), MeOH (10 mL), 70 °C. b) All products were characterized by ^{1}H NMR and Mass spectra. c) Yields of products were determined by GC analysis using internal standards, based on carboxylic acid. d) Reuse-1. e) Reuse-2. f) Reuse-3.

Ti domains within the interlayers. In polar organic molecules, the interlayer space is effectively expanded, allowing access to the substrates to the catalytic site of the Ti species. Vide supra, water molecules adsorbed on the interlamellar surfaces expel the hydrophobic esters from the Ti species, which prevents hydrolysis of the product esters.

2.3.3 Michael Reaction Using the Cu²⁺-Mont Catalyst: The Michael reaction of 1,3-dicarbonyl compounds with enones provides access to 1,5-dioxo synthons, which can be facilely transformed into cyclohexenone derivatives for use as important intermediates in steroid and terpenoid synthesis.[89] The Michael reactions of ethyl 2-oxocyclopentanecarboxylate with 2-cyclohexen-1-one in various solvents were conducted in the presence of Cu²⁺-mont (Eq. 24).

$$\text{(24)}$$
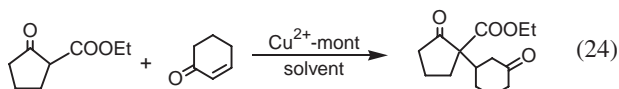
Nitromethane was an optimal solvent to give 2-oxo-1-(3-oxocyclohexyl)cyclopentanecarboxylate in 82% yield. In marked contrast to the Sc³⁺-mont-catalyzed Michael reaction, vide infra, water was a poor solvent (6%). Interestingly, Cu²⁺-mont exhibited the greatest catalytic activity under neat conditions (96%).

The catalytic activity for the Michael reaction without solvents was compared using various M^{n+}-monts. Cu²⁺-mont gave the highest yield and the Michael reaction did not occur in the presence of the parent Na⁺-mont. Notably, Cu²⁺-mont had greater catalytic activity than Cu(NO₃)₂·3H₂O (59% yield). The yield increased with an increase in Lewis-acid strength of the metal cation in the mont.[90]

The scope of substrates for the Michael reaction catalyzed by Cu²⁺-mont under solvent-free conditions was examined and typical results are shown in Table 10. The Michael reactions of various β-keto esters and 1,3-diketones with 3-buten-2-one occurred efficiently to afford the corresponding 1,5-dioxo compounds, even at room temperature (Entries 1–4). In the solvent-free Michael reaction, Cu²⁺-mont was effective for cyclic enones to give the corresponding Michael adducts within 5 h (Entries 6 and 9), while FeCl₃·6H₂O[91] and Cu(OAc)₂·H₂O[92] were reported to be ineffective. In all cases, the desired 1,4-addition products were obtained exclusively without formation of 1,2-addition compounds.

It is notable that 100 mmol of diethyl malonate readily reacted with 2-cyclopenten-1-one under solvent-free conditions using only 0.25 mol % of the Cu²⁺-mont catalyst to afford diethyl 3-oxocyclopentylmalonate in 91% isolated yield (Eq. 25).

$$\text{(25)}$$
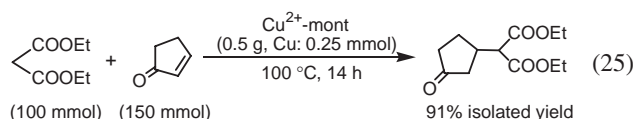
Generally, the Michael reaction of dialkyl malonates does not proceed easily under traditional Lewis acid-catalyzed conditions,[89] but some base catalysts such as sodium ethoxide show high catalytic activity toward these substrates.[93] Shibasaki et al. recently reported that the La-linked-BINOL catalysts were highly efficient for the asymmetric Michael

Table 10. Solvent-Free Michael Reaction Catalyzed by Cu²⁺-Mont[a]

Entry	Donor	Acceptor	Product	Time/h	Yield/%[b]
1				1	99
2				1	97
3				1	97
4				1	97
5				2	96
6[c]				2	92[f]
7[c,d]				2	92[f]
8[c,e]				2	92[f]
9[c]				5	99[f]

a) Reaction conditions: donor (4 mmol), acceptor (4.4 mmol), Cu²⁺-mont (Cu: 0.05 mmol), 20 °C. b) Yields of products were determined by GC based on donor. c) 70 °C. d) Reuse-1. e) Reuse-2. f) 1:1 Ratio of diastereomeric mixture.

reaction of dialkyl malonates with enones, in which the metal center and naphthoxide moiety act as a Lewis acid and Brønsted base, respectively.[94] In a similar fashion, the Michael reaction by Cu²⁺-mont likely proceeds via bifunctional-catalysis between the Lewis acidic Cu complex and silicate layer of the mont; the latter efficiently abstracts a proton from 1,3-dicarbonyl compounds.

Upon completion of the Michael reaction, the Cu²⁺-mont catalyst was readily recovered from the reaction mixture by simple filtration, and could be reused without any discernible loss in activity and selectivity. As shown in Table 10, yields of 92% were obtained in two recycling experiments (Entries 7 and 8). Elemental analysis of the used Cu²⁺-mont confirmed no leaching of Cu species from the catalyst. The retention of monomeric Cu²⁺ species in the recovered Cu-mont catalyst was supported by EXAFS. In the reaction of 2-oxocyclopentanecarboxylate with 2-cyclohexen-1-one, removal of Cu²⁺-mont at ca. 50%-conversion by hot filtration did not afford any additional product. These observations clearly demonstrate that the Michael reaction occurred at the Cu species within the mont layers.

Transition and rare earth metal catalysts have been extensively used for the Michael reaction of 1,3-dicarbonyl compounds with enones. The reaction mechanism is considered to involve a ternary complex, in which both the 1,3-dicarbonyl compound and the enone are coordinated to a Lewis-acid metal center.[58] A shift in the infrared (IR) spectrum of the coordinated ketone is a measure of the Lewis-acid strength of metal cations.[95] The IR spectrum of the $\nu(CO)$ band of adsorbed cyclopentanone onto Cu²⁺-mont appeared at 1685 cm⁻¹, which

is lower than that of the free cyclopentanone ($1751\,cm^{-1}$). This $66\,cm^{-1}$ shift was larger than those found for Sc^{3+}-, Y^{3+}-, Yb^{3+}-, and La^{3+}-monts ($34\,cm^{-1}$), demonstrating that the Cu^{2+}-mont catalyst possesses significantly stronger Lewis-acid strength than the other M^{n+}-monts do. Yields of the Michael adduct increased with increasing Lewis-acid strength of the metal cation. Thus, it is reasonable that the Lewis-acid sites of M^{n+}-monts play an important role in these carbon–carbon bond-forming reactions. Presumably, the silicate layers of the monts might act as a macroanion with low nucleophilicity, leading to the formation of a cationic copper center with extremely strong Lewis acidity.

Upon treatment of Cu^{2+}-mont with 2-cyclohexen-1-one, the IR spectrum contained a $\nu(CO)$ band at $1658\,cm^{-1}$, ascribed to 2-cyclohexen-1-one coordinated to the copper Lewis-acid site. Addition of acetylacetone as a donor gave new bands at 1580, 1558, and $1539\,cm^{-1}$, assigned to the acetylacetonatocopper species.[96] EXAFS analysis of the same sample supported the generation of two Cu–O bonds with a $1.86\,Å$ length and one Cu–O bond with a $2.60\,Å$ length, along with the loss of three H_2O ligands from the original Cu^{2+}-mont, as shown in Table 6. On the basis of these results, it is reasonable that the Cu^{2+}-mont-catalyzed Michael reactions involve the ternary copper complex **II**, in which both the 1,3-dicarbonyl compound and the enone coordinate to the Cu^{2+} center (Scheme 4).[97] The carbon–carbon bond formation produces a alcoholatocopper intermediate **III**, followed by protolysis to afford the Michael adduct together with regeneration of the original Cu species **I**. The same reaction mechanism has been proposed for the Sc^{3+}-mont-catalyzed Michael reactions in water (vide infra).[98] Notably, Michael reactions of nitriles such as ethyl cyanoacetate and malononitrile as donors instead of 1,3-dicarbonyl compounds hardly proceeded under these conditions. It is likely that such nitrile compounds strongly coordinate to copper and prevent the interaction of enones with the Cu complexes.

It seems that the Lewis-acid site originating from the Cu^{2+} aqua species induces both Sakurai–Hosomi and Diels–Alder reactions via coordination of carbonyl compounds (vide infra).

The interlayer space of Cu^{2+}-mont was expanded from 2.9 to $11.5\,Å$ when soaked in a mixture of acetylacetone and 2-cyclohexen-1-one under solvent-free conditions, as confirmed by XRD. Prominent catalysis by Cu^{2+}-mont under solvent-free conditions could be related to the expansion of the interlayer space as well as the strong Lewis-acid nature of the aqua Cu^{2+} cation enwrapped in the macro anion of the mont interlayer.

2.3.4 Catalysis of Sc^{3+}-Mont for Michael Reactions in Water:

Performing carbon–carbon bond-forming reactions with water as the solvent is of great interest due to practical and environmental considerations.[4g,29] While many Lewis acids, such as Ti, Al, Sn, and B complexes, are hydrolyzed to form inactive corresponding hydroxides and oxides in the presence of water,[99] rare earth metal (RE) complexes can act as Lewis acids. $RE(OTf)_3$ (OTf: trifluoromethanesulfonate) compounds are known as water-compatible catalysts.[100] However, these catalysts exhibit low activity or require long reaction times.

The Michael reaction of 2-oxocyclopentanecarboxylate with 3-buten-2-one was carried out under aqueous conditions using various M^{n+}-monts and the results are summarized in Table 11. No reaction proceeded in the absence of catalyst. As expected, M^{n+}-monts having RE^{3+} metal cations were effective in 0.5 h (Entries 1–4); Sc^{3+}-mont gave the highest yield of ethyl 2-oxo-1-(3-oxobutyl)cyclopentanecarboxylate (Entry 1) and exhibited significantly higher catalytic activity than the homogeneous $Sc(OTf)_3$ (Entry 7).[101] In contrast, the catalytic activities of Cu^{2+}- and Zn^{2+}-monts under similar conditions were extremely low (Entries 5 and 6). A similar phenomenon is also observed for Mukaiyama-aldol reactions using various metal salts under aqueous conditions.[58]
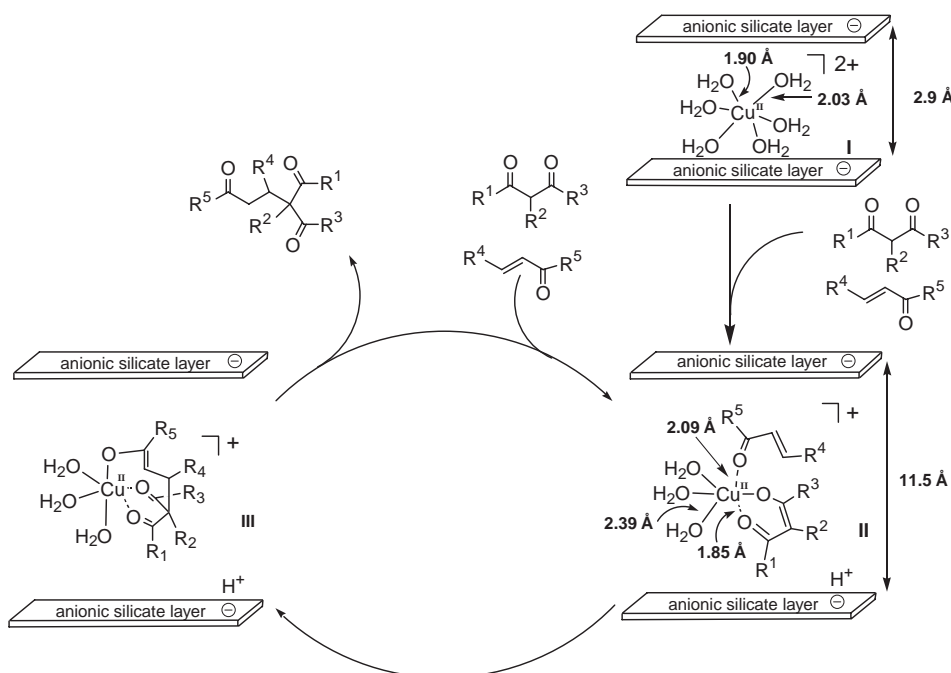
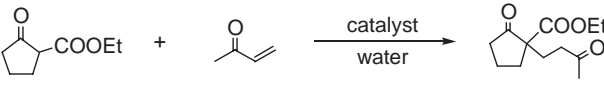Scheme 4. Proposed mechanism for Michael reaction using the Cu^{2+}-mont catalyst.

Generally, treatment of RE^{3+} triflates with water gives RE^{3+} aqua complexes surrounded by low nucleophilic OTf counter anions in the second coordination sphere, which act as Lewis acids.[102] Yb salts with less nucleophilic counteranions, such as OTf and ClO_4^- catalyze the aldol reaction of silyl enol ethers with aldehydes in aqueous media, whereas combining Yb salts with Cl^-, OAc^-, NO_3^-, and SO_4^{2-} anions results in low catalytic activity. Elemental analysis of Sc^{3+}-

mont revealed an absence of OTf groups in the mont catalyst. Additionally, Sc/Al_2O_3 and Sc/SiO_2 were completely inactive for Michael reactions. Presumably, Sc^{3+} aqua complexes partnering with the anionic silicate layers of monts, whose negative charge is delocalized along the layer,[55,91,103] provide outstanding catalytic activity.
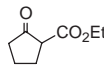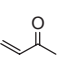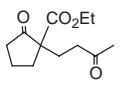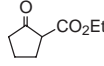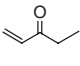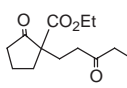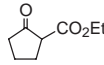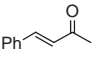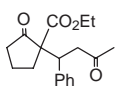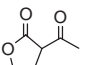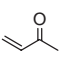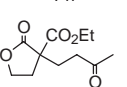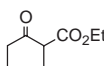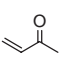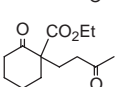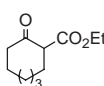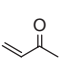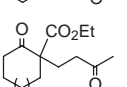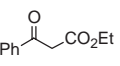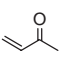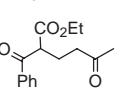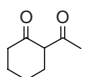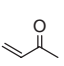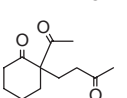
Sc^{3+}-mont-catalyzed Michael reactions were extended to other 1,3-dicarbonyl substrates under aqueous conditions (Table 12). In all cases, the reaction proceeded smoothly in the presence of 2–4 mol% Sc catalyst within 3 h to afford the corresponding Michael adducts in excellent yields. Hydrolysis of the ester moieties did not occur (Entries 1–11). Recently, heterogeneous Michael reactions in water using organic polymer-supported[104] and surfactant-combined[105] Sc catalysts as Lewis acids have been reported. These systems have the drawback of waste production because activated donors such as silyl enol ethers and/or 1.5–3 equiv of acceptors are required. Sc^{3+}-mont overcomes these limitations and is the most active Lewis-acid catalyst for Michael reaction of 1,3-dicarbonyls with enones using water as a solvent. Importantly, even after three recycling experiments, no appreciable loss of catalytic activity or selectivity was observed. For reaction of 2-oxo-cyclopentanecarboxylate with 3-buten-2-one, 99% yields were obtained during three recycling experiments (Entries 2–4). The original Sc content was kept for the used catalyst as confirmed by elemental analysis and the XAFS measurement es-

Table 11. Michael Reaction Using Various Catalysts[a)]

Entry	Catalyst	Yield/%[b)]
1	Sc^{3+}-mont	99
2	Y^{3+}-mont	83
3	Yb^{3+}-mont	62
4	La^{3+}-mont	62
5	Cu^{2+}-mont	17
6	Zn^{2+}-mont	16
7	$Sc(OTf)_3$	7
8	without cat.	0

a) Reaction conditions: donor (2 mmol), acceptor (2.2 mmol), active metal species (0.04 mmol), 30 °C, 0.5 h. b) Yields of products were determined by GC based on donor.

Table 12. Michael Reaction of Various 1,3-Dicarbonyl Compounds with Enones Catalyzed by Sc^{3+}-Mont in Water[a)]

Entry	Donor	Acceptor	Product	Temp/°C	Time/h	Yield/%[b)]
1				30	0.5	99
2[c)]				30	0.5	99
3[d)]				30	0.5	99
4[e)]				30	0.5	99
5				30	1	98
6				50	1	90
7				50	2	99
8				45	3	99
9[f)]				60	2	80
10				50	2	97
11				50	1	96

a) Reaction conditions: donor (2 mmol), acceptor (2.2 mmol), Sc^{3+}-mont (Sc: 0.04 mmol), H_2O (3 mL). b) Yields of products were determined by GC based on donor. c) Reuse-1. d) Reuse-2. e) Reuse-3. f) Donor (0.5 mmol), acceptor (0.55 mmol), Sc^{3+}-mont (Sc: 0.02 mmol), H_2O (1 mL).

Table 13. Allylation of Carbonyl Compounds with Allyltrimethylsilane[a]

$$R^1\overset{O}{\underset{}{\parallel}}R^2 \quad + \quad \diagup\!\!\!\diagdown SiMe_3 \quad \xrightarrow[(ii)]{(i)} \quad R^1\underset{R^2}{\overset{OH}{\mid}}\diagup\!\!\!\diagdown$$

Entry	Carbonyl compound	Allyltrimethyl silane/equiv	Product	Temp/°C[b]	Time/h[b]	Yield/%[c]
1	Ph–C–H ‖ O	1.1	Ph ⤸ OH	45	1	99
2	(t-Bu)C–H ‖ O	1.5	⤸ OH	45	1	97
3[d]	Cy–C–H ‖ O	1.5	Cy ⤸ OH	rt	6	95
4[d]	(⤸)₅C–H ‖ O	1.5	(⤸)₅ OH	rt	1	90
5[d]	Cy=O	2	⤸ OH	40	2	80
6[d]	(⤸)₄ O	2	(⤸)₄ OH	55	3	81

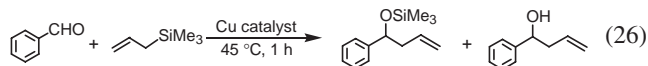a) Reaction conditions: (i) carbonyl compounds (4 mmol), allyltrimethylsilane (1.1–2 equiv), Cu²⁺-mont (Cu: 0.05 mmol), (ii) EtOH (1 mL), 80 °C, 1 h. b) For the allylation reaction (i). c) Yields of products were determined by GC based on carbonyl compound. d) Nitromethane (3 mL) was used as the solvent.

tablished stability of the $[Sc(H_2O)_6]^{3+}$ species in the recovered catalyst.

2.3.5 Application of the Cu²⁺-Mont Catalyst to Sakurai–Hosomi and Diels–Alder Reactions: To expand the applicability of Cu²⁺-mont as a Lewis-acid catalyst, we conducted the Sakurai–Hosomi reaction, i.e., allylation of carbonyl compounds with allylalkylsilanes, which is of great interest in organic chemistry because of the synthetic utility of homoallylic alcohols.[106] The catalytic activity for the reaction of benzaldehyde with allyltrimethylsilane under solvent-free conditions was compared with other copper catalysts (Eq. 26).

$$\text{PhCHO} + \diagup\!\!\!\diagdown SiMe_3 \xrightarrow[\text{45 °C, 1 h}]{\text{Cu catalyst}} \text{Ph}\underset{OSiMe_3}{}\diagup\!\!\!\diagdown + \text{Ph}\underset{OH}{}\diagup\!\!\!\diagdown \quad (26)$$

Among the Cu catalysts tested, Cu²⁺-mont possessed the greatest activity (99% yield after 1 h) to afford trimethyl-[(1-phenyl-3-butenyl)oxy]silane and 4-phenyl-1-buten-4-ol in 98 and 1% yields, respectively. In contrast, the allylation reaction hardly occurred in the presence of Cu²⁺-hydrotalcite, Cu²⁺-zeolite-(X), Cu/Al₂O₃, Cu/SiO₂, and Cu(NO₃)₃·3H₂O.

In the above reaction, after complete conversion of benzaldehyde, addition of ethanol to the reaction mixture afforded 4-phenyl-1-buten-4-ol in 99% yield, which is simple and efficient proton-mediated desilylation to homoallylic alcohols. The one-pot syntheses of various homoallylic alcohols were performed using the Cu²⁺-mont catalyst, as exemplified in Table 13. A variety of aldehydes and ketones smoothly reacted with allyltrimethylsilane to give the corresponding homoallylic alcohols. Cyclic and linear aliphatic aldehydes, as well as ketones, required nitromethane as a solvent to obtain the desired products in high yields.

The recovered catalysts showed activity and selectivity comparable to those of fresh catalysts, yielding the homoallyl-
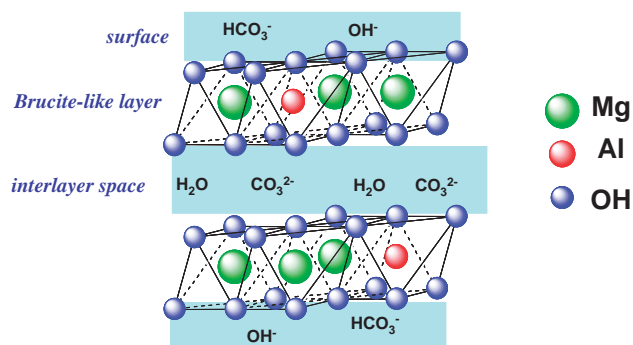
Fig. 10. Schematic side view of layered structure of hydrotalcite.

ic alcohol in 99% during three recycling cycles. A 100 mmol-scale reaction of benzaldehyde with allyltrimethylsilane in the presence of the Cu²⁺-mont catalyst afforded 4-phenyl-1-buten-4-ol in 86% yield. In contrast to previously reported homogeneous aluminum bis(trifluoromethylsulfonyl)amides,[107] ytterbium trichlorides,[108] trimethylsilylmethanesulfonates,[109] indium trichloride/chlorotrimethylsilane,[110] and heterogeneous Al- and K-10 montmorillonites,[111] the Cu²⁺-mont catalyst system is non-polluting and recyclable, and eliminates halogenated reagents and solvents.

3. Hydrotalcite

Hydrotalcites, $Mg_6Al_2(OH)_{16}CO_3 \cdot nH_2O$ (Mg–Al–CO₃), consist of a positively charged two-dimensional Brucite-like layer, with anionic species in the interlayer to form neutral materials.[112] A structural model of the hydrotalcite is illustrated in Fig. 10.

Numerous transition metals can be facilely introduced into

(B) *Mg-M_1-Al-CO$_3$*

Mg M_1 Al Mg
CO$_3^{2-}$ H$_2$O CO$_3^{2-}$
Mg Al M_1 Mg

(C) *M_1-M_2-Al-CO$_3$*

M_2 M_1 Al M_2
CO$_3^{2-}$ H$_2$O CO$_3^{2-}$
M_2 Al M_1 M_2

**MgCl$_2$, AlCl$_3$
(MgO, Al$_2$O$_3$)**

Brucite-like layer

(A) *Mg-Al-CO$_3$*

Surface

HCO$_3^-$ OH$^-$
Mg Mg Al Mg
CO$_3^{2-}$ H$_2$O CO$_3^{2-}$
Mg Al Mg Mg

Brucite-like layer

Interlayer space

Interlayer space

(D) *Mg-Al-A*

HCO$_3^-$ OH$^-$
Mg Mg Al Mg
A^{2-} H$_2$O A^{2-}
Mg Al Mg Mg

Surface

(G) *Mg-Al oxide*

(E) *M_1/Mg-Al-CO$_3$*

M_1
Mg Mg Al Mg
CO$_3^{2-}$ H$_2$O CO$_3^{2-}$
Mg Al Mg Mg

(F) *M_1M_2/Mg-Al-CO$_3$*

M_1 M_2
Mg Mg Al Mg
CO$_3^{2-}$ H$_2$O CO$_3^{2-}$
Mg Al Mg Mg

Chart 3. Strategy for designing highly-functionalized hydrotalcite catalysts.

the Brucite-like layer, interlayer space, or surface by using the following characteristics: (i) the cation-exchange ability of the Brucite layer, (ii) the anion-exchange ability of the interlayer, (iii) surface tunable basicity, and (iv) adsorption capacity.[113] We consider the hydrotalcites as advanced catalyst supports that allow control of the location of catalytically active metal species. Furthermore, the immobilized metal species can cooperate with base sites to create multifunctional catalysts capable of promoting sequential reactions. In this part, the unique catalytic property of functionalized hydrotalcites are described for a variety of oxidation reactions and one-pot syntheses. Our strategy for designing heterogeneous catalysts based on the characteristics of the hydrotalcite is illustrated in Chart 3.

3.1 Monooxygenations. One of the important features of hydrotalcite materials is the base character[114] of the surface anion species such as HCO$_3^-$ and OH$^-$ anions, which compensates for the cationic charge of the Brucite-like layer. As well 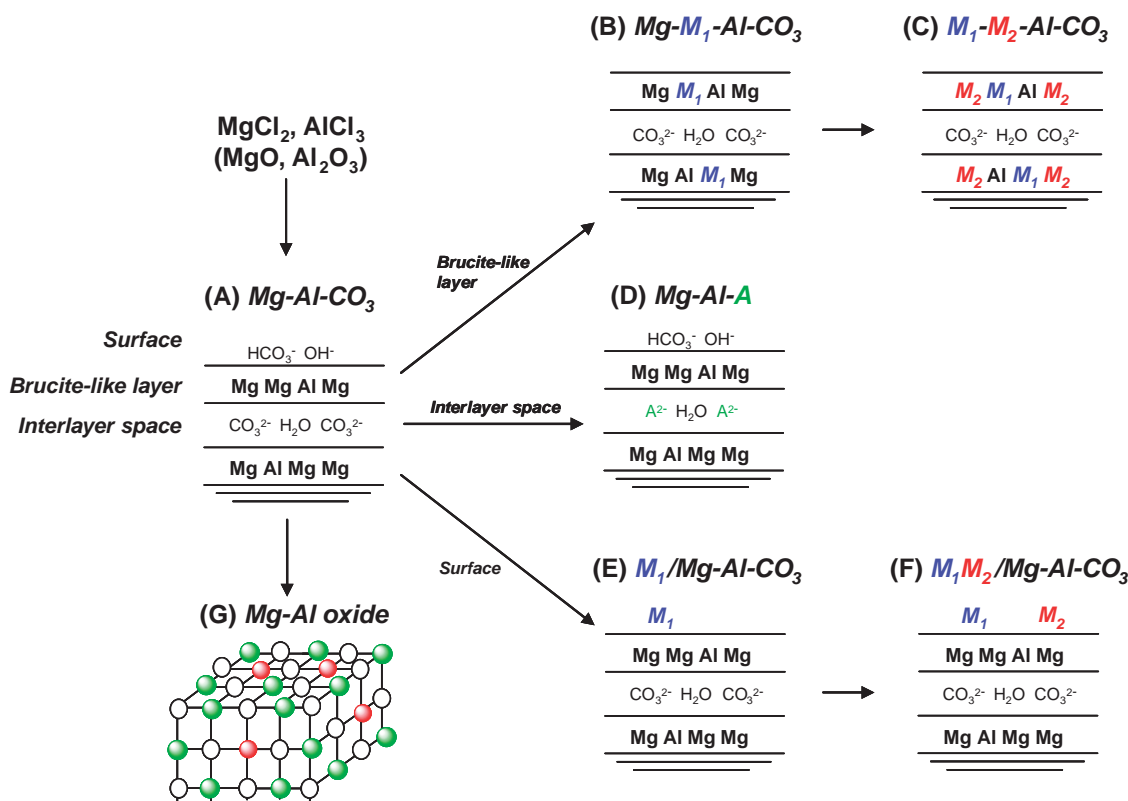as carbon–carbon bond-forming reactions such as aldol and Michael reactions,[115] oxidation reactions are catalyzed by base materials by activation of either the substrate or the oxidant, giving rise to electrophilic attack on carbanions or nucleophilic attack with peroxoanions.[116]

This section describes two types of monooxygenation reactions of Baeyer–Villiger oxidation and epoxidation that are efficiently promoted by heterogeneous base hydrotalcites using combined oxidant of aldehydes and molecular oxygen, and hydrogen peroxide, respectively.

3.1.1 Baeyer–Villiger Oxidation Using Molecular Oxygen and Aldehydes Catalyzed by Base Hydrotalcites: The Baeyer–Villiger oxidation reaction is one of the most well-known and widely applied reactions in organic synthesis and

promoted by acid, base, and transition metals.[95,117,118] A variety of carbonyl compounds can be stereoselectively oxidized into esters or lactones, where a large number of functional groups are tolerated and a wide range of oxidants, such as organic peracids and hydrogen peroxide, may be used (Eq. 27-1).

$$R_1 \overset{O}{\underset{}{\diagup}} R_2 \; + [O] \longrightarrow R_1 \overset{O}{\underset{}{\diagup}} O^{-R_2} \qquad (27\text{-}1)$$
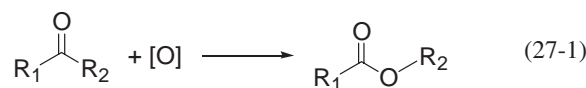
Free radical autoxidation of an aldehyde with molecular oxygen is facile and affords the corresponding peracid. The peracid can transfer an oxygen atom to a substrate, e.g., an olefin or a ketone, resulting in the formation of one equivalent of an epoxide or ester and acid as a coproduct in the absence of metal catalysts.[119–122] We found that both epoxidation and the Baeyer–Villiger oxidation using a system consisting of molecular oxygen and aldehydes were strongly dependent on the kinds of aldehydes used. For example, the Baeyer–Villiger oxidation of cyclohexanone with benzaldehyde smoothly occurred to give $\mathcal{E}$-caprolactone, and benzoic acid was also formed as a coproduct, whereas aliphatic aldehydes such as isobutyraldehyde and isovaleraldehyde, which have high reactivities for epoxidation, showed lower yields of $\mathcal{E}$-caprolactone than benzaldehyde.[121]

Hydrotalcites, Mg$_{10}$Al$_2$(OH)$_{24}$CO$_3$ (Chart 3, type A), have been found to show high catalytic activity for the heterogeneous Baeyer–Villiger oxidation of various carbonyl compounds using a combination system of molecular oxygen and benzaldehyde.[123] A possible reaction mechanism of the Baeyer–Villiger oxidation can be considered as follows:[124] (i) autoxidation of benzaldehyde with molecular oxygen affording per-

benzoic acid (Eq. 27-2) and (ii) oxygen transfer from perbenzoic acid to ketone, which undergoes rearrangement to give the corresponding lactone, and benzoic acid (Eqs. 27-1, 27-3).

$$\text{step 1} \qquad (27\text{-}2)$$

$$\text{step 2} \qquad (27\text{-}3)$$
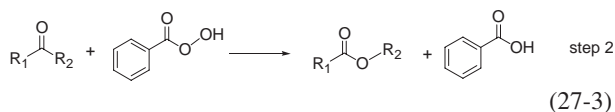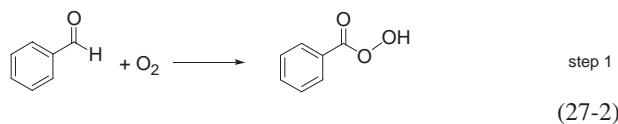
To ensure the role of base sites of hydrotalcites in the heterogeneous Baeyer–Villiger oxidation, various hydrotalcites with different base properties were prepared and used as catalysts for the oxidation of cyclopentanone to δ-valerolactone as a model reaction.[125] The base property of hydrotalcites can be precisely tuned by changing the Mg/Al ratio and the content of interlayer anion species, e.g., CO_3^{2-}, Cl^-, and SO_4^{2-} (Chart 3, type D). The amount of base sites of the hydrotalcites was measured by the zeta-potential method and calorimetric heat of benzoic acid adsorption.[126] We found that the yields of δ-valerolactone increase as the calorimetric heats of benzoic acid adsorption and zeta-potential increase; the hydrotalcites with a large number of base sites gave high catalytic activities. The Baeyer–Villiger oxidation of cyclopentanone was carried out using *m*-CPBA instead of O_2/benzaldehyde as an oxidant with and without the hydrotalcite catalyst. Oxidation in the presence of the hydrotalcite catalyst gave a higher yield of δ-valerolactone than without the hydrotalcite. Yields of δ-valerolactone were 80 and 23% with and without the hydrotalcite catalyst, respectively, after only 1 h. Furthermore, the product yield in the Baeyer–Villiger oxidation of cyclopentanone using *m*-CPBA also correlates with the base amount of hydrotalcites. These facts support the suggestion that hydrotalcites strongly promote the step of oxygen transfer from perbenzoic acid to ketone (step 2).[127] Scheme 5 shows a possible mechanism of the Baeyer–Villiger oxidation catalyzed by base sites of the hydrotalcite surface. Autoxidation of benzaldehyde with O_2 produces perbenzoic acid, and the reaction of the base

OH group on the hydrotalcite surface with perbenzoic acid gives a metal perbenzoate species and H_2O. Then, the perbenzoate species attacks ketone to form a metal alkoxide intermediate, which further reacts with H_2O to convert into lactone or ester accompanied with the formation of benzoic acid and the fresh hydrotalcite surface.

We also found that the catalysis of base hydrotalcites in the heterogeneous Baeyer–Villiger oxidation using O_2 and benzaldehyde was significantly improved by introducing transition metals, e.g., Fe and Cu, into the Brucite-like layer to form multi-metallic hydrotalcite catalysts (Chart 3, type B).[128,129] In particular, Mg–Al–Fe–CO_3 hydrotalcite efficiently oxidized various cyclic ketones to give high yields of the corresponding lactones, while in the case of Mg–Al–Cu–CO_3 hydrotalcite, bicyclic ketones were oxidized almost quantitatively. The improved catalytic activity of multi-metallic hydrotalcites could be ascribed to the cooperative action originating from base sites and transition-metal sites. The concept of the above multi-metallic hydrotalcite catalysts has been developed for creating highly functionalized hydrotalcites for alcohol oxidation and one-pot synthesis (see; sections **3.2** and **3.3**).

3.1.2 Epoxidation of Alkenes Using Hydrogen Peroxide by Base Hydrotalcite Catalyst: Epoxides are an important class of industrial chemical products that have been used as versatile chemical intermediates.[130] A number of epoxidation processes in the presence of various catalysts and oxidants have been extensively developed.[131] However, a chlorine-based noncatalytic processes such as the chlorohydrin method, and catalytic processes using expensive oxidants, including organic peroxides and peracids, are still used frequently. Hydrogen peroxide is a preferable "green" oxidant because it has a high content of active oxygen, and is rather inexpensive compared with organic peroxides and peracid. Furthermore, H_2O_2 is converted into H_2O as a sole coproduct by releasing an oxygen atom to a substrate. Since hydrogen peroxide is commonly purchased as a 30–60% aqueous solution for safety reasons, development of a water-tolerant catalytic system is needed.[132]

Hydrogen peroxide is often used under base conditions, in which it acts as an active hydrogenperoxide ion (HOO^-).[133,134] By the use of the basicity of the hydrotalcite surface, hydrogen
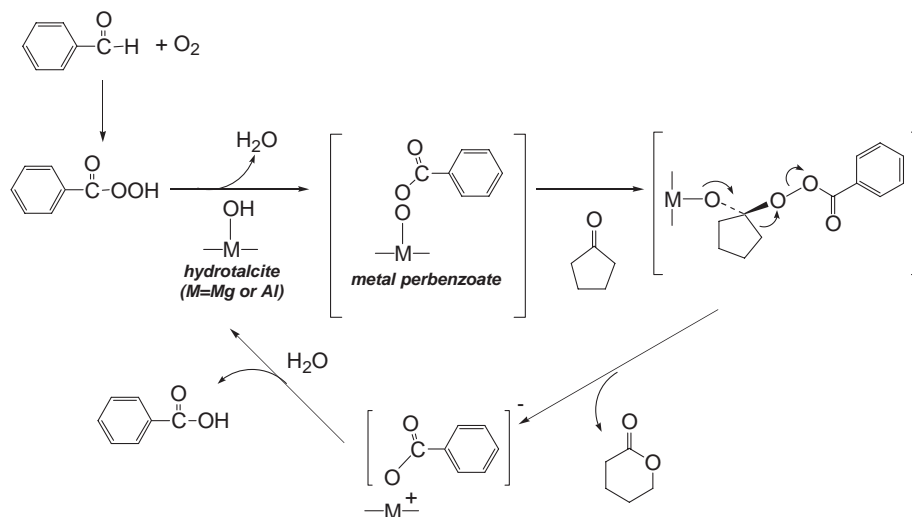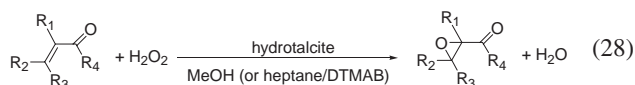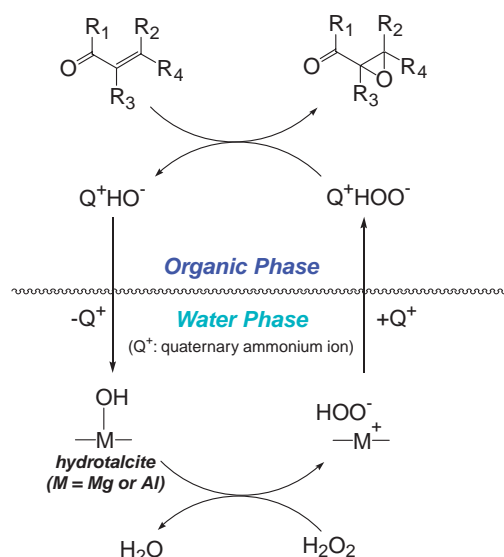

Scheme 5.

peroxide can act as an effective oxidant for monooxygenation-type reactions, e.g., epoxidation of various olefins.[135] Concerning the epoxidation of olefins using hydrogen peroxide in the presence of hydrotalcite catalysts, shape-selective epoxidation was observed in the case of polyoxometalate-intercalated hydrotalcite.[113e] The selectivity for epoxides was, however, extremely low due to the formation of diols and oxolanes by successive cleavage of the epoxides.[136] Notably, our oxidation systems using hydrotalcites exclusively give epoxides without other oxidation products.

3.1.3 Epoxidation of α,β-Unsaturated Ketones: In contrast to the electrophilic epoxidation of common olefins, nucleophilic oxidants are required for the epoxidation of electron-deficient olefins. It is well known that the epoxidation of α,β-unsaturated ketones using hydrogen peroxide under alkaline conditions proceeds by nucleophilic attack of the HOO^- on olefin carbons. We found that the hydrotalcites efficiently catalyzed the epoxidation of various α,β-unsaturated ketones using hydrogen peroxide under mild reaction conditions (Eq. 28).

$$R_2\overset{R_1}{\underset{R_3}{=}}\overset{O}{\underset{}{}}R_4 + H_2O_2 \xrightarrow[\text{MeOH (or heptane/DTMAB)}]{\text{hydrotalcite}} R_2\overset{R_1}{\underset{R_3}{}}O\overset{O}{}R_4 + H_2O \quad (28)$$

Oxidation of various α,β-unsaturated ketones using $Mg_{10}Al_2(OH)_{24}CO_3$ was carried out in methanol solution at 40 °C. Simple cyclic enones such as cyclopentenone and cyclohexenone could be smoothly oxidized into the corresponding epoxyketones. 2-Cyclohexen-1-one was converted into 2,3-epoxycyclohexanone in 91% yield after 5 h. A β-substituted cyclohexenone of 3-methyl-2-cyclohexen-1-one gave a quantitative yield of the corresponding epoxyketone when the reaction time was prolonged to 24 h. It is said that selective epoxidation of cyclopentenone is not attainable under base conditions using NaOH because of the competing aldol-type condensation. Notably, in our catalytic system using base hydrotalcites, 97% of 2,3-epoxycyclopentanone could be obtained from 2-cyclopenten-1-one after 3 h without formation of the aldol products. However, the epoxidation of chalcone resulted in only 57% yield of 2,3-epoxy-1,3-diphenylpropanone after 24 h. Reactivity of the above α,β-unsaturated ketones can be explained in terms of orbital energies in the LUMO, i.e., electrophilicity of the enones.[137,138]

The epoxidation described above consists of three phases: an organic phase of ketones, an aqueous phase of hydrogen peroxide, and solid hydrotalcites. It is well known that in a biphasic medium, surfactants enhance the rates of many organic reactions due to increasing the contact area of the interfacial boundary between water and the organic phase.[132b,139] The effect of various surfactants on the epoxidation of chalcone was examined in *n*-heptane solvent. Interestingly, the use of a cationic surfactant having long alkyl chain such as [CH₃-(CH₂)₁₁N(CH₃)₃]Br (DTMAB) and [CH₃(CH₂)₁₅N(CH₃)₃]Br gave high yields of 2,3-epoxy-1,3-diphenylpropanone, while [*n*-C₄H₉)₄N]Br and [CH₃(CH₂)₇N(CH₃)₃]Br, having a short alkyl chains, were not effective. Both an anionic surfactant [CH₃(CH₂)₁₁SO₄]Na and a nonionic surfactant of sorbitan monolaurate did not promote the epoxidation. Under our phase-transfer conditions, a HOO^- species might move into

Scheme 6.

the organic phase by forming an ion pair such as a Q^+HOO^- species in order to react with a lipophilic enone substrate (Scheme 6). The long alkyl chains of cationic surfactants bring about an increase in the lipophilicity of cationic surfactant molecules, which facilitates the transfer of a lipophilic enone from the organic phase to the interface at the reaction zone.

The phase-transfer procedure using DTMAB could be widely applied to the epoxidation of various α,β-unsaturated ketones (Table 14). The reaction of common open-chain α,β-unsaturated ketones, such as 4-hexen-3-one and 3-nonen-2-one, proceeded smoothly to give epoxyketones in high yields. It is said that the epoxidation of isophorone does not easily proceed due to the steric hindrance of the β-substituted methyl group and *gem*-dimethyl group. Notably, we found that isophorone could be efficiently oxidized into epoxyisophorone in 95% yield (Entry 7). In the case of (R)-$(-)$-carvone, which contains two reactive olefinic double bonds, this hydrotalcite regioselectively oxidized the conjugated double bond to afford 2,3-epoxy-5-isopropenyl-2-methylcyclohexanone, with one diastereomer and *cis* configuration of the methyl group to the isopropenyl group, obtained as the main product (Entry 8).

Yields of the epoxyketone in the reaction of isophorone increased with increasing the basicity evaluated by heat of benzoic acid adsorption on hydrotalcites. The base sites derived from the surface hydroxy groups on hydrotalcites may play an important role in this selective epoxidation. The use of NaOH as a water-soluble base catalyst resulted in low selectivity due to an oxidative cleavage of the epoxyketone to form 3,3-dimethyl-5-oxohexanoic acid.

Hydrotalcites have been conventionally prepared from nitrates or chlorides of magnesium and aluminium under base conditions.[112] Highly active base hydrotalcite catalysts were prepared from MgO and Al_2O_3,[140] HT(MO), for the epoxidation of various α,β-unsaturated ketones using hydrogen peroxide.[135b] HT(MO) showed much higher activity for many α,β-unsaturated ketones than the conventional hydrotalcite, MgO, $Mg(OH)_2$, Al_2O_3, and $Al(OH)_3$.[141] The activity of HT(MO) was significantly greater than that of a physical mixture of MgO and Al_2O_3. Notably, even with low concentrations of hy-

Table 14. Epoxidation of Various α,β-Unsaturated Ketones Catalyzed by $Mg_{10}Al_2(OH)_{24}CO_3$ Using H_2O_2 under Phase-Transfer Conditions with DTMAB[a)]

Entry	Substrate	Product	Time /h	Convn. /%[b)]	Yield /%[b)]
1			4	95	80[c)]
2			4	99	96
3			6	95	94(70)
4	Ph	Ph	24	79	72(70)
5	Ph Ph	Ph Ph	2	99	99(82)
6			3.5	95	92
7			24	97	95(73)
8			24	99	99(80) (*cis/trans* = 96:4)

a) Reaction conditions: substrate (2 mmol), $Mg_{10}Al_2(OH)_{24}$-CO_3 (0.15 g), 30% aq H_2O_2 (0.9 mL, 8 mmol), *n*-heptane (5 mL), DTMAB (0.3 mmol), water (3 mL), 40 °C, b) Determined by GC or HPLC using an internal standard technique. Values in parentheses are isolated yields. For the isolation experiment, the reaction scale was three times as much as that of reaction consitions a). c) Yields were determined by ^{1}H NMR of the reaction mixture. 3-Hydroxy-3,3,5-trimethyl-1,2-dioxolane was also formed in 13% yield.

drogen peroxide, this HT(MO) catalyst had high activity for epoxidation without organic solvents. For example, reaction of 2-cyclopenten-1-one using 1.5 equivalents of 5% H_2O_2 for 2 h gave the corresponding epoxyketone in 94% yield (Eq. 29). Using 5% H_2O_2, other cyclic enones such as 3-methyl-2-cyclopenten-1-one, 2-cyclohexen-1-one, and 3-methyl-2-cyclohexen-1-one were also smoothly epoxidized in high yields.

$$\text{(Eq. 29)}\quad \xrightarrow[\text{HT(MO), 2h}]{\text{1.5 equiv. of 5\% aq.H}_2\text{O}_2} \quad 94\% \tag{29}$$
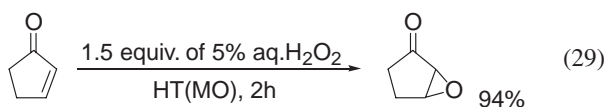
3.1.4 Epoxidation of Common Olefins: In a previous epoxidation of α,β-unsaturated ketones, the reaction of hydrogen peroxide with base sites on the hydrotalcite surface gave a HOO^- anion species. In the presence of nitriles, the HOO^- can react with the nitrile to form peroxycarboximidic acid, the oxygen being transferred into an olefin to produce an epoxide together with a carboxyamide.[134] We found that the hydrotalcite catalyzed the oxidation of common olefins using hydrogen peroxide in the presence of nitriles to afford the corresponding epoxides in excellent yields.[142] Notably, this epoxidation system has a high catalytic activity, especially for the terminal olefins.

Table 15. Epoxidation of Various Olefins Using H_2O_2 and PhCN Catalyzed by Ketones Catalyzed by $Mg_{10}Al_2$-$(OH)_{24}CO_3$[a)]

Entry	Substrate	Convn./%[b)]	Yield/%[b)]
1		95	95
2	Ph	91	91
3		100	>99
4		100	94
5		100	>99
6		99	95
7		94	93
8		100	96

a) Reaction conditions: substrate (4 mmol), $Mg_{10}Al_2(OH)_{24}$-CO_3 (0.05 g), PhCN (10.5 mmol), 30% aq H_2O_2 (2.4 mL, 21 mmol), MeOH (10 mL), 60 °C, 24 h. b) Yields of epoxides were determined by GC using an internal standard method based on the olefin.

Nitriles, hydrogen peroxide, and hydrotalcites were indispensable components for this oxidation system. Among the nitriles used, benzonitrile was the most effective and methanol was the best solvent. Table 15 shows the oxidation of olefins with H_2O_2 and benzonitrile catalyzed by the most active hydrotalcite, $Mg_{10}Al_2(OH)_{24}CO_3$, in methanol. Common linear and cyclic olefins gave the corresponding epoxides as the sole products in excellent yields. Remarkably, styrene was oxidized into styrene oxide in a high yield without formation of other oxidation products, e.g., acetophenone and benzaldehyde. Norbornene afforded only *exo*-norbornene oxide in a quantitative yield. The *cis* and *trans* olefins gave the corresponding epoxides stereospecifically, with retention of the configuration of double bonds.

A possible reaction mechanism for this epoxidation is shown in Scheme 7. First, hydrogen peroxide reacts with a base site on the hydrotalcite surface to form a HOO^- species, which attacks a nitrile to generate a peroxycarboximidic acid as an active intermediate oxidant. Then, the oxygen of the peroxycarboximidic acid is transferred to an olefin.

Interestingly, the resultant amide can be further employed for the epoxidation of olefins in the presence of hydrotalcite catalysts.[142b] For example, the epoxidation of various olefins using isobutyramide instead of benzonitrile proceeded efficiently to afford the corresponding epoxides in excellent yields (Eq. 30).

$$\begin{array}{c} R_1 \quad R_2 \\ R_3 \quad R_4 \end{array} + H_2O_2 \xrightarrow[\text{SDS, solvent}]{\text{isobutyramide, hydrotalcite}} \begin{array}{c} R_1 \quad O \quad R_2 \\ R_3 \quad R_4 \end{array} + H_2O \tag{30}$$
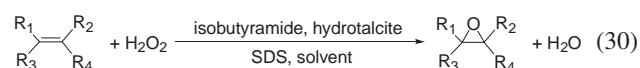
Using the above monooxygenation catalytic system, we found that various pyridines were efficiently oxidized to yield the corresponding pyridine *N*-oxide, as shown in Eq. 31.[142c]

$$\text{pyridine-X} + H_2O_2 \xrightarrow[\text{MeOH, 60°C}]{\text{benzonitrile, hydrotalcite}} \text{pyridine-N}^+\text{-X} + H_2O \tag{31}$$
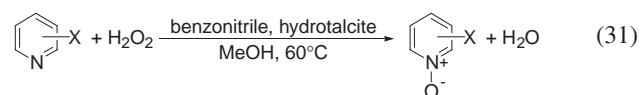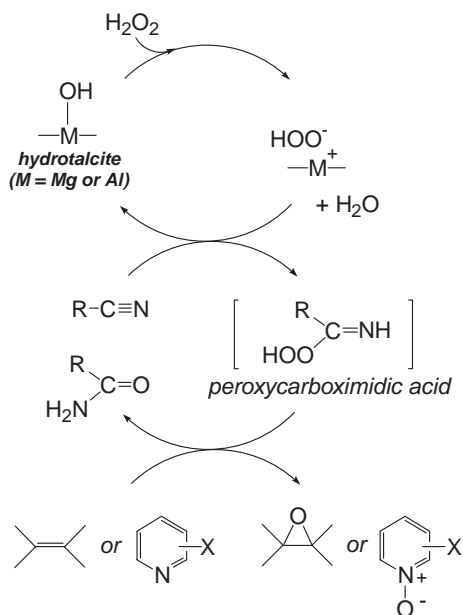
Scheme 7.

In this oxidation system, the corresponding pyridine N-oxides were exclusively obtained without other oxidation products. For example, 4-pyridylcarbinol was oxidized to give 4-pyridylcarbinol N-oxide without formation of other oxidation products, e.g., pyridinealdehyde and pyridine carboxylic acid, while the use of m-CPBA resulted in the formation of a mixture of 4-pyridylcarbinol N-oxide and 4-pyridinecarboxylic acid (9:1). It is notable that excellent efficiency in the hydrogen peroxide utilization toward oxidation products was attained in this catalytic system; the yield of pyridine N-oxide based on the consumed hydrogen peroxide reached 70%.

3.2 Aerobic Alcohol Oxidation.   As mentioned in section **2.1**, selective oxidations of alcohols to the corresponding carbonyl compounds using molecular oxygen as an oxidant by heterogeneous catalysts has attracted much attention from the standpoint of GSC.[11,12,143] This section summarizes the development of immobilized ruthenium catalysts as an active center for aerobic alcohol oxidation using the cation-exchange ability and adsorption capacity of the hydrotalcite (Chart 3, types B, C, E, and F).

3.2.1 Functionalization of Ru-Hydrotalcite Catalysts: Various kinds of Mg–M$_1$–Al–A$_n$ type hydrotalcites (M$_1$: transition metal, A$_n$: interlayer anion, Mg:Al:M$_1$ = 3:1:0.3) were synthesized and examined as catalysts for the oxidation of cinnamyl alcohol in toluene using molecular oxygen. Hydrotalcites containing Ru in the Brucite-like layer showed the highest catalytic activity for oxidation among the hydrotalcites containing other transition metals such as Fe, Ni, Mn, V, Cr, and Co. The most effective anion in the interlayer of the Mg–Al–Ru–A$_n$ was the CO$_3{}^{2-}$ ion. Mg–Al–Ru–CO$_3$ was an effective catalyst for the oxidation of aromatic allylic and benzylic alcohols.[144a] For example, cinnamyl alcohol afforded a 95% yield of cinnamaldehyde after 8 h. The XPS and Ru K-edge XAFS analyses showed that the monomeric Ru^{3+} cations are surrounded by six hydroxy groups, suggesting a partial substitution of Al cations with Ru^{3+} species at the octahedral sites in the Brucite-like layer of the hydrotalcite.

Table 16. Oxidation of Cinnamyl Alcohol with Various M′–Al–Ru–CO$_3$ Type Hydrotalcites[a]

Entry	Catalyst	Convn./%[b]	Yield/%[b]
1	Co–Al–Ru–CO$_3$	100	94
2	Mn–Al–Ru–CO$_3$	99	92
3	Fe–Al–Ru–CO$_3$	64	50
4	Zn–Al–Ru–CO$_3$	23	23
5	Mg–Al–Ru–CO$_3$	31	20
6	Co–Al–CO$_3$ + Mg–Al–Ru–CO$_3$[c]	33	22

a) Reaction conditions: cinnamyl alcohol (2 mmol), catalyst (0.3 g), toluene (5 mL), O$_2$ flow, 60 °C, 40 min. b) Determined by GC using an internal standard technique. c) Physical mixture of the two catalysts which contained the same amounts of Ru and Co as Entry 1.

It was found that the catalytic activity of Mg–Al–Ru–CO$_3$ was greatly enhanced by replacing Mg cations in the Brucite-like layer by other cations M$_2$ (M$_2$:Al:Ru = 3:1:0.3).[144b] The effect of metal cations of the M$_2$–Al–Ru–CO$_3$ hydrotalcite on the aerobic oxidation of cinnamyl alcohol is shown in Table 16. The introduction of the Co cation led to the highest yield of cinnamaldehyde (Entry 1). The Co–Al–CO$_3$ hydrotalcite (Co:Al = 3:1) hardly catalyzed the oxidation at all, and the catalytic activity of Co–Al–Ru–CO$_3$ was much higher than that of a physical mixture of the Co–Al–CO$_3$ and Mg–Al–Ru–CO$_3$ (Entry 1 vs 6). Therefore, it is likely that the prominent catalytic properties of Co–Al–Ru–CO$_3$ may be ascribed to a synergism from the interaction of Co and Ru cations. The XPS and Ru K-edge XAFS analyses showed that isolated Ru^{4+} cations are incorporated into the Brucite-like layer. The Ru^{4+} species in Co–Al–Ru–CO$_3$ might be formed by the redox interaction between the neighboring Ru^{3+} and Co^{3+} cations; the Co^{3+} cation can oxidize Ru^{3+} to Ru^{4+}.

Co–Al–Ru–CO$_3$ efficiently catalyzed the oxidation of various alcohols, including aromatic allylic, benzylic, secondary saturated alcohols, to the corresponding carbonyl compounds in high yields.[144b] Interestingly, the Co–Al–Ru–CO$_3$ catalyst could also efficiently oxygenate at benzylic positions of aromatic compounds, such as diphenylmethane, fluorene, and xanthene, to give the corresponding ketones (Scheme 8). The above two Ru-hydrotalcite catalysts were applicable to the oxidation of alcohols with high reactivity such as allylic and benzylic alcohols; however, the less-reactive aliphatic primary alcohols could not be efficiently oxidized.
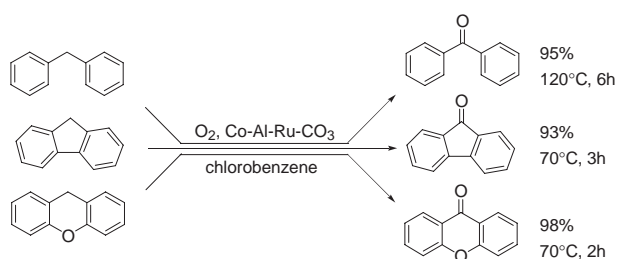
Scheme 8.

For the oxidation of aliphatic primary alcohols into the corresponding carboxylic acids, stoichiometric amounts of hazardous and/or toxic inorganic oxidants that generate copious amounts of environmentally damaging wastes are used even at present.[145] Therefore, the development of catalytic systems for the aerobic oxidation of aliphatic primary alcohols using O_2 at atmospheric as the sole oxidant still remains as a challenging task in this field. We found that the Co–Ce–Ru system acted as a highly efficient and heterogeneous catalyst for the one-pot synthesis of carboxylic acids from primary alcohols without any additives.[144c,d]

Co–Ce–Ru could efficiently catalyze the allylic, benzylic, and aliphatic secondary alcohols in the presence of molecular oxygen in high yields. The above results have encouraged us to apply the Co–Ce–Ru catalyst to the oxidation of less-reactive aliphatic primary alcohols. To evaluate the catalytic properties of Co–Ce–Ru, the oxidation of 1-octanol was carried out using various Ru catalysts under an O_2 atmosphere, and the results are listed in Table 17. Among the hydrotalcite- and hydroxyapatite-immobilized Ru catalysts, and Ru/CeO$_2$,[146] Co–Ce–Ru exhibited the highest catalytic activity for the oxidation of 1-octanol into octanoic acid. In the cases of Mg–Ce–Ru–CO$_3$ and Mg–Al–Ru–CO$_3$ catalysts, the conversion of 1-octanol was low and gave only octanal as a product.

Using Co–Ce–CO$_3$ without the Ru component, the oxidation of 1-octanol scarcely proceeded. It is suggested that a combination of Ru with both Co and Ce elements is necessary to achieve a high yield of carboxylic acid. Obviously, the Ru species acts as a catalytically active site for this alcohol oxidation and the Co component plays an essential role in the production of carboxylic acid.[147]

Subsequently, the Co–Ce–Ru catalyst was applied to the oxidation of aliphatic primary alcohols, and typical results are shown in Table 18. Linear primary alcohols were readily oxidized to the corresponding carboxylic acids in excellent yields without formation of esters (Entries 1 and 2), whereas branched and cyclic primary aliphatic alcohols were oxidized in moderate yields (Entries 3–5). A 20 mmol-scale oxidation of 1-octanol proceeded at 80 °C to afford octanoic acid in 90% yield after 30 h. The high chemoselectivity for the primary hydroxy function is exemplified in the intramolecular competitive oxidation of 1,4-pentanediol, affording methyl-γ-butyrolactone in 87% yield at 80 °C after 6 h (Entry 6).

To the best of our knowledge, the Co–Ce–Ru catalyst is the most effective catalyst for one-pot oxidation of primary aliphatic alcohols into carboxylic acids using O_2 atmospheric pressure as the sole oxidant. Although the use of other homogeneous transition-metal complexes and heterogeneous catalysts can also achieve the effective oxidation of primary alcohols using O_2 as a sole oxidant, the major products are aldehydes; only a few reports can be found on the selective formation of carboxylic acid.[17c,22,146,148]

An efficient transformation of aldehyde to carboxylic acid may involve a free radical process associated with the Co species, since octanal was formed quantitatively without formation of octanoic acid when 2,6-di-*tert*-butyl-*p*-cresol was added as a radical scavenger in the oxidation of 1-octanol using

Table 17. Effect of Catalysts in Aerobic Oxidation of 1-Octanol[a]

Entry	Catalyst	Convn. /%[b]	Yield/%[b] Octanoic acid	Octanal
1	Co^{III}–Ce^{IV}–Ru^{IV}	100	97	1
2	Co–Al–Ru–CO$_3$	90	63	26
3	Ru/CeO$_2$[c]	30	28	0
4	Mg–Ce–Ru–CO$_3$	58	1	48
5	RuHAP[d]	95	0	94
6	Mg–Al–Ru–CO$_3$	16	0	15
7	Co–Ce–CO$_3$	<2	0	<1

a) Reaction conditions: 1-octanol (2 mmol), catalyst (0.3 g, Ru: 6 wt %), trifluorotoluene (5 mL), O_2 flow, 60 °C, 4 h.
b) Determined by GC using an internal standard technique.
c) Prepared by literature procedure (Ref. 146). d) Cited from Ref. 4a; RuHAP (0.2 g), 16 h.

Table 18. Oxidation of Primary Alcohols by Co–Ce–Ru Catalyst Using Molecular Oxygen[a]

Entry	Substrate	Product	Time/h	Convn./%[b]	Yield/%[b]
1	$\sim\!\!\sim\!\!\sim$CH$_2$OH	$\sim\!\!\sim\!\!\sim$CO$_2$H	4	95	97(90)
2	CH$_2$OH (15)	CO$_2$H (15)	5	99	82(78)
3[c]	CH$_2$OH	CO$_2$H	14	95	79
4	CH$_2$OH	CO$_2$H	24	79	64
5	CH$_2$OH	CO$_2$H	5	99	85(80)
6[d]	CH$_2$OH, OH	$O\!\!=\!\!$ lactone	4	95	87

a) Reaction conditions: substrate (2 mmol), Co–Ce–Ru (0.3 g, Ru: 0.20 mmol), trifluorotoluene (5 mL), O_2 flow, 60 °C. b) Determined by GC, LC, or GCMS using an internal standard technique. Values in parentheses are isolated yields using 20 mmol of substrate. c) Deionized water (0.2 mL) was added. d) Diol (1 mmol), 80 °C.

the Co–Ce–Ru catalyst. It is well known that the Co^{III} species mediates the formation of peracids by a radical chain reaction of aldehydes with molecular oxygen.[149] Aliphatic aldehyde reacts with the surface Co^{III} species to give an acyl radical, RC•(O), a Co^{II} species and H$^+$ (Eq. 32). Reaction of an acyl radical with molecular oxygen affords an acylperoxy radical that abstracts a hydrogen from the aldehyde to give the peracid, RC(O)OOH (Eqs. 33 and 34). The Co^{III} species is regenerated by the reaction of the peracid and the Co^{II}/H$^+$ together with formation of carboxylic acid and H$_2$O (Eq. 35).

$$RCHO + Co^{III} \rightarrow RC{\bullet}(O) + Co^{II} + H^+, \qquad (32)$$

$$RC{\bullet}(O) + O_2 \rightarrow RC(O)OO{\bullet}, \qquad (33)$$

$$RC(O)OO{\bullet} + RCHO \rightarrow RC(O)OOH + RC{\bullet}(O), \qquad (34)$$

$$RC(O)OOH + 2Co^{II} + 2H^+$$
$$\rightarrow RCOOH + 2Co^{III} + H_2O. \qquad (35)$$
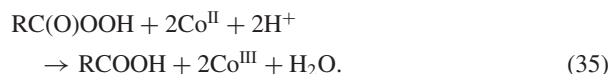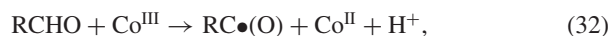
Correspondingly, Co–Ce–Ru efficiently catalyzed the oxidation of aliphatic aldehydes into the carboxylic acids even at room temperature.[144c] The peracid may participate in the oxidation of alcohol in combination with the Ru species,[149b] and in the reoxidation of the Ce^{II} to Ce^{IV} species. It is notable that Co–Ce–Ru serves as a unique heterogeneous catalyst that generates radical species under mild reaction conditions.

3.2.2 Aerobic Oxidation of Alcohols Catalyzed by Ru/Hydrotalcite: The effectiveness of the Ru species in the above hydrotalcite-based catalyst systems seems to be insufficient because the Ru cations in the Brucite-like layer are mostly located within the crystalline structure. Accordingly, the formation of the Ru species on the surface of hydrotalcite should provide solid catalysts with high utilization efficiency for the Ru element. We employed a triad of hydroxy groups of the hydrotalcite surface for the immobilization of Ru cations as the active species to form a Ru/Mg–Al–CO$_3$ catalyst (Chart 3, type E). Ru/Mg–Al–CO$_3$ was prepared simply by treating Mg–Al–CO$_3$ with an aqueous solution of RuCl$_3\cdot$ nH$_2$O at room temperature. The XAFS analysis showed that a monomeric Ru(IV) species having one hydroxy and two aqua ligands is grafted onto a triad of oxygen atoms on the hydrotalcite surface.[144e]

The yield of benzaldehyde in the oxidation of benzylalcohol catalyzed by Ru/Mg–Al–CO$_3$ was nearly five times that of Mg–Al–Ru–CO$_3$, and similar to that of the trimetallic Co–Ce–Ru catalyst. The high catalytic activity of Ru/Mg–Al–CO$_3$ was attributed to the greater utilization efficiency of the Ru species with high-valence states on the surface of the hydrotalcite crystalline as well as the potential coordinative unsaturation of the Ru species. Additionally, the basicity of the hydrotalcite surface may provide a preferable situation for the alcohol oxidation; bases such as K$_2$CO$_3$, amines, and NaOH, facilitate the deprotonation of alcohols to give a metal–alkoxide intermediate species (vide infra). A cooperative action between the Ru species and the base sites for one-pot sequential reactions is described in Section **3.3.1**.

Modifying the coordination sphere of a metal species with other metals as ligands, which is a basic approach in organometallic and bioinorganic chemistry,[150] is also being applied to heterogeneous catalysis because of the potential of performing unique catalytic reactions based on cooperation between
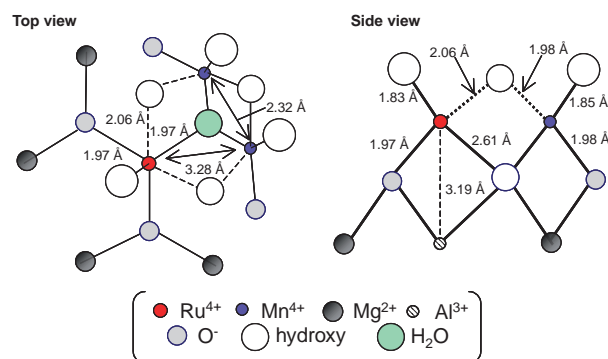

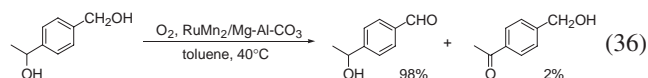Fig. 11. Proposed structure of heterometallic RuMnMn complex on the hydrotalcite.

diverse metal functions within a regular arrangement.[151] We prepared a novel HT-bound heterotrimetallic Ru^{IV}Mn^{IV}Mn^{IV} species (RuMn$_2$/Mg–Al–CO$_3$, Chart 3, type F), structurally characterized on the atomic scale, for highly efficient oxidation of various alcohols to the corresponding carbonyl compounds under O$_2$ at atmospheric pressure and mild reaction conditions.[144g]

We obtained well-defined and robust heterometallic RuMnMn species on the Mg–Al–CO$_3$ surface by immobilizing Mn cations onto Ru/Mg–Al–CO$_3$. The retention of the HT interlayer distance (3.0 Å), as shown by XRD, indicated that both metal species are accommodated on the HT surface. The K-edge XANES spectrum of the Ru and Mn of RuMn$_2$/Mg–Al–CO$_3$ reveals that the surface Ru and Mn cations are in the oxidation state +IV. The curve-fitting analysis of the Fourier transformation of the k^3-weighted EXAFS shows a Ru^{IV}Mn^{IV}Mn^{IV} trimetallic species on the HT surface, as shown in Fig. 11, in which dimeric Mn–Mn species are connected to a single Ru^{IV} cation through OH groups and water. To our knowledge, this is the first report of the preparation of heterometallic species consisting of metal cations on a support involving metal oxide and metal hydroxides, although the preparation of supported heterobimetallic or metal alloy species have been reported.[152] Adjusting the basicity of the hydroxy groups around the Ru^{IV} cation, which were produced by reaction of the surface OH groups of HT with RuCl$_3$ species, brought about selective immobilization of Mn cations in the vicinity of the Ru species to give the unique Ru^{IV}Mn^{IV}Mn^{IV} sites.

The trimetallic RuMn$_2$/Mg–Al–CO$_3$ shows a higher catalytic activity than the above Ru/Mg–Al–CO$_3$, Ru/Al$_2$O$_3$,[24] and RuO$_2$,[143a] which are typical heterogeneous Ru catalysts for the oxidation of benzyl alcohol. Benzyl alcohol was oxidized to benzaldehyde quantitatively within 1 h in the presence of the RuMn$_2$/Mg–Al–CO$_3$ catalyst. The initial turnover frequency based on Ru for RuMn$_2$/Mg–Al–CO$_3$ (140 h^{-1}) is almost five times larger than that for Ru/Mg–Al–CO$_3$. On a 10 mmol-scale oxidation of benzyl alcohol in the presence of 0.1 mol % Ru, the turnover number based on Ru reached 840 at 90 °C. Moreover, the high catalytic activity of RuMn$_2$/Mg–Al–CO$_3$ was demonstrated by the quantitative oxidation of benzyl alcohol within 10 h, even at 40 °C. The RuMn$_2$/Mg–Al–CO$_3$ catalyst selectively oxidized a wide variety of alcohols including primary and secondary benzylic and aromatic allylic alcohols. In the case of cyclopropyl(phenyl)methanol,

the hydroxy group was oxidized without cleavage of the cyclo-propyl ring. Notably, RuMn$_2$/Mg–Al–CO$_3$ effectively catalyzed the oxidation of (2-hydroxymethyl)thiophene, a hetero-aromatic alcohol to 2-thiophenecarboxaldehyde in high yield, and the oxidation of 2-aminobenzyl alcohol to 2-aminobenzaldehyde, quantitatively, in contrast to the homogeneous complexes of Pd and Ru.[15,17]

The catalysis is also chemoselective; RuMn$_2$/Mg–Al–CO$_3$ preferentially oxidized primary over secondary hydroxy groups, as shown by the selective oxidation of 1-[(4′-hydroxy-methyl)phenyl]ethanol to 1-[(4′-formyl)phenyl]ethanol in 98% yield (Eq. 36).

$$\text{[structure]} \xrightarrow[\text{toluene, 40 °C}]{\text{O}_2,\ \text{RuMn}_2/\text{Mg-Al-CO}_3} \text{[structure]}\ 98\% + \text{[structure]}\ 2\% \quad (36)$$

The spent RuMn$_2$/Mg–Al–CO$_3$ could be readily separated from the reaction mixture by filtration. The EXAFS spectrum of the recovered RuMn$_2$/Mg–Al–CO$_3$ catalyst confirmed retention of the original RuMnMn structure, and ICP analysis of the filtrate indicated no leaching of Ru and Mn species during the oxidation. The RuMn$_2$/Mg–Al–CO$_3$ catalyst could be reused while maintaining high catalytic activity and selectivity. When the catalyst was removed at about 50% conversion of alcohol, no further oxidation was detected, which shows that the present alcohol oxidation proceeds at the interface between the catalyst surface and the liquid phase.

The Mn cations in the RuMnMn species evidently play a pivotal role in improving the Ru-catalyzed alcohol oxidation since Mn$_2$/Mg–Al–CO$_3$ does not catalyze the reaction. We have proposed a catalytic cycle for the alcohol oxidation (Scheme 9) that proceeds via a ruthenium alkoxide intermediate, which undergoes β-hydrogen elimination to produce the carbonyl compound and a ruthenium hydride species, as observed by IR spectroscopy. Reaction of this hydride species with O$_2$ and subsequent ligand-exchange with the alcohol

Scheme 9.

completes the catalytic cycle.

A rate equation based on a Michaelis–Menten-type model for this proposed mechanism (Eq. 37) agrees well with the kinetic data. For the RuMn$_2$/Mg–Al–CO$_3$-catalyzed oxidation of benzyl alcohol, K_M and k_2 were calculated to be 2.96 nM and 0.047 s^{-1}, respectively, at 60 °C.

$$\text{Ru–OH} + \text{RCH}_2\text{OH} \underset{k_{-1}}{\overset{k_1}{\rightleftharpoons}} [\text{Ru–OCH}_2\text{R}] \overset{k_2}{\rightarrow} \text{R–H} + \text{RCHO}. \quad (37)$$

The rate constant (k_2) of β-hydrogen elimination from the ruthenium alkoxide intermediate is therefore almost twice that for the Mn-free Ru/Mg–Al–CO$_3$. The β-hydrogen elimination is considered to be the rate-determining step in the overall alcohol oxidation due to the primary kinetic isotope effect in the competitive oxidation of benzyl alcohol and C$_6$D$_5$CD$_2$OH (4.2). Thus, the Mn cations in the heterometallic sites facilitate β-hydrogen elimination. Removing the water molecule that binds the Ru and Mn cations improves the situation of the Ru species during β-hydrogen elimination by, for example, producing a coordinatively unsaturated Ru site.

For the secondary alcohol 1-phenylethanol, K_M and k_2 were found to be 133 mM and 0.026 s^{-1}, respectively, at 60 °C. Importantly, the K_M value is significantly greater than that for the oxidation of benzyl alcohol, which is reflected in the preferential oxidation of primary hydroxy groups by this species. The formation of metal alkoxide intermediates of primary alcohols is favored over secondary alcohols in the ligand-exchange step. A similarly high chemoselectivity for primary alcohols has been observed in the Zr(OAc)$_2$-catalyzed oxidation of alcohols.[153]

3.3 One-Pot Syntheses. Multireaction in a single pot is considered as an ideal chemical process due to operational simplicity and the minimization of energy input, time, and reagents.[154,155] A significant problem in one-pot synthesis is the mutual destruction of reagents. To overcome this problem, several attractive methods, for example, the anchoring active sites onto polymers and doping of reactive species into sol–gel materials, have been developed.[156] However, solid reagents still suffer from deactivation by interaction between opposing anchored reagents and require expensive dopants as active sites as well as a tedious preparation method.

Solid catalysts that accommodate various active sites on their surfaces show promise for promoting multiple reactions in a single pot without the destruction of several catalytically active species.[157] This part describes highly efficient one-pot syntheses of α-alkylated nitriles[144e] and quinolines[144f] using the Ru-grafted hydrotalcite, Ru/Mg–Al–CO$_3$ (vide supra), based on the cooperative catalysis between Ru and base sites on the surface of hydrotalcites. The one-pot sequential reactions by combination of heterogeneous acid and base catalysts, e.g., Ti^{4+}-mont and hydrotalcite, are also demonstrated.[158]

3.3.1 Synthesis of α-Alkylated Nitriles and Quinolines Catalyzed by Ru/Mg–Al–CO$_3$: α-Alkylated nitriles are important building blocks in the construction of amides, carboxylic acids, ketones, and biologically active compounds and are traditionally synthesized with alkyl halides using stoichiometric amounts of inorganic bases.[159] Alternatively, catalytic α-alkylation of nitriles with alcohols is particularly attractive from both an economical and environmental point of view.

K. Kaneda et al.

Bull. Chem. Soc. Jpn. Vol. 79, No. 7 (2006)   1007
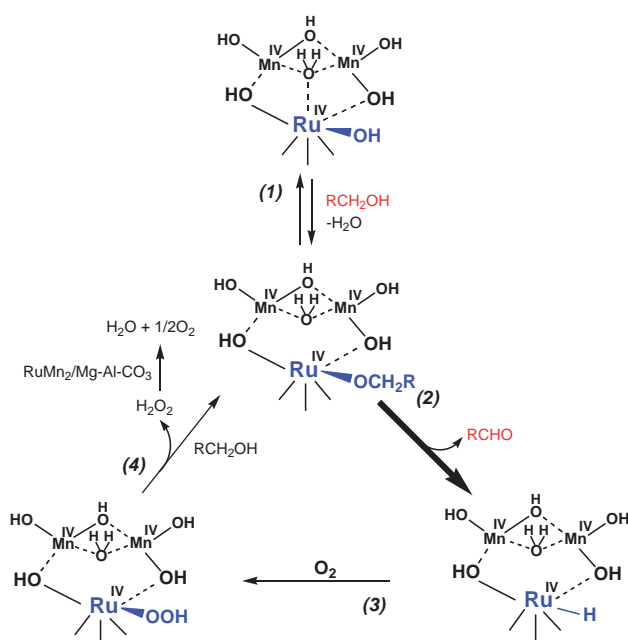
Table 19. Reaction of Phenylacetonitrile (**1a**) with Ethanol (**2a**) by Various Catalysts[a]

Ph–CN + EtOH $\xrightarrow{\text{catalyst}}$ Ph–CH(Et)–CN + Ph–C(=CHCH$_3$)–CN

1a   **2a**   **3a**   **4a**

Entry	Catalyst	Yield/%[b]	
		3a	**4a**
1	Ru/Mg–Al–CO$_3$	98	trace
2[c]	Ru/Mg–Al–CO$_3$	trace	10
3	Ru/Al$_2$O$_3$	14	trace
4	Ru/MgO	2	trace
5	Ru/Al(OH)$_3$	5	16
6	Ru/Mg(OH)$_2$	2	8
7[d]	HT	n.r.[e]	n.r.
8[f]	RuCl$_3 \cdot n$H$_2$O	n.r.	n.r.

a) Reaction conditions: **1a** (1 mmol), **2a** (2 mL), Ru catalyst (0.15 g, Ru: 0.0075 mmol), Ar, 180 °C, 20 h. b) Based on **1a**. c) Under O$_2$. d) 0.15 g of Mg–Al–CO$_3$ was used. e) No reaction. f) 0.0075 mmol of Ru was used.

Y = H, Me, *n*-Pr, *i*-Pr, Ph
X = H, Cl, Me, MeO, 1-naphthyl, 2-thiophenyl
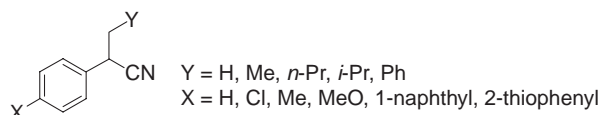
Scheme 10.

Some homogeneous transition-metal complexes accomplish this transformation; however, all such catalysts suffer from either low activity or low stability and also require inorganic bases as additives.[160]

α-Ethylated phenylacetonitrile (**3a**) was obtained by the reaction of phenylacetonitrile (**1a**) with ethanol (**2a**) in the presence of various Ru catalysts under an Ar atmosphere, as shown in Table 19. The Ru/Mg–Al–CO$_3$ catalyst exhibited the highest activity, giving **3a** in 98% yield (Entry 1). The α-alkylation hardly occurred in the presence of only parent Mg–Al–CO$_3$ or RuCl$_3 \cdot n$H$_2$O (Entries 7 and 8). Other heterogeneous Ru catalysts, such as Ru/Al$_2$O$_3$, Ru/MgO, Ru/Mg(OH)$_2$, and Ru/Al(OH)$_3$, were found to be less active (Entries 3–6). For Ru/Mg–Al–CO$_3$, (*Z*)-2-phenylcrotononitrile (**4a**) was obtained as the major product under an O$_2$ atmosphere (Entry 2).

A wide variety of arylacetonitriles efficiently reacted with ethanol, affording the corresponding α-ethylated nitriles in excellent yields, as shown in Scheme 10, without the formation of dialkylated products. The Ru/Mg–Al–CO$_3$ catalyst system was also applicable to a heteroarylacetonitrile including a sulfur atom as a donor. A diverse set of primary alcohols was usable for this α-alkylation reaction; interestingly, the reaction of phenylacetonitrile with *n*-butanol gave 2-phenylhexanonitrile, a precursor of the systemic fungicide Systhane,[159c] in 94% yield.

The Ru/Mg–Al–CO$_3$ catalyst was also found to promote the α-alkylation of carbonyl compounds as a donor (Eq. 38). This is the first report of the α-alkylation of ketones with alcohols achieved using a heterogeneous catalyst.[160] A 20 mmol-scale reaction of phenylacetonitrile with ethanol afforded the corresponding product in 82% yield with a high TOF of 14 h^{-1} and a high TON of 412, which are considerably higher than those

L = a triad of oxy ligand
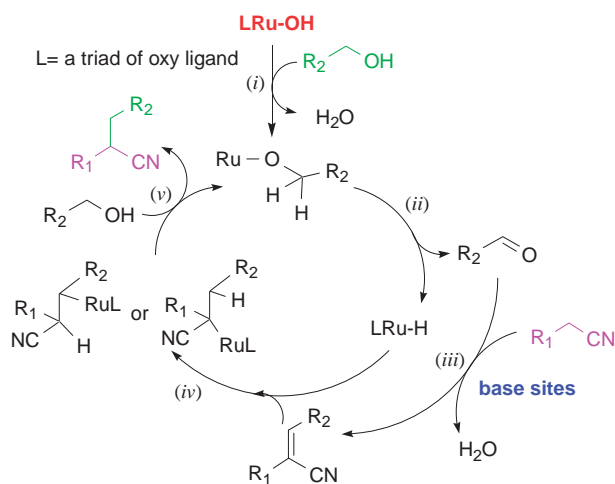
Scheme 11.

of a previously reported homogeneous Ru catalyst combined with a stoichiometric amount of Na$_2$CO$_3$ (TOF, 0.77 h^{-1}; TON, 18).[161]

$$\text{(38)}$$
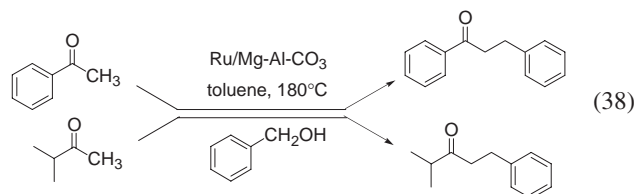
Hydrogen transfer from benzyl alcohol to (*Z*)-2-phenylcinnamonitrile in the presence of Ru/Mg–Al–CO$_3$ yielded 2,3-diphenylpropionitrile along with benzaldehyde.[162] In a separate experiment, the parent Mg–Al–CO$_3$ promoted aldol condensation of phenylacetonitrile with benzaldehyde to afford (*Z*)-2-phenylcinnamonitrile. From the above results, it is reasonable that the present α-alkylation consists of the following three consecutive reactions (Scheme 11): (i, ii) oxidative dehydrogenation of alcohols to aldehydes, (iii) base-catalyzed aldol condensation of nitriles with aldehydes, (iv, v) and hydrogenation of α,β-unsaturated nitriles with a Ru–H species. In the reaction of phenylacetonitrile with benzyl-d_7-alcohol, the deuterium was transferred to the alkylated product. The formation of two deuterated regio-isomers supports the involvement of two different hydride intermediates in the α-alkylation. Upon treatment of Ru/Mg–Al–CO$_3$ with benzyl alcohol, the IR spectrum showed a signal at 2120 cm^{-1} assignable to ν(Ru–H).[15e] Vide supra, the reaction of the Ru–H species with O$_2$ might lead to the exclusive formation of the α,β-unsaturated nitrile (Table 19, Entry 1).

The applicability of the Ru/Mg–Al–CO$_3$ catalyst is highlighted by a one-pot synthesis of α,α-dialkylated phenylacetonitriles (Scheme 12). For example, after completion of the alkylation of phenylacetonitrile with ethanol, acrylonitrile was added and the mixture was allowed to react at 150 °C after 1 h. A base-catalyzed Michael reaction occurred to afford 2-ethyl-2-phenylglutarodinitrile, a highly useful intermediate of the sedative Glutethimide,[159b,d] in 93% yield.

The conventional method for the synthesis of 2-ethyl-2-phenylglutarodinitrile from phenylacetonitrile using iodoethane, NaNH$_2$, and Triton B gave less than 39% yield.[159b]
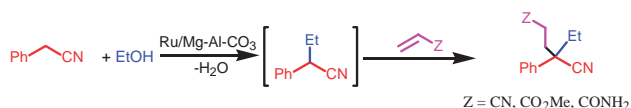
Scheme 12.

For this single-pot synthesis, the Ru species and base sites on the Ru/Mg–Al–CO$_3$ surface participate in four sequential reactions: oxidative dehydrogenation, aldol condensation, hydrogenation, and Michael reaction, finally producing α,α-dialkylated phenylacetonitriles.

The heterogeneous Ru/Mg–Al–CO$_3$ catalyst also enables one-pot quinoline synthesis from 2-aminobenzyl alcohol and various carbonyl compounds in the presence of molecular oxygen (Eq. 39).

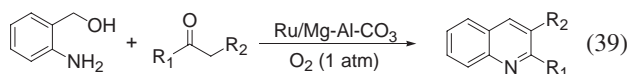Shim and co-workers proposed the direct formation of quinolines from 2-aminobenzyl alcohol and ketones via a hydrogen-transfer reaction and cyclization mediated by a homogeneous Ru complex catalyst system combined with a stoichiometric amount of KOH.[163] This one-pot method is superior to traditional Friedlaender quinoline synthesis[164] because 2-amino-benzyl alcohol is less expensive and more stable than 2-amino-benzaldehyde. Significant advantages of our catalyst system include (i) high catalytic activity and wide applicability to various carbonyl compounds, (ii) no need for homogeneous bases, and (iii) the use of molecular oxygen as a green oxidant.

In the reaction of 2-aminobenzyl alcohol (**5**) with acetophenone in the presence of molecular oxygen, Ru/Mg–Al–CO$_3$ exhibited the highest catalytic activity to give 2-phenylquinoline (**6**) in 87% yield. The reaction hardly occurred using the parent HT, and other solid Ru catalysts such as Ru/Al$_2$O$_3$, Ru/MgO, Ru/Mg(OH)$_2$, and Ru/Al(OH)$_3$ were inactive for this quinoline synthesis. Compared with the conventional synthesis method using hydrogen transfer to ketones from **16**, only 1.2 equiv of ketones were required in this catalyst system.

Various quinolines were synthesized from ketones in the presence of the Ru/Mg–Al–CO$_3$ catalyst. Both oxidation and aldol reactions occurred on the surface of Ru/Mg–Al–CO$_3$, because the reactions completely stopped when the solid catalyst was removed from the reaction mixture by simple filtration. The mechanism of a one-pot quinoline synthesis using Ru/Mg–Al–CO$_3$ is proposed as follows: the surface Ru species oxidizes 2-aminobenzyl alcohol to 2-aminobenzaldehyde under an O$_2$ atmosphere, followed by aldol reaction with ketones catalyzed by the base sites of Mg–Al–CO$_3$ to yield quinolines.

The applicability of the Ru/Mg–Al–CO$_3$-catalyzed one-pot synthesis is exemplified by the reaction of α,β-unsaturated ketones with carbon–carbon double bonds that are easily reduced by metal–hydride species.[162] The reactions of benzalacetone derivatives with 2-aminobenzyl alcohol afforded styryl quinolines, precursors of naturally occurring tetrahydroquinoline alkaloids and inhibitors of viral proliferation.[165] Reduction of carbon–carbon double bonds did not occur because of the smooth oxidation of the Ru–H species by molecular oxygen. Furthermore, 1-octanal and phenylacetonitrile were also react-

ed as donors to afford 3-amylquinoline and 2-amino-3-phenyl-quinoline in 81 and 90% yields, respectively (Eqs. 40 and 41). To the best of our knowledge, this is the first example of a one-pot quinoline synthesis from 2-aminobenzyl alcohol with unsaturated ketones, aldehydes, and nitrile compounds.
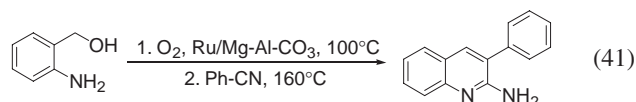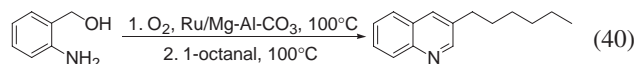
The reaction of nitriles and carbonyl compounds using hydrotalcite-supported palladium nanoparticles as a multifunctional catalyst under atmospheric hydrogen pressure afforded α-alkylated nitriles (Eq. 42).[144h] The alkylated nitriles were formed through aldol reaction of nitriles with carbonyl compounds at base sites on the hydrotalcite surface followed by hydrogenation of unsaturated nitriles by molecular hydrogen on the palladium nanoparticle.
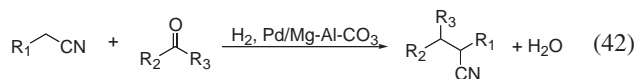
3.3.2 One-Pot Sequential Reactions Combined with Solid Acid Ti^{4+}-Mont Catalyst:
The use of acid and base materials in a single pot fatally results in a disappearance of both catalytic functions as they neutralize each other. The development of catalytic system in which acid and base sites independently function in a single pot is a matter of great importance for the one-pot sequential reactions promoted by acid and base. The Ti^{4+}-exchanged montmorillonite (Ti^{4+}-mont) acted as a heterogeneous Brønsted-acid catalyst as a result of Ti^{4+} cations in the interlayer spaces (vide supra). Since the large hydrotalcite particles cannot enter the narrow interlayer space of Ti^{4+}-mont, these catalysts have the potential to be combined, allowing both acid and base sites to act independently as catalytically active centers without mutual destruction even in the same reactor.[158]

Deacetalization is an important acid-catalyzed reaction in organic synthesis, forming carbonyl compounds that are often further reacted to the target products using base catalysts. One-pot synthesis of benzylidenemalononitrile (**9**) from malononitrile (**8**) with benzaldehydedimethyl acetal (**7**) was demonstrated using various acid–base catalyst pairs (Table 20).

Remarkably, reaction of **7** with **8** directly proceeded in the presence of both the Ti^{4+}-mont and the HT catalysts to afford **9** in 93% yield (Entry 1). In the absence of the HT catalyst, benzaldehyde became the only product (Entry 2), while no reaction occurred without Ti^{4+}-mont (Entry 3). From these results, **20** was considered to form via the Ti^{4+}-mont-catalyzed deacetalization of **1**, followed by the aldol reaction of **8** with benzaldehyde at the base sites of the HT. When either Ti^{4+}-mont or the HT was replaced by a homogeneous reagent, such as *p*-toluenesulfonic acid or piperidine, both the deacetalization and aldol reaction scarcely occurred (Entries 4 and 5). Furthermore, this one-pot system did not need the addition of water because the successive aldol reaction produced water to efficiently accelerate the deprotection of **7**. Deacetalization

has often been performed in aqueous organic solvents despite tedious separating procedures.

The scope of the one-pot deprotection-aldol reaction of acetals with equimolar amounts of donors is shown in Table 21. The reaction of **1** with methyl cyanoacetate proceeded quantitatively to afford methyl benzylidenecyanoacetate (Entry 4), and ethylene ketal also gave the corresponding unsaturated nitrile in a high yield (Entry 8). 2-(3-(Trimethylsilyl)phenyl)-1,3-dioxolane reacted smoothly without decomposition of the TMS groups (Entry 3), in contrast to some acid catalysts that promote hydrolysis of the TMS during the deprotection process. The base-promoted cross aldol reaction of aldehydes with α-protons of carbonyl groups often leads to undesirable side reactions. Using our combined catalyst system, the reaction of hexane dimethylacetal with phenylacetonitrile gave 2-phenyl-2-octenenitrile in 92% GC yield, in which the formation of a self-aldol product was depressed because of the low concentration of the aldehyde during this one-pot reaction (Entry 7). On the contrary, the use of *n*-hexanal itself in place of hexanal dimethylacetal resulted in the desired product in 71% GC yield together with 2-butyl-2-octenal.

The solid mixture consisting of Ti^{4+}-mont and the HT catalysts was easily recovered by simple filtration and could then

be reused at least five times with retention of high catalytic activity and selectivity.

The present catalyst system is also applicable to tandem Michael reaction and acetalization, as summarized in Table 22. These reactions gave excellent yields of nitrodioxolanes, which are highly useful precursors for several nitro-group transfer reactions. For example, nitromethane underwent the Michael reaction with methyl vinyl ketone, followed by acetalization with ethane-1,2-diol to afford an 89% yield of 2-methyl-2-(3-nitropropyl)-1,3-dioxolane, whereas the conventional two-step method gave less than 70% yield. Also, the tandem reaction of dimethyl malonate with 2-cyclohexene-1-one readily proceeded and in the case of β-ketoester, chemoselective acetalization toward an aldehyde function occurred to give a protected Michael adduct.

The potential benefits of using these clay catalysts together are highlighted by the development of novel one-pot synthetic processes (Scheme 13). Epoxynitrile, an intermediate for the synthesis of various heterocyclic compounds, was successfully obtained using methanol, cyanoacetic acid, **7**, and hydrogen peroxide in four sequential acid and base reactions, namely, (i) esterification, (ii) deacetalization, (iii) aldol reaction, and (iv) epoxidation, in a single reactor. We also succeeded in a one-pot synthesis of glutaronitrile using the Ti^{4+}-mont and the Pd/HT catalysts. After reaction of the unsaturated nitrile under 1 atm of H_2, the Michael reaction with acrylonitrile occurred at the base sites of Pd/HT to afford 2-carbomethoxy-2-benzyl glutaronitrile in an excellent overall yield.

Isolated catalytically active centers created on different clay materials bring about a variety of acid–base tandem reactions. The description in the next section focuses on the development of acid–base bifunctional surfaces on the metal oxides derived from hydrotalcites.

3.4 Acid–Base Bifunctional Surface for Fixation of Carbon Dioxide. Hydrotalcites have been often used as precursors for active magnesium–aluminium mixed oxide (Mg–Al mixed oxide) catalysts with strong base sites on their surface (Chart 3, type G). We found that the Mg–Al mixed oxide possesses an acid–base bifunctional surface for the fixation of CO_2 to various epoxides into the corresponding five-membered cyclic carbonates.[166] Compared with other reported catalysts for

Table 20. Tandem Deprotection-Aldol Reaction with Acids and Bases[a]

Entry	Acid	Base	Convn. of **7** /%[b]	Yield of **9** /%[b]
1	Ti^{4+}-mont	HT	>99	93
2	Ti^{4+}-mont	—	30	trace
3	—	HT	trace	trace
4[c]	Ti^{4+}-mont	piperidine	10	trace
5[d]	*p*-TsOH H_2O	HT	trace	trace

a) **7** (1 mmol), **8** (1 mmol), Ti^{4+}-mont (0.02 g; Ti: 0.013 mmol), HT (0.15 g), toluene (3 mL), 1 h, 80 °C. b) Determined by GC. c) Piperidine (0.15 mmol), d) *p*-Toluenesulfonic acid (0.1 mmol).

Table 21. Tandem Deprotection-Aldol Reaction Using the Ti^{4+}-Mont and HT Catalysts in a Single Pot[a]

Entry	Acetal				Donor		Time/h	Isolated yield/%
	R_1	R_2	R_3	R_4	R_5	R_6		
1	Me	Me	Ph	H	CN	CN	1	90
2[b]	–C_2H_4–		Ph	H	CN	CN	1	88
3[b]	–C_2H_4–		3-TMS-Ph	H	CN	CN	1	82
4	Me	Me	Ph	H	CN	COOMe	1	95
5[c]	Me	Me	Ph	H	H	PhC(O)	12	83
6[d]	Me	Me	PhC_2H_2	H	CN	COOMe	1	79
7[e]	Me	Me	*n*-C_5H_{11}	H	CN	Ph	2.5	81[f]
8[b]	–C_2H_2–		–C_5H_{10}–		CN	CN	10	68

a) Acetal (1 mmol), donor (1 mmol), Ti^{4+}-mont (0.02 g), HT (0.2 g), toluene (3 mL), 80 °C. b) 1,4-Dioxane was used as solvent. c) 100 °C. d) 60 °C, (*E*)-acetal was used. e) 150 °C. f) *E/Z* = 1/11.

Table 22. Tandem Michael Reaction-Protection Using the HT and Ti^{4+}-Mont Catalysts in a Single Pot[a)]

Entry	Acceptor	Donor	Conditions of Michael reaction	Product	Isolated yield/%
1	**10a**	**11a**	40 °C, 2 h	**12a**	89
2	**10a**	**11b**	40 °C, 3 h	**12b**	89
3	**10b**	**11a**	50 °C, 3 h	**12c**	86
4	**10c**	**11a**	50 °C, 3 h	**12d**	70
5[b),c)]	**10c**	**11c**	100 °C, 10 h	**12e**	82
6[c),d)]	**10d**	**11d**	40 °C, 3 h	**12f**	64

a) Acceptor (1 mmol), donor (2 mL), Ti^{4+}-mont (0.15 g), HT (0.1 g). After the completion of Michael reaction, ethane-1,2-diol (1.5 mmol) and toluene (10 mL) were added followed by acetalization under Dean–Stark conditions for 1 h. b) Donor (1.2 mmol) was used. c) Toluene (2 mL) was used as solvent for Michael reaction. d) Donor (1 mmol) and ethane-1,2-diol (1.1 mmol) were used.
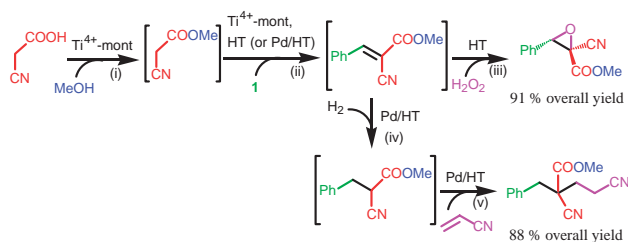
Scheme 13.

Scheme 14.

this addition reaction, the Mg–Al mixed oxides have the following advantages: (1) highly catalytic activity even under a CO$_2$ atmosphere, (2) reusable catalysts without any toxic metals, and (3) stereospecific addition via retention of the configuration of epoxides.

Mg–Al oxide with a Mg/Al ratio of 5, calcined at 400 °C, was found to be the most active catalyst for the reaction of CO$_2$ and styrene oxide, and DMF was the best solvent. Using this Mg–Al oxide, various kinds of epoxides could be quantitatively converted to the corresponding cyclic carbonates. This addition reaction proceeded with retention of the stereochemistry of epoxides; the reaction of CO$_2$ with (R)- and (S)-benzyl glycidyl ether gave (R)- and (S)-4-(benzyloxymethyl)-1,3-dioxolane-2-one with >99% ee, respectively.

In the reaction of CO$_2$ and styrene oxide, the yields of styrene carbonate were proportional to the base amount of Mg–Al oxides. Although the uncalcined hydrotalcites had high basicity, their catalytic activities were lower than those of the above calcined catalysts. Furthermore, the Mg–Al oxides showed higher catalytic activities than MgO.[167] From the temperature-programmed desorption (TPD) of ammonia, it became clear that the acid sites also existed on the surface of the active Mg–Al mixed oxides and that no acid sites could be observed on MgO. Therefore, the noble catalysis of the Mg–Al mixed
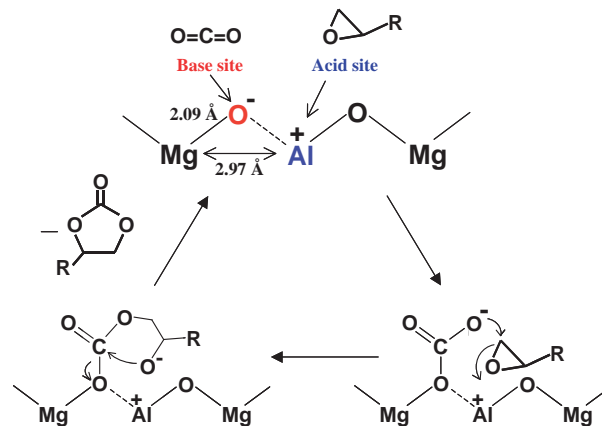
oxide may be attributed to the cooperation of the Lewis-acid sites and the strong base sites. XRD and XAFS analyses of the Mg–Al oxides shows that Mg^{2+} ions are isomorphically substituted by Al^{3+} ions to form Mg–O–Al bonds to disorder the small portion of the Mg–Mg shell, which would bring about the formation of acid and strong base sites on the surfaces of the mixed oxides. We propose a possible reaction mechanism of the addition reaction, shown in Scheme 14. The addition reaction is initiated by adsorption of CO$_2$ on the Lewis-base sites to form a carbonate species, and independently, an epoxide is coordinated on the neighboring acid site on the surface. The coordinated epoxide is ring-opened by a nucleophilic attack on the carbonate species, which leads to an oxy-anion species yielding the corresponding cyclic carbonate as a product. The activity of the Mg–Al mixed oxide was much greater than that of a physical mixture of MgO and Al$_2$O$_3$. Therefore, it is likely that a prominent feature of the active Mg–Al mixed oxide catalysts can be found to orig-

inate from the cooperative action of both the base and acid sites located as neighbors on the surface. Kinetic data of this addition reaction could be well accommodated with a rate equation based on the Langmuir–Hinshelwood model where the CO_2 and epoxide are independently adsorbed on the different sites, i.e., base sites and acid sites, respectively. This is the first distinct instance of an acid–base bifunctional mechanism.

4. Conclusion and Further Perspective

In this account, we demonstrate an effective approach to GSC by designing heterogeneous metal catalysts using inorganic solids as macroligands, and describe their outstanding catalytic performances for a variety of organic syntheses including oxidations, carbon–carbon bond-forming reactions, one-pot syntheses, dehalogenation, and fixation of carbon dioxide. Catalytic systems incorporating the heterogeneous metal catalysts described above can offer significant benefits in achieving simple and clean organic syntheses because they have the following advantages: (i) they allow the use of non-polluting oxidants, (ii) they possess high catalytic activity and selectivity, (iii) they have high substrate tolerance, (iv) they allow a simple work-up procedure and easy recovery of the catalyst, and (v) they are recyclable. By applying concepts from coordination chemistry, we have developed a preparation for nanostructured metal species that is much simpler than previous synthetic methods for solid-supported metal catalysts and provides a strong protocol for preparing catalytically active compounds that are uniform in composition and distribution on solid surfaces. These catalyst systems bridge the gap between homogeneous and heterogeneous catalysis.

The catalyst-based chemical industry contributes to the improvement of our quality of life by manufacturing valuable products such as manure and artificial fibers. Catalytic chemistry has laid emphasis on the pursuit of their function. In the 21st century, the development of solutions for environmental and energy issues has become a central subject in the field of catalytic chemistry. For example, a pivotal challenge for the future is the creation of nano-structured and highly functionalized catalytic materials that allow the utilization of hydrogen and biomass as a resource with the aid of solar energy. The design of such high-performance catalysts requires not only modification of conventional catalysts, but also breakthroughs in science and technology that result from a knowledge of biological and materials sciences.

References

1   a) B. M. Trost, *Science* **1991**, *254*, 1471. b) R. A. Sheldon, *CHEMTECH* **1994**, 38. c) P. T. Anastas, J. C. Warner, *Green Chemistry: Theory and Practice*, Oxford Press, Oxford, **1998**. d) J. H. Clark, *Green Chem.* **1999**, *1*, 1. e) P. T. Anastas, L. B. Bartlett, M. M. Kirchhoff, T. C. Williamson, *Catal. Today* **2000**, *55*, 11. f) R. A. Sheldon, H.-U. Blaser, *Adv. Synth. Catal.* **2003**, *345*, 413.

2   K. Kaneda, S. Ueno, K. Ebitani, *Curr. Top. Catal.* **1997**, *1*, 91; K. Kaneda, K. Yamaguchi, K. Mori, T. Mizugaki, K. Ebitani, *Catal. Surv. Jpn.* **2000**, *4*, 31; K. Kaneda, K. Yamaguchi, K. Mori, T. Mizugaki, K. Ebitani, *Recent Res. Dev. Org. Chem.* **2002**, *6*, 281; K. Kaneda, *J. Synth. Org. Chem., Jpn.* **2003**, *61*, 436; K. Kaneda, K. Mori, T. Mizugaki, K. Ebitani, *Current Organic Chemistry*, ed. by J. G. Heredia, Bentham Science Publishers, San Francisco, **2006**, Vol. 10, p. 241.

3   J. C. Elliott, *Structure and Chemistry of the Apatites and Other Calcium Orthophosphates*, Elsevier, Amsterdam, **1994**.

4   a) K. Yamaguchi, K. Mori, T. Mizugaki, K. Ebitani, K. Kaneda, *J. Am. Chem. Soc.* **2000**, *122*, 7144. b) K. Mori, K. Yamaguchi, T. Mizugaki, K. Ebitani, K. Kaneda, *Chem. Commun.* **2001**, 461. c) K. Mori, M. Tano, T. Mizugaki, K. Ebitani, K. Kaneda, *New J. Chem.* **2002**, *26*, 1536. d) K. Mori, K. Yamaguchi, T. Hara, T. Mizugaki, K. Ebitani, K. Kaneda, *J. Am. Chem. Soc.* **2002**, *124*, 11572. e) M. Murata, T. Hara, K. Mori, M. Ooe, T. Mizugaki, K. Ebitani, K. Kaneda, *Tetrahedron Lett.* **2003**, *44*, 4981. f) T. Hara, K. Mori, T. Mizugaki, K. Ebitani, K. Kaneda, *Tetrahedron Lett.* **2003**, *44*, 6207. g) K. Mori, T. Hara, T. Mizugaki, K. Ebitani, K. Kaneda, *J. Am. Chem. Soc.* **2003**, *125*, 11460. h) K. Mori, T. Hara, T. Mizugaki, K. Ebitani, K. Kaneda, *J. Am. Chem. Soc.* **2004**, *126*, 10657. i) T. Hara, K. Mori, M. Oshiba, T. Mizugaki, K. Ebitani, K. Kaneda, *Green Chem.* **2004**, *6*, 507. j) K. Mori, M. Oshiba, T. Hara, T. Mizugaki, K. Ebitani, K. Kaneda, *Tetrahedron Lett.* **2005**, *46*, 4283. k) K. Mori, Y. Mitani, T. Hara, T. Mizugaki, K. Ebitani, K. Kaneda, *Chem. Commun.* **2005**, 3331. l) K. Mori, T. Hara, M. Oshiba, T. Mizugaki, K. Ebitani, K. Kaneda, *New J. Chem.* **2005**, *29*, 1174.

5   R. A. Sheldon, J. K. Kochi, *Metal-Catalyzed Oxidations of Organic Compounds*, Academic Press, London, **1981**.

6   M. Hudlucky, *Oxidations in Organic Chemistry*, ACS Monograph Series, American Chemical Society, Washington, DC, **1990**.

7   S. S. Stahl, *Angew. Chem., Int. Ed.* **2004**, *43*, 3400.

8   G. Cainelli, G. Cardillo, *Chromium Oxidants in Organic Chemistry*, Springer, Berlin, **1984**.

9   D. G. Lee, U. A. Spitzer, *J. Org. Chem.* **1970**, *35*, 3589.

10   F. M. Menger, C. Lee, *Tetrahedron Lett.* **1981**, *22*, 1655.

11   T. Mallat, A. Baiker, *Chem. Rev.* **2004**, *104*, 3037.

12   R. A. Sheldon, M. Wallau, I. W. C. E. Arends, U. Schuhardt, *Acc. Chem. Res.* **1998**, *31*, 485.

13   S. Sugiyama, T. Minami, H. Hayashi, M. Tanaka, N. Shigemoto, J. B. Moffat, *J. Chem. Soc., Faraday Trans.* **1996**, *26*, 293.

14   W.-C. Chen, W.-Y. Yu, C.-K. Li, C.-M. Che, *J. Org. Chem.* **1995**, *60*, 6840.

15   a) S. Kanemoto, S. Matsubara, K. Takai, K. Oshima, K. Utimoto, H. Nozaki, *Bull. Chem. Soc. Jpn.* **1988**, *61*, 3607. b) R. Lenz, S. V. Ley, *J. Chem. Soc., Perkin Trans. 1* **1997**, 3291. c) A. Hanyu, E. Takezawa, S. Sakaguchi, Y. Ishii, *Tetrahedron Lett.* **1998**, *39*, 5557. d) I. E. Markó, P. R. Giles, M. Tsukazaki, A. Gautier, I. Chellé-Regnaut, S. M. Brown, C. J. Urch, *J. Org. Chem.* **1999**, *64*, 2433. e) A. Dijksman, A. Marino-González, A. M. i. Payeras, I. W. C. E. Arends, R. A. Sheldon, *J. Am. Chem. Soc.* **2001**, *123*, 6826.

16   T. F. Blackburn, J. Schwartz, *J. Chem. Soc., Chem. Commun.* **1977**, 157.

17   Recent reports for Pd-catalyzed alcohol oxidation: a) K. P. Peterson, R. C. Larock, *J. Org. Chem.* **1998**, *63*, 3185. b) T. Nishimura, T. Onoue, K. Ohe, S. Uemura, *J. Org. Chem.* **1999**, *64*, 6750. c) G.-J. ten Brink, I. W. C. E. Arends, R. A. Sheldon, *Science* **2000**, *287*, 1636. d) S. S. Stahl, J. L. Thorman, R. C. Nelson, M. A. Kozee, *J. Am. Chem. Soc.* **2001**, *123*, 7188. e) B. A. Steinhoff, S. R. Fix, S. S. Stahl, *J. Am. Chem. Soc.* **2002**, *124*, 766. f) B. A. Steinhoff, S. S. Stahl, *Org. Lett.* **2002**, *4*, 4179. g) D. R. Jensen, M. J. Schultz, J. A. Mueller, M. S. Sigman, *Angew. Chem., Int. Ed.* **2003**, *42*, 3810.

18   T. Mallat, A. Baiker, *Catal. Today* **1994**, *19*, 247.

19   L. F. Liotta, A. M. Venezia, G. Deganello, A. Longo, A. Martorana, Z. Schay, L. Guczi, *Catal. Today* **2001**, *66*, 271.

20   N. Kakiuchi, Y. Maeda, T. Nishimura, S. Uemura, *J. Org. Chem.* **2001**, *66*, 6220.

21   a) K. Kaneda, M. Fujii, K. Morioka, *J. Org. Chem.* **1996**, *61*, 4502. b) K. Kaneda, Y. Fujie, K. Ebitani, *Tetrahedron Lett.* **1997**, *38*, 9023. c) K. Ebitani, Y. Fujie, K. Kaneda, *Langmuir* **1999**, *15*, 3557. d) K. Ebitani, K.-M. Choi, T. Mizugaki, K. Kaneda, *Langmuir* **2002**, *18*, 1849. e) K.-M. Choi, T. Akita, T. Mizugaki, K. Ebitani, K. Kaneda, *New J. Chem.* **2003**, *27*, 324. f) K.-M. Choi, T. Mizugaki, K. Ebitani, K. Kaneda, *Chem. Lett.* **2003**, *32*, 180. g) K. Kaneda, K.-M. Choi, T. Mizugaki, K. Ebitani, *Palladium Nanoclusters: Preparation and Catalysis in Encyclopedia of Nanoscience and Nanotechnology*, ed. by J. A. Schwarz, C. Contescu, K. Putyera, Marcel Dekker, New York, **2004**, p. 2803.

22   Y. Uozumi, R. Nakao, *Angew. Chem., Int. Ed.* **2003**, *42*, 194.

23   C. Döbler, G. M. Mehltretter, U. Sundermeier, M. Eckert, H.-C. Militzer, M. Beller, *Tetrahedron Lett.* **2001**, *42*, 8447.

24   a) K. Yamaguchi, N. Mizuno, *Angew. Chem., Int. Ed.* **2002**, *41*, 4538. b) K. Yamaguchi, N. Mizuno, *Chem. Eur. J.* **2003**, *9*, 4353.

25   G. Csjernyik, A. H. Ell, L. Fadini, B. Pugin, J.-E. Bäckvall, *J. Org. Chem.* **2002**, *67*, 1657.

26   a) M. Santelli, J.-M. Pons, *Lewis Acids and Selectivity in Organic Synthesis*, CRS Press, Boca Raton, FL, **1995**. b) *Lewis Acids in Organic Synthesis*, ed. by H. Yamamoto, Wiley-VCH, Weinheim, **2000**.

27   a) A. Hosomi, H. Sakurai, *Tetrahedron Lett.* **1976**, *16*, 1295. b) T. Mukaiyama, *Angew. Chem., Int. Ed.* **1977**, *16*, 817.

28   W. Odenkirk, A.-L. Rheingold, B. Bosnich, *J. Am. Chem. Soc.* **1992**, *114*, 6392.

29   a) *Organic Reactions in Aqueous Media*, ed. by C.-J. Li, T.-H. Chan, Wiley, New York, **1997**. b) *Organic Synthesis in Water*, ed. by P. A. Grieco, Blackie Academic and Professional, London, **1998**.

30   S.-I. Murahashi, T. Naota, H. Taki, M. Mizuno, H. Takaya, S. Komiya, Y. Mizuho, N. Oyasato, M. Hiraoka, M. Hirano, A. Fukuoka, *J. Am. Chem. Soc.* **1995**, *117*, 12436.

31   a) B. H. Yang, S. L. Buchwald, *J. Organomet. Chem.* **1999**, *576*, 125. b) J. F. Hartwing, *Angew. Chem., Int. Ed.* **1998**, *37*, 2046. c) B. H. Yang, S. L. Buchwald, *J. Organomet. Chem.* **1999**, *576*, 125.

32   a) W. A. Herrmann, C. Brossmer, K. Öfele, C.-P. Reisinger, T. Priermeier, M. Beller, H. Fischer, *Angew. Chem., Int. Ed.* **1995**, *34*, 1844. b) W. A. Herrmann, V. P. W. Boehm, *J. Organomet. Chem.* **1999**, *576*, 23.

33   M. Ohff, A. Ohff, M. E. van der Boom, D. Milstein, *J. Am. Chem. Soc.* **1997**, *119*, 11687.

34   a) W. A. Herrmann, M. Elison, C. Ficher, C. Köcher, G. R. J. Artus, *Angew. Chem., Int. Ed.* **1995**, *34*, 2371. b) W. A. Herrmann, K. Ofele, D. Von Preysing, S. K. Schneider, *J. Organomet. Chem.* **2002**, *41*, 1291.

35   J.-F. Fauvarque, F. Pflüger, *J. Organomet. Chem.* **1981**, *208*, 419.

36   a) A. Suzuki, *Chem. Commun.* **2005**, 4759. b) V. V. Grushin, H. Alper, in *Activation of Unreactive Bonds and Organic Synthesis*, ed. by S. Murai, Springer, Berline, **1999**.

37   a) F. Alonso, I. P. Beletskaya, M. Yus, *Chem. Rev.* **2002**, *102*, 4009. b) V. V. Grushin, H. Alper, *Chem. Rev.* **1994**, *94*,

1047. c) A. R. Pinder, *Synthesis* **1980**, 425.

38   M. D. Erickson, S. E. Swanson, J. J. D. Flora, Jr., G. D. Hinshaw, *Environ. Sci. Technol.* **1989**, *23*, 462.

39   a) C. Desmarrets, S. Kuhl, R. Schneider, Y. Fort, *Organometallics* **2002**, *21*, 1554. b) M. S. Viciu, G. A. Grasa, S. P. Nolan, *Organometallics* **2001**, *20*, 3607.

40   R. E. Maleczka, Jr., R. J. Rahaim, Jr., R. R. Teixeira, *Tetrahedron Lett.* **2002**, *43*, 7087.

41   R. Hara, K. Sato, W.-H. Sun, T. Takahashi, *Chem. Commun.* **1999**, 845.

42   P. P. Cellier, J.-F. Spindler, M. Taillefer, H.-J. Cristau, *Tetrahedron Lett.* **2003**, *44*, 7191.

43   a) M. A. Atienza, M. A. Esteruelas, M. Fernández, J. Herrero, M. Oliván, *New J. Chem.* **2001**, *25*, 775. b) I. Pri-Bar, O. Buchman, *J. Org. Chem.* **1986**, *51*, 734.

44   M. E. Cucullu, S. P. Nolan, T. R. Belderrain, R. H. Grubbs, *Organometallics* **1999**, *18*, 1299.

45   D. T. Ferrughelli, I. T. Horváth, *J. Chem. Soc., Chem. Commun.* **1992**, 806.

46   Y. Zhang, S. Liao, Y. Xu, *Tetrahedron Lett.* **1994**, *35*, 4599.

47   C. A. Marques, M. Selva, P. Tundo, *J. Org. Chem.* **1993**, *58*, 5256.

48   a) V. Felis, C. D. Bellefon, P. Fouilloux, D. Schweich, *Appl. Catal., B* **1999**, *20*, 91. b) C. Schuth, M. Reinhard, *Appl. Catal., B* **1998**, *18*, 215.

49   a) A. Behr, *Carbon Dioxide Activation by Metal Complexes*, VCH publishers, New York, **1988**. b) *Carbon Dioxide Fixation and Reduction in Biological and Model Systems*, ed. by C.-I. Brauden, G. Schneider, Oxford University Press, Oxford, **1994**. c) D. H. Gibson, *Chem. Rev.* **1996**, *96*, 2063.

50   a) A. A. G. Shaikh, S. Sivaram, *Chem. Rev.* **1996**, *96*, 951. b) D. J. Darensbourg, M. W. Holtcamp, *Coord. Chem. Rev.* **1996**, *153*, 155. c) M. Yoshida, M. Ihara, *Chem. Eur. J.* **2004**, *10*, 2886.

51   R. L. Paddock, S. T. Nguyen, *J. Am. Chem. Soc.* **2001**, *121*, 11498.

52   Y. M. Shen, W. L. Duan, M. Shi, *J. Org. Chem.* **2003**, *68*, 1559.

53   R. L. Paddock, Y. Hiyama, J. M. McKay, S. T. Nguyen, *Tetrahedron Lett.* **2004**, *45*, 2023.

54   L. B. Ryland, M. W. Tamele, J. N. Wilson, *Catalysis*, ed. by P. H. Emmett, Reinhold, New York, **1960**, Vol. 70, Chap. 1.

55   a) P. Laszlo, *Science* **1987**, *235*, 1473. b) T. J. Pinnavaia, *Science* **1983**, *220*, 365.

56   Excellent reviews of mont-catalyzed organic syntheses: a) J. H. Clark, D. J. Macquarrie, *Chem. Soc. Rev.* **1996**, *25*, 303. b) Y. Izumi, M. Onaka, *Adv. Catal.* **1992**, *38*, 245. c) P. Laszlo, *Acc. Chem. Res.* **1986**, *19*, 121.

57   Ti: a) T. Kawabata, T. Mizugaki, K. Ebitani, K. Kaneda, *Tetrahedron Lett.* **2003**, *44*, 9205. b) T. Kawabata, M. Kato, T. Mizugaki, K. Ebitani, K. Kaneda, *Chem. Lett.* **2003**, *32*, 648. c) T. Kawabata, T. Mizugaki, K. Ebitani, K. Kaneda, *Tetrahedron Lett.* **2001**, *42*, 8329. d) K. Ebitani, T. Kawabata, K. Nagashima, T. Mizugaki, K. Kaneda, *Green Chem.* **2000**, *2*, 157. Fe: e) K. Ebitani, M. Ide, T. Mitsudome, T. Mizugaki, K. Kaneda, *Chem. Commun.* **2002**, 690. Sc: f) T. Kawabata, T. Mizugaki, K. Ebitani, K. Kaneda, *J. Am. Chem. Soc.* **2003**, *125*, 10486. Cu: g) T. Kawabata, M. Kato, T. Mizugaki, K. Ebitani, K. Kaneda, *Chem. Eur. J.* **2005**, *11*, 288. V: h) T. Mitsudome, K. Mori, T. Mizugaki, K. Ebitani, K. Kaneda, *Chem. Lett.* **2005**, *34*, 1626.

58   S. Kobayashi, S. Nagayama, T. Busujima, *J. Am. Chem. Soc.* **1998**, *120*, 8287.

59   R. Raja, G. Sanker, J. M. Thomas, *J. Am. Chem. Soc.* **1999**, *121*, 11926.

60   S. Bordiga, S. Collucia, C. Lamberti, L. Marchese, A. Zecchina, F. Boscherini, F. Buffa, F. Genoni, G. Leofanti, G. Petrini, G. Vlaic, *J. Phys. Chem.* **1994**, *98*, 4125.

61   A. Fahmi, C. Minot, B. Silvi, M. Causá, *Phys. Rev. B* **1993**, *47*, 11717.

62   J. Wong, F. W. Lytle, R. P. Messmer, D. H. Haylotte, *Phys. Rev. B* **1984**, *30*, 5596.

63   a) H. G. Bachmann, F. R. Ahmed, W. H. Barnes, *Z. Kristallogr. Mineral.* **1961**, *115*, 110. b) T. Tanaka, H. Yamashita, R. Tsuchitani, T. Funabiki, S. Yoshida, *J. Chem. Soc., Faraday Trans. 1* **1988**, *84*, 2987.

64   F. A. Cotton, G. Wilkinson, *Advanced Inorganic Chemistry*, 5th ed., Wiley, New York, **1988**, p. 755.

65   C. Lamberti, G. Spoto, D. Scarano, C. Pazé, M. Salvalaggio, S. Bordiga, A. Zecchina, G. T. Palomino, F. D'Acapito, *Chem. Phys. Lett.* **1997**, *269*, 500.

66   H. Ohtaki, M. Maeda, *Bull. Chem. Soc. Jpn.* **1974**, *47*, 2197.

67   M. B. McBride, T. J. Pinnavaia, M. M. Mortland, *J. Phys. Chem.* **1975**, *79*, 2430.

68   K. Ebitani, K. Nagashima, T. Mizugaki, K. Kaneda, *Chem. Commun.* **2000**, 869.

69   N. Mizuno, C. Nozaki, I. Kiyoto, M. Misono, *J. Am. Chem. Soc.* **1998**, *120*, 9267.

70   R. H. Fish, M. S. Konings, K. J. Oberhausen, R. H. Fong, W. M. Yu, G. Christou, J. B. Vincent, D. K. Coggin, R. M. Buchana, *Inorg. Chem.* **1991**, *30*, 3002.

71   G. B. Sul'pin, A. E. Shilov, G. Süss-Fink, *Tetrahedron Lett.* **2001**, *42*, 7253.

72   G. Süss-Fink, S. Stanislas, G. B. Shul'pin, G. V. Nizova, H. Stoeckli-Evans, A. Neels, C. Bobillier, S. Claude, *J. Chem. Soc., Dalton Trans.* **1999**, 3169.

73   Y. Lvov, K. Ariga, I. Ichinose, T. Kunitake, *Langmuir* **1996**, *12*, 3038.

74   R. A. Leising, B. A. Brenna, L. Que, B. G. Fox, E. Münck, *J. Am. Chem. Soc.* **1991**, *113*, 3988.

75   a) *Modern Oxidation Methods*, ed. by J.-E. Bäckvall, Wiley-VCH, Weinheim, **2004**. b) *The Activation of Dioxygen and Homogeneous Catalytic Oxidation*, ed. by D. H. R. Barton, A. E. Martell, D. T. Sawyer, Plenum, New York, **1993**.

76   a) Q. Tang, Y. Wang, J. Liang, P. Wang, Q. Zhang, H. Wan, *Chem. Commun.* **2004**, 440. b) C.-X. Yin, R. G. Finke, *Inorg. Chem.* **2005**, *44*, 4175. c) Y. Nishiyama, Y. Nakagawa, N. Mizuno, *Angew. Chem., Int. Ed.* **2001**, *40*, 3639. d) A. S. Goldstein, R. H. Beer, R. S. Drago, *J. Am. Chem. Soc.* **1994**, *116*, 2424. e) M. M. T. Khan, A. P. Rao, *J. Mol. Catal.* **1987**, *39*, 331. f) J. T. Groves, R. Quinn, *J. Am. Chem. Soc.* **1985**, *107*, 5790.

77   A review on vanadium-catalyzed organic syntheses: T. Hirao, *Chem. Rev.* **1997**, *97*, 2707.

78   a) S. Shinachi, M. Matsushita, K. Yamaguchi, N. Mizuno, *J. Catal.* **2005**, *233*, 81. Vanadium-substituted phosphomolybdates catalyst (84%). b) K. Yamaguchi, N. Mizuno, *New J. Chem.* **2002**, *26*, 972. Ru-substituted silicotungstate catalyst (42%). c) N. Mizuno, M. Tateishi, T. Hirose, M. Iwamoto, *Chem. Lett.* **1993**, 2137. Ni- and Fe-substituted heteropolyanion catalyst (29%). d) M. M. T. Khan, D. Chatterjee, S. Kumar, A. P. Rao, *J. Mol. Catal.* **1987**, *75*, L49. Ru–saloph complex catalyst (13%). e) R. Neumann, M. Dahan, *J. Am. Chem. Soc.* **1998**, *120*, 11969. Ru-substituted polyoxometalate catalyst (57%).

79   a) Y. Ishii, *J. Mol. Catal. A: Chem.* **1997**, *117*, 123. b) Y. Ishii, T. Iwahama, S. Sakaguchi, K. Nakayama, Y. Nishiyama, *J. Org. Chem.* **1996**, *61*, 4520.

80   C. S. Chen, B. J. Bulkin, E. M. Pearce, *J. Appl. Polym. Sci.* **1982**, *27*, 1177.

81   G. S. Papava, N. A. Maisuradze, Z. L. Zarkua, N. S. Dokhturishvili, Z. M. Sarishvile, G. B. Razmadze, S. V. Vinogradova, V. V. Korshak, *Acta Polym.* **1988**, *8*, 445.

82   M. Yamada, J. Sun, Y. Suda, T. Nakaya, *Chem. Lett.* **1988**, 1055.

83   M. Hino, S. Kobayashi, K. Arata, *J. Am. Chem. Soc.* **1979**, *110*, 6439.

84   T. Yamaguchi, T. Jin, K. Tanabe, *J. Phys. Chem.* **1986**, *90*, 3148.

85   S. Bodoardo, R. Chiappetta, B. Onida, F. Figueras, E. Garrone, *Microporous Mesoporous Mater.* **1998**, *20*, 187.

86   a) T. W. Greene, P. G. M. Wuts, *Protective Groups in Organic Synthesis*, John Wiley & Sons, New York, **1999**, p. 293. b) A. R. Katritzky, M.-C. Otto, *Comprehensive Organic Functional Group Transformations*, Pergamon Press, Oxford, **1995**, Vol. 4, p. 176. c) P. J. Kocienski, *Protecting Groups*, George Thieme Verlag, New York, **1994**, p. 156.

87   a) R. Ballini, G. Bosica, B. Frullanti, R. Maggi, G. Sartori, F. Schroer, *Tetrahedron Lett.* **1998**, *39*, 1615. b) A. Corma, M. J. Climent, H. Garcia, J. Primo, *Appl. Catal.* **1990**, *59*, 333.

88   Representative examples of homogeneous catalytic esterifications. a) S. Palaniappan, M. S. Ram, *Green Chem.* **2002**, *4*, 53. Polyaniline salt. b) K. Ishihara, S. Ohara, H. Yamamoto, *Science* **2000**, *290*, 1140. Hafnium salt. c) K. Wakasugi, T. Misaki, K. Yamada, Y. Tanabe, *Tetrahedron Lett.* **2000**, *41*, 5249. Diphenylammonium triflate. d) P. Goswani, P. Chowdhury, *New J. Chem.* **2000**, *24*, 955. Ceric ammonium nitrate. e) J. Otera, N. Dan-oh, J. Nozaki, *J. Org. Chem.* **1991**, *56*, 5307. Distannoxane.

89   J. Christoffers, *Eur. J. Org. Chem.* **1998**, 1259.

90   a) S. Fukuzumi, K. Ohkubo, *J. Am. Chem. Soc.* **2002**, *124*, 10270. b) S. Fukuzumi, K. Ohkubo, *Chem. Eur. J.* **2000**, *6*, 4532.

91   J. Christoffers, *Chem. Commun.* **1997**, 943.

92   A. C. Coda, G. Desimoni, P. Righetti, G. Tacconi, *Gazz. Chim. Ital.* **1984**, *114*, 417.

93   H. O. House, *Modern Synthetic Reactions*, 2nd ed., Benjamin, Calif, **1972**, p. 595.

94   S. Matsunaga, T. Ohshima, M. Shibasaki, *Adv. Synth. Catal.* **2002**, *344*, 3.

95   a) A. Corma, L. T. Nemeth, M. Renz, S. Valencia, *Nature* **2001**, *412*, 423. b) A. Corma, M. E. Domine, L. Nemeth, S. Valencia, *J. Am. Chem. Soc.* **2002**, *124*, 3194. c) S. R. Bare, S. D. Kelly, W. Sinkler, J. J. Low, F. S. Modica, S. Valencia, A. Corma, L. T. Nemeth, *J. Am. Chem. Soc.* **2005**, *127*, 12924.

96   a) J. W. Carmichael, Jr., L. K. Steinrauf, R. L. Belford, *J. Chem. Phys.* **1965**, *43*, 3959. b) K. Nakamoto, *Infrared and Raman Spectra of Inorganic and Coordination Compounds*, 5th ed., pt. B, Wiley, New York, **1997**, p. 91.

97   J. Christoffers, *Chem. Eur. J.* **2003**, *9*, 4862.

98   B. M. Choudary, C. Sridhar, M. Sateesh, B. Sreedhar, *J. Mol. Catal. A: Chem.* **2004**, *212*, 237.

99   C. F. Baes, Jr., R. Mesmer, *The Hydrolysis of Cations*, Wiley, New York, **1976**.

100   S. Kobayashi, M. Sugiura, H. Kitagawa, W. W.-L. Lam, *Chem. Rev.* **2002**, *102*, 2227.

101   S. Kobayashi, *Eur. J. Org. Chem.* **1999**, 15.

102   S. Kobayashi, K. Manabe, *Acc. Chem. Res.* **2002**, *35*, 209.

103   M. Onaka, *J. Synth. Org. Chem., Jpn.* **1995**, *53*, 392.

104   a) W. Gu, W.-J. Zhou, D. L. Gin, *Chem. Mater.* **2001**, *13*, 1949. b) R. Anwander, H. W. Gcrlitzer, G. Gerstberger, C. Palm, O. Runte, M. Spiegler, *J. Chem. Soc., Dalton Trans.* **1999**, 3611.

105   Y. Mori, K. Kakumoto, K. Manabe, S. Kobayashi, *Tetrahedron Lett.* **2000**, *41*, 3107.

106   a) J. A. Marshall, *Chem. Rev.* **1996**, *96*, 31. b) Y. Yamamoto, N. Asao, *Chem. Rev.* **1993**, *93*, 2207. c) A. Hosomi, *Acc. Chem. Res.* **1988**, *21*, 200.

107   A. Marx, H. Yamamoto, *Angew. Chem., Int. Ed.* **2000**, *39*, 178.

108   X. Fang, J. G. Watkin, B. P. Warner, *Tetrahedron Lett.* **2000**, *41*, 447.

109   M. W. Wang, Y. J. Chen, D. Wang, *Synlett* **2000**, 385.

110   Y. Onishi, T. Ito, M. Yasuda, A. Baba, *Eur. J. Org. Chem.* **2002**, 1578.

111   M. Kawai, M. Onaka, Y. Izumi, *Chem. Lett.* **1986**, 381.

112   S. Miyata, *Clays Clay Miner.* **1980**, *28*, 50; F. Cavani, F. Trifiró, A. Vaccari, *Catal. Today* **1991**, *11*, 173; B. F. Sels, D. E. De Vos, P. A. Jacobs, *Catal. Rev. Sci. Eng.* **2001**, *43*, 443.

113   a) T. Nakatsuka, H. Kawasaki, S. Yamashita, S. Kohjiya, *Bull. Chem. Soc. Jpn.* **1979**, *52*, 2449. b) W. T. Reichle, *J. Catal.* **1985**, *94*, 547. c) E. Suzuki, Y. Ono, *Bull. Chem. Soc. Jpn.* **1988**, *61*, 1008. d) A. Corma, V. Fornes, R. M. Martin-Aranda, F. Rey, *J. Catal.* **1992**, *134*, 58. e) T. Tatsumi, K. Yamamoto, H. Tajima, H. Tominaga, *Chem. Lett.* **1992**, 815. f) B. Sels, D. De Vos, M. Buntinx, F. Pierard, A. Kirsch-De Mesmaeker, P. Jacobs, *Nature* **1999**, *400*, 855. g) T. Nishimura, N. Kakiuchi, M. Inoue, S. Uemura, *Chem. Commun.* **2000**, 1245. h) B. M. Choudary, N. Choudary, S. Madhi, M. Kantam, *Angew. Chem., Int. Ed.* **2001**, *40*, 4620.

114   H. Hattori, *Chem. Rev.* **1995**, *95*, 537; Y. Ono, T. Baba, *Catal. Today* **1997**, *38*, 321.

115   For example, see: M. L. Kantam, B. M. Choudary, C. V. Reddy, K. K. Rao, F. Figueras, *Chem. Commun.* **1998**, 1033.

116   H. Pines, W. M. Stalick, *Base-Catalyzed Reactions of Hydrocarbons and Related Compounds*, Academic Press, New York, **1977**; J. M. Fraile, J. I. Garcia, J. A. Mayoral, *Catal. Today* **2000**, *57*, 3.

117   A recent review: G.-J. ten Brink, I. W. C. E. Arends, R. A. Sheldon, *Chem. Rev.* **2004**, *104*, 4105.

118   Na_2CO_3: a) J. K. Ehitesell, R. S. Matthews, A. M. Helbling, *J. Org. Chem.* **1978**, *43*, 784. Ni: b) T. Yamada, K. Takahashi, K. Kato, T. Takai, S. Inoki, T. Mukaiyama, *Chem. Lett.* **1991**, 641. Fe: c) S.-I. Murahashi, Y. Oda, T. Naota, *Tetrahedron Lett.* **1992**, *33*, 7557. Cu: d) C. Bolm, G. Schlinggloff, K. Weickhardt, *Tetrahedron Lett.* **1993**, *34*, 3405.

119   T. Yamada, T. Takai, O. Rhode, T. Mukaiyama, *Bull. Chem. Soc. Jpn.* **1991**, *64*, 2109.

120   K. Kaneda, S. Haruna, T. Imanaka, M. Hamamoto, Y. Nishiyama, Y. Ishii, *Tetrahedron Lett.* **1992**, *33*, 6827. This epoxidation method is applied to the synthesis of isotopically pure [^{18}O]-epoxides from alkenes and $^{18}O_2$ in the presence of isobutyraldehyde (*Kaneda epoxidation*). Unlike peracids, the system allows the selective epoxidation of the double bond in a keto-alkene without competing Baeyer–Villiger oxidation of the carbonyl group. See: M. Schöttler, W. Boland, *Synlett* **1997**, 91.

121   K. Kaneda, S. Ueno, T. Imanaka, E. Shimotsuma, Y. Nishiyama, Y. Ishii, *J. Org. Chem.* **1994**, *59*, 2915.

122   In-situ generated peracids from O_2 and aldehydes oxidize ruthenium dioxide into ruthenium compounds with higher oxidation state, e.g., RuO_4, which act as catalysts for the oxidative cleavage of olefins. See: K. Kaneda, S. Haruna, T. Imanaka, K. Kawamoto, *J. Chem. Soc., Chem. Commun.* **1990**, 1467.

123   K. Kaneda, S. Ueno, T. Imanaka, *J. Chem. Soc., Chem. Commun.* **1994**, 797.

124   R. Criegee, *Justus Liebigs Ann. Chem.* **1948**, *560*, 127; G. R. Krow, *Org. React.* **1993**, *43*, 251.

125   S. Ueno, K. Ebitani, A. Ookubo, K. Kaneda, *Appl. Surf. Sci.* **1997**, *121/122*, 366.

126   R. J. Hunter, *Zeta Potential in Colloid Science*, Academic press, New York, **1981**.

127   The hydrotalcites also efficiently catalyzed the Baeyer–Villiger oxidation using *m*-CPBA as an oxidant. See: K. Kaneda, T. Yamashita, *Tetrahedron Lett.* **1996**, *37*, 4555.

128   K. Kaneda, S. Ueno, T. Imanaka, *J. Mol. Catal. A: Chem.* **1995**, *102*, 135.

129   K. Kaneda, S. Ueno, in *Heterogeneous Hydrocarbon Oxidation*, ACS Symposium Series, No. 638, **1996**, Chap. 22, p. 300.

130   A recent review: I. W. C. E. Arends, R. A. Sheldon, *Top. Catal.* **2002**, *19*, 133.

131   A typical example for stereoselective epoxidation using TBHP in the presence of a V catalyst, see: T. Ito, K. Jitsukawa, K. Kaneda, S. Teranishi, *J. Am. Chem. Soc.* **1979**, *101*, 159; T. Ito, K. Kaneda, S. Teranishi, *J. Chem. Soc., Chem. Commun.* **1976**, 421.

132   For selected catalytic systems for epoxidation using H_2O_2, see: a) C. Venturello, E. Alneri, M. Ricci, *J. Org. Chem.* **1983**, *48*, 3831. b) Y. Ishii, K. Yamawaki, T. Ura, H. Yamada, T. Yoshida, M. Ogawa, *J. Org. Chem.* **1988**, *53*, 3587. c) K. Sato, M. Aoki, M. Ogawa, T. Hashimoto, R. Noyori, *Bull. Chem. Soc. Jpn.* **1997**, *70*, 905. d) P. Wu, T. Tatsumi, *Chem. Commun.* **2001**, 897. e) K. Kamata, K. Yonehara, Y. Sumida, K. Yamaguchi, S. Hikichi, N. Mizuno, *Science* **2003**, *300*, 964.

133   E. Rohrmann, R. G. Jhones, H. A. Shonle, *J. Am. Chem. Soc.* **1944**, *66*, 1856.

134   G. B. Payne, P. H. Williams, *J. Org. Chem.* **1959**, *24*, 54; G. B. Payne, P. H. Deming, P. H. Williams, *J. Org. Chem.* **1961**, *26*, 659; G. B. Payne, *Tetrahedron* **1962**, *19*, 763.

135   a) K. Yamaguchi, K. Mori, T. Mizugaki, K. Ebitani, K. Kaneda, *J. Org. Chem.* **2000**, *65*, 6897. b) T. Honma, M. Nakajo, T. Mizugaki, K. Ebitani, K. Kaneda, *Tetrahedron Lett.* **2002**, *43*, 6229.

136   C. Cativiela, F. Figueras, J. M. Fraile, J. I. García, J. A. Mayoral, *Tetrahedron Lett.* **1995**, *36*, 4125; J. M. Fraile, J. I. García, C. Cativiela, J. A. Mayoral, F. Figueras, *Tetrahedron Lett.* **1996**, *37*, 665; B. F. Sels, D. E. De Vos, P. A. Jacobs, *Tetrahedron Lett.* **1996**, *37*, 8557.

137   J. J. P. Stewart, *J. Comput. Chem.* **1989**, *10*, 221.

138   R. J. Loncharich, F. K. Brown, K. N. Houk, *J. Org. Chem.* **1989**, *54*, 1129.

139   S. Sakaguchi, Y. Nishiyama, Y. Ishii, *J. Org. Chem.* **1996**, *61*, 5307; B. Boyer, A. Hambardzoumian, G. Lamaty, A. Leydet, J.-P. Roque, P. Bouchet, *New J. Chem.* **1996**, *20*, 985.

140   M. Rajamathi, G. D. Nataraja, S. Ananthamurthy, P. V. Kamath, *J. Mater. Chem.* **2000**, *10*, 2754; S. P. Newman, W. Jones, P. O'Conner, P. N. Stamires, *J. Mater. Chem.* **2002**, *12*, 153.

141   We think that high catalytic activity of the HT(MO) might be ascribed to its large surface area and high hydrophilicity.

142   a) S. Ueno, K. Yamaguchi, K. Yoshida, K. Ebitani, K. Kaneda, *Chem. Commun.* **1998**, 295. b) K. Yamaguchi, K. Ebitani, K. Kaneda, *J. Org. Chem.* **1999**, *64*, 2966. c) K. Yamaguchi, T.

Mizugaki, K. Ebitani, K. Kaneda, *New J. Chem.* **1999**, *23*, 799.

143 a) M. Matsumoto, M. Watanabe, *J. Org. Chem.* **1984**, *49*, 3435. b) M. Musawir, P. N. Davey, G. Kelly, I. V. Kozhevnikov, *Chem. Commun.* **2003**, 1414. c) A. Abad, P. Concepción, A. Corma, H. García, *Angew. Chem., Int. Ed.* **2005**, *44*, 4066. d) Z. Opre, J.-D. Grunwaldt, M. Maciejewski, D. Ferri, T. Mallat, A. Baiker, *J. Catal.* **2005**, *230*, 406. e) D. V. Bavykin, A. A. Lapkin, P. K. Plucinski, J. M. Friedrich, F. C. Walsh, *J. Catal.* **2005**, *235*, 10.

144 a) K. Kaneda, T. Yamashita, T. Matsushita, K. Ebitani, *J. Org. Chem.* **1998**, *63*, 1750. b) T. Matsushita, K. Ebitani, K. Kaneda, *Chem. Commun.* **1999**, 265. c) H.-B. Ji, T. Mizugaki, K. Ebitani, K. Kaneda, *Tetrahedron Lett.* **2002**, *43*, 7179. d) K. Ebitani, H.-B. Ji, T. Mizugaki, K. Kaneda, *J. Mol. Catal. A: Chem.* **2004**, *212*, 161. e) K. Motokura, D. Nishimura, K. Mori, T. Mizugaki, K. Ebitani, K. Kaneda, *J. Am. Chem. Soc.* **2004**, *126*, 5662. f) K. Motokura, T. Mizugaki, K. Ebitani, K. Kaneda, *Tetrahedron Lett.* **2004**, *45*, 6029. g) K. Ebitani, K. Motokura, T. Mizugaki, K. Kaneda, *Angew. Chem., Int. Ed.* **2005**, *44*, 3423. h) K. Motokura, N. Fujita, K. Mori, T. Mizugaki, K. Ebitani, K. Kaneda, *Tetrahedron Lett.* **2005**, *46*, 5507.

145 Typical examples of primary aliphatic alcohol oxidations using inorganic oxidants: CrO_3/H_2SO_4: a) J. G. Millar, A. C. Oehlschlager, J. W. Wong, *J. Org. Chem.* **1983**, *48*, 4404. $RuCl_3/H_5IO_6$: b) P. H. J. Carlsen, T. Katsuki, V. S. Martin, K. B. Sharpless, *J. Org. Chem.* **1981**, *46*, 3936. CrO_3/H_5IO_6: c) M. Zhao, J. Li, Z. Song, R. Desmond, D. M. Tschaen, E. J. J. Grabowski, P. J. Reider, *Tetrahedron Lett.* **1998**, *39*, 5323. TEMPO/NaClO: d) M. Zhao, J. Li, E. Mano, Z. Song, D. M. Tschaen, E. J. J. Grabowski, P. J. Reider, *J. Org. Chem.* **1999**, *64*, 2564. e) K. Yasuda, S. V. Ley, *J. Chem. Soc., Perkin Trans. 1* **2002**, 1024.

146 F. Vocanson, Y. P. Guo, J. L. Namy, H. B. Kagan, *Synth. Commun.* **1998**, *28*, 2577.

147 From the results of the Ru K-edge XAFS of the Co^III–Ce^IV–Ru^IV catalyst., the monomeric Ru^4+ species had a coordination with one short Ru–O distance (1.81 Å) and four long Ru–O distances (1.97 Å). The short Ru–O bond was assigned to a Ru^IV–OH moiety. Together with the result for XRD and Co K-edge XAFS, the monomeric Ru^IV cation species is located on the surface of the $CeO_2/CoO(OH)$ support.

148 T. Iwahama, S. Sakaguchi, Y. Nishiyama, Y. Ishii, *Tetrahedron Lett.* **1995**, *36*, 6923; M. Akada, S. Nakano, T. Sugiyama, K. Ichitoh, H. Nakao, M. Akita, Y. Moro-oka, *Bull. Chem. Soc. Jpn.* **1993**, *66*, 1511.

149 a) C. E. H. Bawn, J. B. Williamson, *Trans. Faraday Soc.* **1951**, *47*, 721. b) S.-I. Murahashi, T. Naota, N. Hirai, *J. Org. Chem.* **1993**, *58*, 7318.

150 N. Wheatley, P. Kalck, *Chem. Rev.* **1999**, *99*, 4479; B. H. Holm, E. I. Solomon, *Chem. Rev.* **2004**, *104*, 347.

151 This allows local compositional modeling for the strong metal-support interaction (SMSI) seen in supported metal catalysts. See: S. J. Tauster, S. C. Fung, L. R. Garten, *J. Am. Chem. Soc.* **1978**, *100*, 170.

152 *Handbook of Heterogeneous Catalysis*, ed. by G. Ertl, H. Knözinger, J. Weitkamp, VCH, Weinheim, **1997**.

153 K. Kaneda, Y. Kawanishi, S. Teranishi, *Chem. Lett.* **1984**, 1481.

154 N. Hall, *Science* **1994**, *266*, 32.

155 Excellent reports of one-pot synthesis: a) K. M. Koeller, C.-H. Wong, *Chem. Rev.* **2000**, *100*, 4465. b) T. Kawasaki, Y. Yamamoto, *J. Org. Chem.* **2002**, *67*, 5138. c) G. Balme, E. Bossharth, N. Monterio, *Eur. J. Org. Chem.* **2003**, 4101. d) B. M. Choudary, N. S. Chowdari, S. Madhi, M. L. Kantam, *J. Org. Chem.* **2003**, *68*, 1736. e) K. C. Nicolaou, T. Montagnon, S. A. Snyder, *Chem. Commun.* **2003**, 551.

156 a) B. J. Cohen, M. A. Kraus, A. Patchornik, *J. Am. Chem. Soc.* **1997**, *99*, 4165. b) G. Cainelli, M. Contento, F. Manescalchi, R. Regnoly, *J. Chem. Soc., Perkin Trans. 1* **1980**, 2516. c) F. Gelman, J. Blum, D. Avnir, *J. Am. Chem. Soc.* **2000**, *122*, 11999.

157 One-pot syntheses using multifunctional heterogeneous catalysts: Y. Z. Chen, C. M. Hwang, C. W. Liaw, *Appl. Catal., A* **1998**, *169*, 207. See also Ref. 155d.

158 K. Motokura, N. Fujita, K. Mori, T. Mizugaki, K. Ebitani, K. Kaneda, *J. Am. Chem. Soc.* **2005**, *127*, 9674.

159 a) S. S. Kulp, M. J. McGee, *J. Org. Chem.* **1983**, *48*, 4097. b) R. W. Hartmann, C. Batzl, *J. Med. Chem.* **1986**, *29*, 1362. c) D. S. Im, C. S. Cheong, S. H. Lee, B. H. Youn, S. C. Kim, *Tetrahedron* **2000**, *56*, 1309. d) H. Takaya, K. Yoshida, K. Isozaki, H. Terai, S.-I. Murahashi, *Angew. Chem., Int. Ed.* **2003**, *42*, 3302.

160 α-Alkylation of ketones using homogeneous transition-metal complexes in the presence of base: a) C. S. Cho, B. T. Kim, T.-J. Kim, S. C. Shim, *Tetrahedron Lett.* **2002**, *43*, 7987. b) K. Taguchi, H. Nakagawa, T. Hirabayashi, S. Sakaguchi, Y. Ishii, *J. Am. Chem. Soc.* **2004**, *126*, 72.

161 R. Grigg, T. R. B. Mitchell, S. Sutthivaiyakit, N. Tongpenyai, *Tetrahedron Lett.* **1981**, *22*, 4107.

162 Metal-catalyzed hydrogen-transfer reactions: T. Naota, H. Takaya, S.-I. Murahashi, *Chem. Rev.* **1998**, *98*, 2599; G. Zassinovich, G. Mestroni, S. Gladiali, *Chem. Rev.* **1992**, *92*, 1051.

163 C.-S. Cho, B.-T. Kim, T.-J. Kim, S.-C. Shim, *Chem. Commun.* **2001**, 2576; Use of alcohols instead of ketones, see: C.-S. Cho, B.-T. Kim, H.-J. Choi, T.-J. Kim, S.-C. Shim, *Tetrahedron* **2003**, *59*, 7997.

164 P. Friedlaender, *Chem. Ber.* **1882**, *15*, 2572; Review: C.-C. Cheng, S.-J. Yan, *Org. React.* **1982**, *28*, 37.

165 a) C. Stephane, S. Desfosses, R. Dionne, N. Theberge, R. H. Burnell, *J. Nat. Prod.* **1993**, *56*, 138. b) A. Fournet, R. Mahieux, M. A. Fakhfakf, X. Franck, R. Hocquemiller, B. Figadére, *Bioorg. Med. Chem. Lett.* **2003**, *13*, 891.

166 K. Yamaguchi, K. Ebitani, T. Yoshida, H. Yoshida, K. Kaneda, *J. Am. Chem. Soc.* **1999**, *121*, 4526.

167 T. Yano, H. Matsui, T. Koike, H. Ishiguro, H. Fujihara, M. Yoshihara, T. Maeshima, *Chem. Commun.* **1997**, 1129.

Kiyotomi Kaneda is a professor of chemical engineering at Osaka University. He was born in Takamatsu in 1943. He obtained his bachelors (1967), masters (1969), and doctoral (1972) degrees from Osaka University, Faculty of Engineering Science, under the supervision of Professor Shiichiro Teranishi. He joined Osaka University, Faculty of Engineering Science, as a research assistant in 1972, ans spent two years (1986–1987) at Texas A&M University and University of Birmingham as a research fellow from the Ministry of Education, Culture, Sports, Science and Technology, Japan. He has been a professor since 1997, and acted as a director of Research Center for Solar Energy Chemistry of Osaka University (2001–2004). He is a recipient of the first Award of the Green and Sustainable Chemistry Network (2001) and Academic Award from the Catalysis Society of Japan (2003). His research interests include the design of high-performance catalysts for environmentally benign chemical reactions based on knowledge of homogeneous and heterogeneous catalysis.

Kohki Ebitani was born in Yamaguchi in 1965. After he obtained his doctoral degree (1992) from Hokkaido University, Graduate School of Science, under the supervision of Proferssor Kozo Tanabe and Professor Hideshi Hattori, he joined Tokyo Institute of Technology, Faculty of Engineering, as a research assistant in 1992. In 1996, he moved to Osaka University as a research assistant. He has been an associate professor since 1997, and currently studies with Professor Kiyotomi Kaneda. His research interest concerns the structural determination of catalytically active species using spectroscopic methods such as X-ray absorption spectroscopy and acid–base catalysts by a solid surface.

Tomoo Mizugaki was born in Tokyo in 1971. He received his B.S. in 1994 and his M.S. in chemical engineering in 1996 from Osaka University. He obtained his Ph.D. from Osaka University in 1999, working under the direction of Professor Kiyotomi Kaneda. After his Ph.D., he joined Prof. Kaneda's group as a research associate at Osaka University. Currently, his research interests are principally in the areas of organic syntheses using heterogenized catalysts with organic and inorganic macroligands.

Kohsuke Mori was born in Aichi in 1975. He received his B.S. (1999), M.S. (2000), and Ph.D. (2003) degrees from Osaka University under the supervision of Professor Kiyotomi Kaneda. In 2003–2005, he was a research fellow of the Japan Society for the Promotion of Science (JSPS) for Young Scientist. In 2004, he joined the groups of Professor Don Tilley at the University of California, Bekeley, as a postdoctoral fellow. Since 2005, he has been a research assistant at the Faculty of Engineering Science of Osaka University. His research interests are focused on the design and synthesis of novel hydroxyapatite catalysts.